UC San Diego

UC San Diego Electronic Theses and Dissertations

Title

The Molecular Mechanisms of MAP4K3-mediated Autophagy Induction

Permalink

https://escholarship.org/uc/item/7dj6610f

Author

Hsu, Cynthia Li-Shin

Publication Date

2016

Peer reviewed|Thesis/dissertation

eScholarship.org Powered by the California Digital Library
University of California

UNIVERSITY OF CALIFORNIA, SAN DIEGO

The Molecular Mechanisms of MAP4K3-mediated Autophagy Induction

A dissertation submitted in partial satisfaction of the requirements for the degree
Doctor of Philosophy

in

Biomedical Sciences

by

Cynthia Li-Shin Hsu

Committee in charge:

Professor Albert La Spada, Chair
Professor Christopher Glass
Professor Kun-Liang Guan
Professor Tony Hunter
Professor Richard Kolodner

2016

Copyright

Cynthia Li-Shin Hsu, 2016

All rights reserved

This Dissertation of Cynthia Li-Shin Hsu is approved, and it is acceptable in quality and form for publication on microfilm and electronically:

_____

_____

_____

_____

_____

Chair

University of California, San Diego

2016

TABLE OF CONTENTS

LIST OF FIGURES

ACKNOWLEDGEMENTS

I would like to thank Professor Al La Spada for his support and mentorship throughout my time in his lab. He has given me the opportunity to grow both as a scientist and as a person, and has challenged me to stretch outside my comfort zone to achieve my goals. He has also been extremely encouraging of my scientific collaborations, and through this, I have had invaluable opportunities to meet wonderful scientists and friends.

I would also like to thank my dissertation committee members Dr. Glass, Dr. Guan, Dr. Hunter, and Dr. Kolodner for all of your support and feedback, as well as collaboration opportunities and scientific expertise.

In the Guan lab, I would like to thank Steve Plouffe for all of your help getting me started with CRISPR/Cas9 and with the MAP4K3 k.o. cells, and your general willingness to help me whenever I had questions. I would also like to thank Zhipeng Meng for your general extensive knowledge about the MAP4K family and also your willingness to help with any reagents/plasmids/etc. that I needed.

In the Hunter lab, I cannot thank Jill Meisenhelder enough for everything you have done for me. My graduate experience would not have been the same without you. Not only have you taught me everything I know about kinase assays, but you have also been a wonderful friend and mentor.

To everyone in the La Spada lab, thank you for being a wonderful group of scientists, mentors, and friends. Thank you especially to those of you who were kind and patient to me from the very beginning, when I had just joined the lab, and helped me get on my feet. I would especially like to thank Elian Lee, who has been an incredible student. You have been a pleasure to mentor and I truly appreciate all of

your hard work, amazing attitude, and huge heart. Thank you to all of the wonderful past and present members of the autophagy team: Dr. Somasish Dastidar, Dr. Kohta Onishi, and Dr. Edwin Paz, for being an awesome and collaborative team to work with and making science fun. Thank you to Colleen Stoyas and Dr. Kara Gordon for advice of all types. And thank you to Dr. Susan Mayo for being the best lab manager and keeping the lab always in running order.

Chapter 2 is an adaptation of a published manuscript. The full citation is: Dubinsky, A.N., Dastidar, S.G., Hsu, C.L., Zahra, R., Djakovic, S.N., Duarte, S., Esau, C.C., Spencer, B., Ashe, T.D., Fischer, K.M., MacKenna, D.A., Sopher, B.L., Masliah, E., Gaasterland, T., Chau, B.N., Pereira de Almeida, L., Morrison, B.E., and La Spada, A.R. (2014). Let-7 coordinately suppresses components of the amino acid sensing pathway to repress mTORC1 and induce autophagy. Cell metabolism 20, 626-638. The dissertation author was a co-first author of this work.

Chapter 3 is an original document describing scientific work that is currently being prepared as a manuscript for submission. Hsu, C.L., Lee, E.X., Meisenhelder, J., Gordon, K.L., Hunter, T., and La Spada, A.R. “MAP4K3 regulates autophagy induction via direct phosphorylation of TFEB.” The dissertation author is the principal author of this work.

Chapter 4 is an original document describing scientific work that is currently being prepared as a manuscript for submission in a much revised form. Hsu, C.L., Ohnishi, K., Lee, E.X., Meisenhelder, J., Paz, E.P., Hunter, T., and La Spada, A.R. “MAP4K3 regulates mTORC1 activity via AMPK signaling.” The dissertation author is the principal author of this work.

VITA

2016 Doctor of Philosophy, Biomedical Sciences
University of California – San Diego, School of Medicine

2010-2012 Medical student, Medical Scientist Training Program
University of California – San Diego, School of Medicine

2010 Bachelor of Science, Biochemistry
Bachelor of Science, Molecular, Cellular, & Developmental Biology
University of Washington – Seattle

PUBLICATIONS

Dubinsky, A.N., Dastidar, S.G., **Hsu, C.L.*,** Zahra, R., Djakovic, S.N., Duarte, S., Esau, C.C., Spencer, B., Ashe, T.D., Fischer, K.M., MacKenna, D.A., Sopher, B.L., Masliah, E., Gaasterland, T., Chau, B.N., Pereira de Almeida, L., Morrison, B.E., and La Spada, A.R. (2014). Let-7 coordinately suppresses components of the amino acid sensing pathway to repress mTORC1 and induce autophagy. Cell metabolism 20, 626-638.

***** Co-first author

Hsu, C.L., Muerdter, C.P., Knickerbocker, A.D., Walsh, R.M., Zepeda-Rivera, M.A., Depner, K.H., Sangesland, M., Cisneros, T.B., Kim, J.Y., Sanchez-Vazquez, P., Cherezova, L., Regan, R.D., Bahrami, N.M., Gray, E.A., Chan, A.Y., Chen, T., Rao, M.Y., and Hille, M.B. (2012). Cdc42 GTPase and Rac1 GTPase act downstream of p120 catenin and require GTP exchange during gastrulation of zebrafish mesoderm. Dev Dyn 241, 1545-1561.

Mefford, H.C., Yendle, S.C., **Hsu, C.,** Cook, J., Geraghty, E., McMahon, J.M., Eeg-Olofsson, O., Sadleir, L.G., Gill, D., Ben-Zeev, B., Lerman-Sagie, T., Mackay, M., Freeman, J.L., Andermann, E., Pelakanos, J.T., Andrews, I., Wallace, G., Eichler, E.E., Berkovic, S.F., and Scheffer, I.E. (2011). Rare copy number variants are an important cause of epileptic encephalopathies. Ann Neurol 70, 974-985.

ABSTRACT OF THE DISSERTATION

The Molecular Mechanisms of MAP4K3-mediated Autophagy Induction

by

Cynthia Li-Shin Hsu

Doctor of Philosophy in Biomedical Sciences

University of California, San Diego, 2016

Professor Albert R. La Spada, Chair

The ability of cells to maintain metabolic homeostasis in response to changes in nutrient availability is critical for cell survival. Autophagy, the major cellular pathway by which macromolecules and organelles are degraded, is upregulated in the face of nutrient starvation and cell stress. The mammalian target of rapamycin complex 1 (mTORC1) integrates various environmental stimuli to regulate cellular processes,

including autophagy, cell growth, protein synthesis, and lipid metabolism. Of the various inputs to mTORC1, the amino acid sensing pathway is among the most potent. This dissertation describes three studies that aim to elucidate the molecular mechanisms by which cells regulate autophagy and metabolic homeostasis in response to amino acids.

The first study (Chapter 1) identifies *let-7* as a microRNA capable of promoting neuronal autophagy in response to nutrient deprivation by coordinately down-regulating the amino acid sensing pathway to prevent mTORC1 activation. In the course of this work, we identified MAP4K3 as a target of let-7, and found that inhibition of MAP4K3 was sufficient to induce autophagy in neurons.

The second study (Chapter 2) builds upon the MAP4K3 findings from the first study, elucidating MAP4K3 regulation of autophagy via phosphorylation of transcription factor EB (TFEB). In the presence of amino acids, activated MAP4K3 phosphorylates TFEB at serine 3, which is necessary for subsequent mTORC1 phosphorylation of TFEB at serine 211 and sequestration in the cytoplasm by 14-3-3 binding. Loss of MAP4K3 leads to increased TFEB nuclear localization, transcription of TFEB-regulated lysosomal genes, and autophagy induction.

In the final study (Chapter 3), we demonstrate another role for MAP4K3 in autophagy regulation: MAP4K3 regulates both mTORC1 localization and activity via distinct pathways. We hypothesize that MAP4K3 is critical for the activation of mTORC1 through the inhibition of SIRT1, AMPK, and TSC2, upstream inhibitors of mTORC1, in the presence of amino acids. Subsequent to mTORC1 activation, MAP4K3 then regulates the Rag GTPases to mobilize mTORC1 off the lysosome to phosphorylate and activate its substrates.

Through these complex mechanisms, MAP4K3 emerges as a critical regulator of cellular homeostasis in response to amino acids, via both mTORC1 activity and TFEB-mediated autophagy induction.

CHAPTER 1.

MAP4K3 and the mTOR signaling pathway

Cells must be able to respond to a large number of environmental stimuli and extracellular signals in order to survive. However, most extracellular signals cannot cross the plasma membrane in order to activate their corresponding genes. Therefore, cells depend on signaling pathways to transmit their signals to various cytoplasmic and nuclear targets. One such pathway, the mitogen-activated protein kinase (MAPK) signaling cascade, is critical for the regulation of diverse cellular processes such as proliferation, differentiation, stress response, and apoptosis in response to the cellular environment (Avruch, 2007; Dhanasekaran and Johnson, 2007; Krishna and Narang, 2008; Pimienta and Pascual, 2007). The MAPK signaling cascade is initiated when a stimuli activates a small G protein or adaptor protein. This signal is then transmitted through up to five tiers of kinases by phosphorylation of their downstream targets, going through MAP4Ks, MAP3Ks, MAPKKs, MAPKs, and MAPKAPKs from upstream to downstream. This multiplicity of components in the MAPK signaling pathway allows extended specificity and tight regulation, which are hallmarks of these signaling cascades.

MAP4K3

MAP4K3, also known as germinal center kinase-like kinase (GLK), is a member of the MAP4K family, which is a subfamily of the sterile 20 (Ste20) protein kinase family (Diener, 1997). MAP4K3 is in the GCK-I subfamily of Ste20 kinases, and contains a conserved N-terminal kinase domain, a conserved C-terminal citron homology domain and proline-rich motifs in the middle portion. In response to UV radiation and TNF-α, MAP4K3 has been shown to activate the JNK pathway (Diener et al., 1997; Ramjaun et al., 2001). MAP4K3 induces caspase-dependent apoptotic cell death by modulating pro-apoptotic Bcl-2 homology domain 3 (BH3)-only proteins post-transcriptionally via the JNK signaling pathway (Diener et al., 1997; Lam et al., 2009; Lam et al., 2010). Consistent with this, increased MAP4K3 expression has been linked to various autoimmune disorders, including Still's disease, rheumatoid arthritis, and autoimmune encephalomyelitis (Chen et al., 2012; Lock et al., 2002).

Separately, MAP4K3 has also been shown to act upstream of the mTORC1 signaling pathway to induce phosphorylation of S6K and 4E-BP1 (eIF4E-binding protein) in response to amino acids, but not to insulin (Findlay et al., 2007). During conditions of amino acid starvation, the phosphatase PP2A dephosphorylates MAP4K3 at serine 170, which is normally transautophosphorylated, rendering it inactive (Yan et al., 2010). Consistent with these findings, *Drosophila* mutant for MAP4K3 have reduced phosphorylation of TOR targets, which physiologically manifested as retarded growth, reduced size, and low lipid reserves (Bryk et al., 2010; Resnik-Docampo and de Celis, 2011). Interestingly, MAP4K3 mutants showed the same growth delay as wild-type Drosophila when cultured on amino acid-restricted food, supporting amino acid-specific signaling to MAP4K3. In *C. elegans*,

depletion of MAP4K3 led to a small but significant increase in mean lifespan (Khan et al., 2012). These findings support MAP4K3 regulation of mTORC1 signaling in response to amino acids. However, the mechanism by which MAP4K3 regulates mTORC1 signaling has not been elucidated.

mTORC1

Central to the mTORC1 signaling pathway is the mTORC1 complex, composed of six protein subunits – the catalytic mammalian target of rapamycin (mTOR), regulatory-associated protein of mTOR (Raptor), mammalian lethal with Sec13 protein 8 (mLST8, also known as GβL), proline-rich AKT substrate 40 kDa (PRAS40), the Tti1/Tel2 complex and DEP-domain-containing mTOR-interacting protein (DEPTOR) (Hara et al., 2002; Jacinto et al., 2004; Kaizuka et al., 2010; Kim, 2003; Peterson et al., 2009; Sancak et al., 2007). Deregulation of the mTOR signaling pathway has been implicated in aging, as well as a wide array of human diseases including cancer, obesity, type 2 diabetes, and neurodenegeration (Laplante and Sabatini, 2012). The vast reach of mTOR signaling is attributable to its ability to integrate information about nutrient status, in the form of amino acids, growth factors, or energy, and cell stress, and regulate disparate processes such as protein translation, lipid metabolism, glycolysis, angiogenesis, autophagy, and inflammation (Laplante and Sabatini, 2009). Here, we will explore the different upstream nutrients that signal to mTORC1 and their effects on mTORC1 downstream regulation of metabolic homeostasis.

Upstream regulators of mTORC1

Growth factors

Growth factors such as insulin or insulin-like growth factor (IGF) stimulate mTORC1 via the PI3K and ERK-Ras signaling pathways, ultimately culminating in the activation of the small GTPase Rheb, which when loaded with GTP, stimulates the kinase activity of mTORC1 (Saucedo et al., 2003; Stocker et al., 2003). Activation of these pathways leads to the phosphorylation and activation of protein kinase B (PKB, also known as Akt), which activates mTORC1 in two ways. Akt promotes the phosphorylation and dissociation of PRAS40 from mTOR, leading to mTORC1 activation (Sancak et al., 2007; Vander Haar et al., 2007). Additionally, activated Akt also phosphorylates and inactivates TSC2. TSC2, together with TSC1 and TBC1D7, forms the TSC-TBC complex, which acts as a GTPase activating protein (GAP) towards the Rheb GTPase (Inoki et al., 2002; Potter et al., 2002).

Energy

Another nutrient source that regulates mTORC1 activity via activation of Rheb GTPase is energy, stored in the form of ATP. Upon nutrient deprivation, cellular ATP levels drop, countered by an increase in levels of cellular ADP and AMP. Increases in cellular ADP and AMP levels are sensed by AMP-activated protein kinase (AMPK), a serine/threonine kinase composed of a catalytic (α) and two regulatory (β and γ) subunits.

Under nutrient starvation conditions, AMPK is phosphorylated at threonine 172 by liver kinase B1 (LKB1) in the LKB1-STRAD-MO25 complex. LKB1, a tumor suppressor gene mutated in Peutz–Jeghers syndrome, is allosterically activated

through its interaction with STE20-related adapter (STRAD) and the adaptor protein mouse protein 25 (MO25) (Boudeau et al., 2003). LKB1 phosphorylation of the conserved threonine 172 residue in AMPK's activation loop increases its activity more than 100-fold (Suter et al., 2006). Then, the γ subunit of AMPK binds to AMP and ADP, enforcing a conformational change that blocks de-phosphorylation of AMPK to keep it in an activated state. Once active, AMPK phosphorylates TSC2 at serine 1387, which acts as a primer for the phosphorylation and activation of TSC2 by glycogen synthase kinase (GSK)3-β (Inoki et al., 2003; Inoki et al., 2006), stimulating TSC2's GAP activity towards Rheb and ultimately inhibiting mTORC1. Additionally, AMPK phosphorylates Raptor, causing it to dissociate from the mTORC1 complex by binding to 14-3-3 proteins, leading to inhibition of mTORC1 through an allosteric mechanism (Gwinn et al., 2008).

Amino acids

Only recently has it become apparent that amino acids are a critical regulator of mTORC1 signaling, performing a distinct role separate from that of growth factor and energy signaling. A number of amino acid sensors have been identified in the last few years, including SLC38A9 and CASTOR1 as direct arginine sensors (Chantranupong et al., 2016; Rebsamen et al., 2015; Wang et al., 2015), Sestrin2 as a direct leucine sensor (Saxton et al., 2016; Wolfson et al., 2016), and adenosine diphosphate ribosylation factor-1 (Arf1) GTPase to be critical in glutamine sensing (Jewell et al., 2013).

Most of these sensors transduce signals that center upon the regulation of the Rag GTPases. The Rag GTPases belong to the RAS superfamily of GTPases and

function as heterodimers wherein the active complex consists of GTP-bound RagA or B complexed with GDP-bound RagC or D (Gao and Kaiser, 2006; Sekiguchi et al., 2001). In response to the presence of amino acids, mTORC1 is recruited to the cytoplasmic surface of lysosomes via a physical interaction between Raptor and the Rag GTPases. Specifically, amino acids trigger the GTP loading of RagA/B proteins, thus promoting binding to Raptor and assembly of an activated mTORC1 complex (Kim et al., 2008a; Sancak et al., 2008). In the absence of amino acids, the Rags adopt an inactive conformation (GDP-bound RagA/B and GTP-bound RagC/D), and mTORC1 is inactivated and shuttled back to the cytosol.

The activation of Rag GTPases is tightly regulated by GEF and GAP proteins. The pentameric lysosomal Ragulator complex, composed of p18, p14, MP1, HBXIP, and C7orf59 (also known as LAMTORs 1-5), functions as a GEF for RagA/B in response to amino acid stimulation (Bar-Peled et al., 2012). Meanwhile, the GATOR1 complex, a trimeric complex consisting of NPRL2, NPRL3, and DEPDC5, acts as a GAP for RagA/B and negatively regulates mTORC1 activation by promoting the GTPase activity of RagA/B (Bar-Peled et al., 2013). Through regulation of these GEF and GAP proteins, amino acids are able to regulate Rag GTPase activity and mTORC1 localization to the lysosome. Bringing mTOR to lysosomes is critical for the activation of its kinase activity because Rheb GTPase, activated by growth factors and energy signaling, is lysosomally localized (Inoki et al., 2003b).

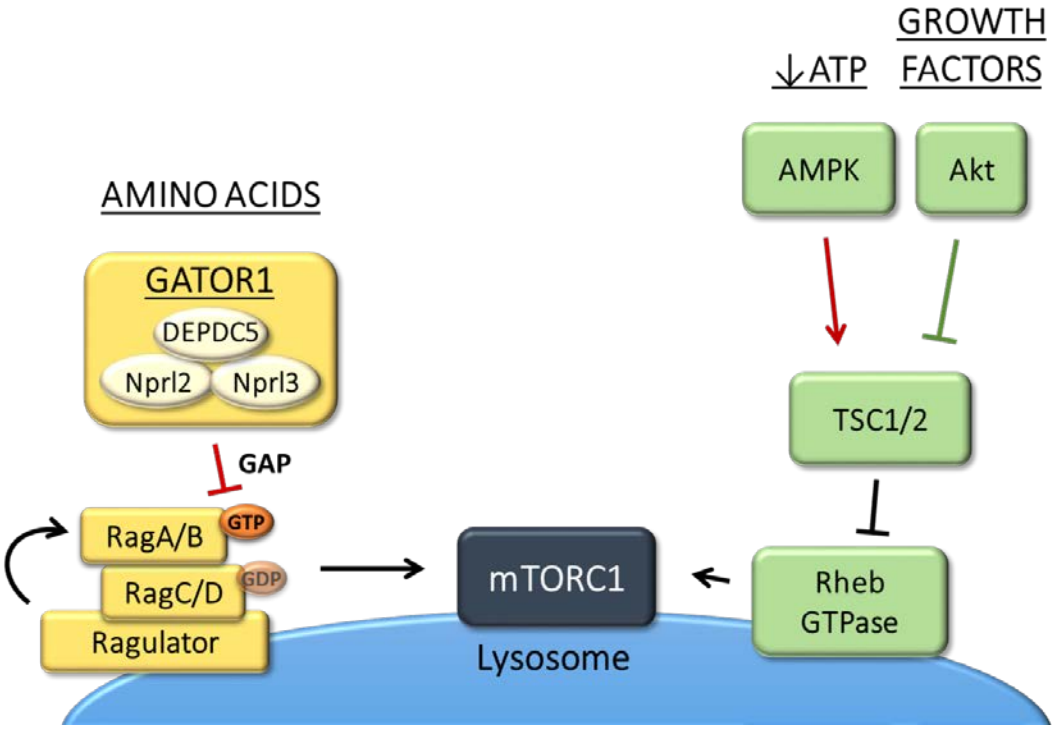

Figure 1.1. Schematic of nutrient signaling to mTORC1 at the lysosome.

Cellular processes regulated by mTORC1

mTORC1 signaling must be tightly regulated in the face of different nutrient stimuli because mTORC1 positively regulates cell growth and proliferation. mTORC1 promotes anabolic processes such as protein and lipid biosynthesis and angiogenesis, and limits catabolic processes such as lysosomal biogenesis and autophagy.

Protein translation

mTORC1 promotes protein synthesis by phosphorylating the p70 ribosomal S6 kinase 1 (S6K1) and eukaryotic initiation factor 4E (eIF4E)-binding protein 1 (4E-BP1). Unphosphorylated 4E-BP1 suppresses mRNA translation by binding to eIF4E, preventing cap-dependent translation. Phosphorylation by mTORC1 causes 4E-BP1 to dissociate from eIF4E, allowing eIF4E to recruit the translation initiation factor eIF4G to the 5′ end of mRNAs (Haghighat et al., 1995; Hara et al., 1997). Phosphorylation of S6K1 leads to increases in mRNA biogenesis, cap-dependent translation initiation and elongation, and the translation of ribosomal proteins through regulation of the activity of many proteins, including eukaryotic elongation factor 2 kinase (eEF2K) (Wang et al., 2001), S6K1 Aly/REF-like target (SKAR; also known as POLDIP3) (Ma et al., 2008), 80 kDa nuclear cap-binding protein (CBP80; also known as NCBP1) (Wilson et al., 2000) and eIF4B (Holz et al., 2005; Ma and Blenis, 2009). The activation of mTORC1 has also been shown to promote ribosome biogenesis by modulating the activity of transcription initiation factor IA (TIF-IA) to stimulate transcription of ribosomal RNA (Mayer et al., 2004).

Autophagy

In addition to upregulating anabolic processes in response to the presence of nutrients, mTORC1 must also inhibit catabolic processes like autophagy. Autophagy is the major eukaryotic cellular pathway by which macromolecules and organelles are degraded (Shintani and Klionsky, 2004). Autophagy involves the initial formation of an isolation membrane, the phagophore, followed by engulfment of cytosolic components and organelles into double membrane-bound vesicles that ultimately fuse with lysosomal compartments to permit degradation of the enclosed contents. When nutrient availability is limited, the degradation of organelles and proteins through autophagy provides biological material to sustain anabolic processes such as protein synthesis and energy production. Importantly, inhibition of mTORC1 is sufficient to induce autophagy in the presence of nutrients in yeast or mammalian cells (Kanazawa et al., 2004; Noda and Ohsumi, 1998). mTORC1 represses autophagy via regulation of ULK1 and 2, homologues to yeast ATG1, which are critical for recruitment of ATG proteins during autophagosome formation (Yan et al., 1998). In mammalian cells, ULK functions in a trimeric complex with ATG13L and FIP200, and mTORC1 phosphorylates Atg13L and phosphorylates ULK1 at serine 757 to repress ULK1 kinase activity (Ganley et al., 2009; Hosokawa et al., 2009a; Jung et al., 2009). When mTORC1 is inhibited under starvation conditions, ULK1 undergoes autophosphorylation and trans-phosphorylation of binding partners ATG13L and FIP200, leading to activation of the kinase complex and subsequently, autophagy induction (Boya et al., 2013).

Lysosomal Biogenesis

In addition to repressing autophagy induction, recent work has also discovered a related role for mTORC1 in regulating lysosomal biogenesis. Lysosomes not only are an important signaling hub for the activation of mTORC1 by nutrients, as discussed above, but is also critical for cellular homeostasis by regulating cellular clearance, lipid homeostasis, and energy metabolism. Transcription factor EB (TFEB) has recently emerged as a master regulator of autophagy and lysosomal biogenesis. TFEB is a member of the basic helix-loop-helix leucine zipper family of transcription factors that recognizes a 10–base pair motif (GTCACGTGAC) enriched in the promoter regions of numerous lysosomal genes (Sardiello et al., 2009). Activation of TFEB induces expression of genes associated with lysosomal biogenesis and function, and TFEB also stimulates the expression of genes necessary for autophagosome formation, fusion of autophagosomes with lysosomes, and lysosome-mediated degradation of the autophagosomal content (Palmieri et al., 2011; Settembre et al., 2011). mTORC1 regulates lysosomal biogenesis by modulating the activity of transcription factor EB (TFEB) (Martina et al., 2012; Roczniak-Ferguson et al., 2012; Settembre et al., 2012).

Under nutrient-rich conditions, TFEB interacts with active Rag GTPases, which promote recruitment of TFEB to the lysosomal surface (Martina and Puertollano, 2013). This facilitates mTORC1 phosphorylation of TFEB on several sites, including serine 211 (Ser211) (Martina et al., 2012; Roczniak-Ferguson et al., 2012; Settembre et al., 2012). Phosphorylation of Ser211 creates a binding site for 14-3-3, a cytosolic chaperone that keeps TFEB sequestered in the cytosol. In contrast, under starvation conditions, mTORC1 is inactivated, permitting the

TFEB/14-3-3 complex to dissociate, and enabling TFEB to translocate to the nucleus, where it stimulates the expression of its target genes, thus leading to lysosomal biogenesis, increased lysosomal degradation, and autophagy induction (Martina et al., 2012; Roczniak-Ferguson et al., 2012).

Conclusion

While there is a clear relationship between MAP4K3 and mTORC1 signaling, the mechanism of action is not understood. In the following chapters, we catalogue our increased understanding of MAP4K3 regulation of mTORC1 signaling and autophagy induction. In Chapter 2, we demonstrate that knockdown of MAP4K3 in neurons is sufficient to induce autophagy. In Chapter 3, we identify MAP4K3 as a critical negative regulator of autophagy through the phosphorylation of transcription factor EB (TFEB). In the presence of amino acids, activated MAP4K3 phosphorylates TFEB at serine 3. This preliminary phosphorylation step is necessary for subsequent mTORC1 phosphorylation of TFEB at serine 211 and sequestration in the cytoplasm by 14-3-3 binding. Loss of MAP4K3 leads to increased TFEB nuclear localization, transcription of TFEB-regulated lysosomal genes, and autophagy induction. The phosphorylation of TFEB at serine 3 is crucial for its interaction with the Rag GTPases and mTORC1 at the lysosome, as well as phosphorylation at serine 211. In Chapter 4, we explore MAP4K3 regulation of mTORC1 localization via the Rag GTPases and the GATOR1 complex, as well as MAP4K3 regulation of mTORC1 activity via SIRT1 and the LKB1-AMPK axis. Increased understanding of MAP4K3 and MTORC1 signaling will lead to better understanding of deregulation in disease states and identification of drug-targetable substrates.

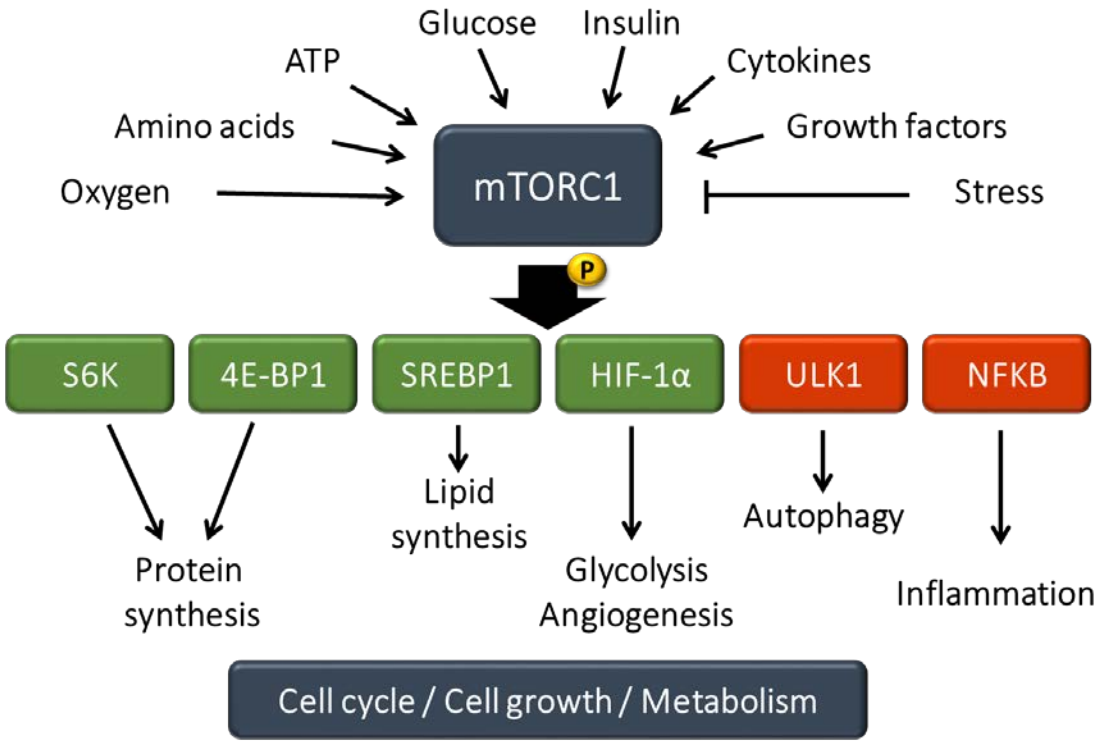

Figure 1.2. Schematic of upstream nutrient and stress signaling to mTORC1 and downstream cellular processes regulated by mTORC1.

CHAPTER 2.

Let-7 coordinately suppresses components of the amino acid sensing pathway to repress mTORC1 and induce autophagy

Abstract

Macroautophagy (hereafter autophagy) is the major pathway by which macromolecules and organelles are degraded. Autophagy is regulated by the mTOR signaling pathway, which is the focal point for integration of metabolic information, with mTORC1 playing a central role in balancing biosynthesis and catabolism. Of the various inputs to mTORC1, the amino acid sensing pathway is among the most potent. Based upon transcriptome analysis of neurons subjected to nutrient deprivation, we identified *let-7* as a microRNA capable of promoting neuronal autophagy. We found that *let-7* activates autophagy by coordinately down-regulating the amino acid sensing pathway to prevent mTORC1 activation. Further we confirmed that inhibition of one specific target of *let-7,* MAP4K3, was sufficient to induce autophagy in neurons. Hence, *let-7* plays a central role in nutrient homeostasis and proteostasis regulation in higher organisms.

Introduction

Autophagy is the major eukaryotic cellular pathway by which macromolecules and organelles are degraded (Shintani and Klionsky, 2004). Autophagy involves the initial formation of an isolation membrane, the phagophore, followed by engulfment of cytosolic components and organelles into double membrane-bound vesicles that ultimately fuse with lysosomal compartments to permit degradation of the enclosed contents. Much of what we know about autophagy regulation and the autophagy pathway comes from work done in yeast (Mizushima et al., 1998; Scott et al., 1996). Although mammals also use autophagy as a cellular survival mechanism when faced with starvation conditions, autophagy has been adapted to perform a wide range of functions in higher organisms, including immune response to pathogen invasion, surveillance against cancer, and maintenance of protein and organelle quality control in the CNS (Mizushima and Komatsu, 2011).

Autophagy activation is tightly regulated in the cell based upon nutrient availability and cell stress. One critical regulator of autophagy is TOR kinase (also known as mTOR, for ‘mammalian target of rapamycin’), which forms the mTORC1 signaling complex along with regulatory-associated protein of mTOR (Raptor), mammalian lethal with Sec13 protein 8 (mLST8, also known as GbL); proline-rich AKT substrate 40 kDa (PRAS40); and DEP-domain-containing mTOR-interacting protein (Deptor) (Peterson et al., 2009). mTORC1 serves as a focal point for integration of metabolic information, growth factor signaling, and stress (Ganley et al., 2009; Hosokawa et al., 2009a). Under conditions of abundant nutrients and absence of cell stress, mTORC1 directly phosphorylates and thereby inactivates Atg1 (ULK1),

which is in complex with Atg13 and FIP200, key upstream autophagy pathway proteins that initiate autophagy induction (Boya et al., 2013).

Recent studies have further demonstrated that sensing of nutrient status by the mTORC1 complex is accomplished by direct association with the lysosome, where nutrient availability both within this organelle and in the cytosol is transduced to the mTORC1 complex through a set of signaling complexes that converge on mTORC1 to determine its activation state (Yan and Lamb, 2012). The Rag family of GTPases are critical for the amino acid sensing ability of mTORC1 (Kim et al., 2008a; Sancak et al., 2008). The Rag GTPases exist as a heterodimer wherein the active complex consists of GTP-bound RagA or B complexed with GDP-bound RagC or D (Gao and Kaiser, 2006; Sekiguchi et al., 2001). Importantly, the $RagA/B^{GTP}$–$RagC/D^{GDP}$ heterodimer physically interacts with Raptor to recruit mTORC1 to the lysosome under AA-rich conditions, placing it in close proximity to Rheb, a potent activator of mTORC1. The Rag proteins lack membrane-targeting sequences, and are instead anchored to the lysosomal surface by the Ragulator complex, which is composed of five proteins: p18, p14, MAPK scaffold protein 1 (MP1), C7orf59, and hepatitis B virus X interacting protein (HBXIP), encoded by the late endosomal/lysosomal adaptor and MAPK and mTOR activator 1, 2, 3, 4, and 5 (LAMTOR1, 2, 3, 4, and 5) genes, respectively (Sancak et al., 2010). This pentameric Ragulator complex also acts as a guanine nucleotide exchange factor (GEF) towards RagA/B (Bar-Peled et al., 2012).

In light of its numerous essential roles in cellular homeostasis, we hypothesized that autophagy would be subject to sophisticated transcriptional regulatory control, not just downstream of mTORC1, but also upstream of mTORC1

to facilitate integration of nutrient sensing information coming from a variety of signaling pathway sources. We predicted that such fine-tuned regulation would be particularly important in the CNS, where autophagy-mediated turnover of misfolded proteins and damaged organelles guards against disruption of crucial cellular processes. To delineate pathways of genetic regulation of autophagy in the CNS, we developed a novel culture system for autophagy induction in primary cortical neurons (Young et al., 2009), and we used this system to interrogate gene expression changes that occur upon nutrient deprivation mediated autophagy induction. We were particularly interested in differential expression of miRNAs due to their ability to regulate approximately 50% of all protein-coding genes and play important roles in all types of biological events, including cell proliferation and differentiation, cell fate determination, signal transduction, organ development, host-viral interactions, tumorigenesis and progression (Huang et al., 2011; Krol et al., 2010). miRNAs are highly conserved, small noncoding RNA molecules that can cause translational inhibition, mRNA destabilization, or mRNA degradation by base pairing with the 3′ untranslated regions (3′-UTRs) of their target mRNAs through the seed sequences of the miRNAs (Bartel, 2009).

Our analysis revealed that a feature of autophagy pathway activation in primary neurons is upregulation of microRNAs belonging to the *let-7* family. We then determined that *let-7* activates neuronal autophagy by repressing the expression of genes that comprise a newly delineated amino acid sensing pathway (Jewell et al., 2013), and confirmed the physiological significance of this *let-7* regulation by documenting *let-7* modulation of autophagy in the brain. These findings reveal a central role for *let-7* in the regulation of cellular metabolic processes.

Results

MicroRNA *let-7* is a potent regulator of neuronal autophagy

To identify the transcriptional basis of autophagy pathway regulation in neurons, we established a system for autophagy induction in primary cortical neurons obtained from GFP-LC3 transgenic mice (Young et al., 2009) This system is based upon culturing GFP-LC3 neurons in a nutrient limited media (NLM), as LC3 incorporation into autophagosomes, which are formed upon autophagy pathway induction, requires a processing – conjugation step that converts diffuse appearing GFP-LC3-I into discrete GFP-LC3-II puncta (Klionsky et al., 2012). The conversion of LC3-I to LC3-II can also be monitored by Western blot analysis, as LC3-II migrates at a lower molecular mass than LC3-I (Klionsky et al., 2012).

As microRNAs (miRNAs) are enriched in the nervous system and coordinate the regulation of essential processes (Fineberg et al., 2009), we hypothesized that miRNAs could regulate neuronal autophagy induction. To identify the miRNAs necessary for neuronal autophagy induction, we performed a miRNA array analysis, comparing GFP-LC3 neurons cultured under normal complete media (CM) conditions and NLM conditions. We identified 19 miRNAs with a fold change of >1.2 at a *P* value of <0.005 and false discovery rate of <0.10. Among these 19 miRNAs, five were members of the *let-7* miRNA family (Roush and Slack, 2008). As Argonaute-2 (Ago) HITS-CLIP analysis of postnatal day 13 mouse cortex established that *let-7* is highly abundant in this brain region (Chi et al., 2009), and therefore likely to be physiologically relevant for neuronal autophagy regulation, we focused on *let-7*, after RT-PCR analysis confirmed increased *let-7* expression in NLM-cultured primary neurons.

Analysis of autophagy activation revealed increased autophagy induction in CM-cultured FFP-LC3 neurons transfected with *let-7* mimic, based upon immunostaining quantification of autophagosome formation and LC3 immunoblot measurement of autophagy flux (Figure 2.1). To assess if autophagy induction is accompanied by proper progression of the autophagy pathway, we treated GFP-LC3 neurons, cultured under normal CM conditions, with *let-7* mimic and found that LC3-II increased relative to actin (Figure 2.1A, B). To determine the flux through the autophagic pathway, we examined the effect of *let-7* mimic in the presence or absence of ammonium chloride, a lysosomal inhibitor, and observed increased autophagy flux upon *let-7* mimic treatment in comparison to treatment with control miR (Figure 2.1A, B). Analysis of GFP-LC3 puncta formation in primary neurons transfected with *let-7* mimic independently corroborated autophagy induction by *let-7* (Figure 2.1C, D). This data suggests that expression of *let-7* is sufficient to induce neuronal autophagy.

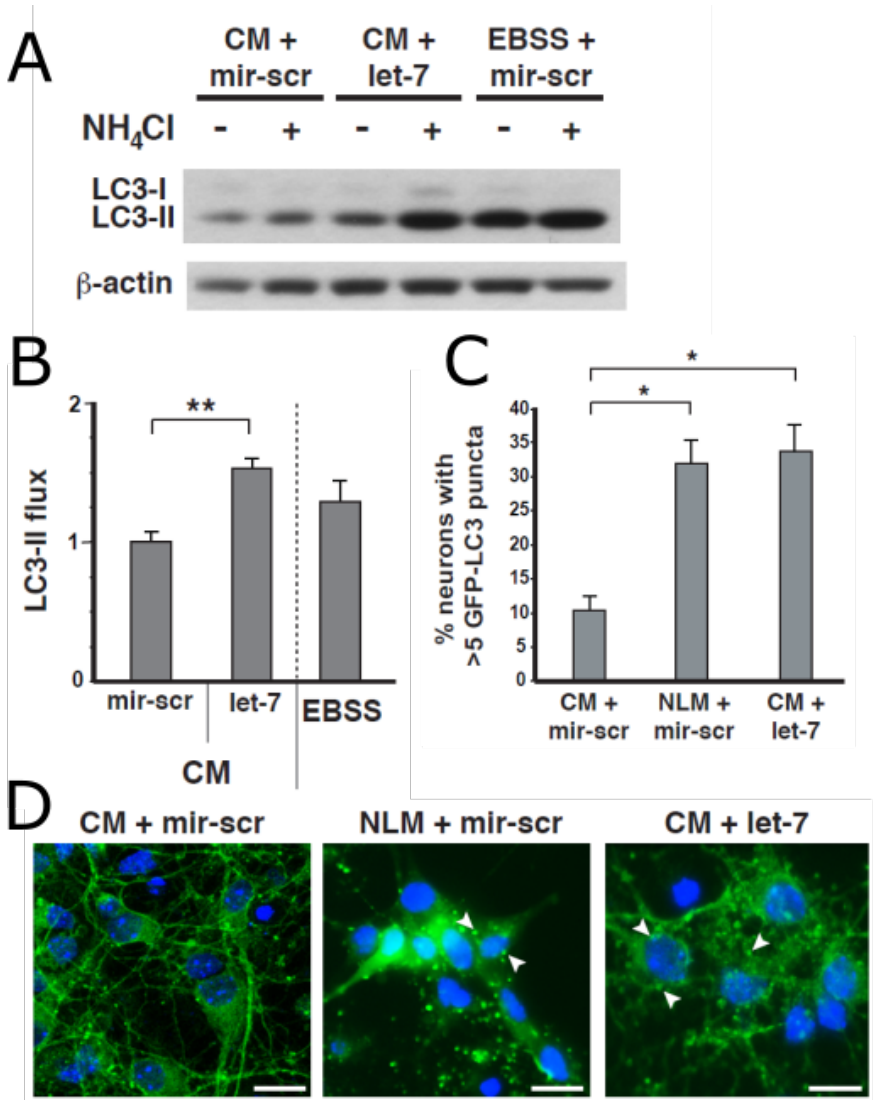

Figure 2.1. *Let-7* activates the autophagy pathway in neurons. **(A)** LC3 immunoblot analysis of GFP-LC3 primary cortical neurons cultured in CM with mir-scr, amino acid deprivation media (EBSS) with mir-scr, or CM with *let-7* mimic, in the absence or presence of the lysosomal inhibitor ammonium chloride. **(B)** Densitometry analysis of LC3 immunoblotting in (A) for autophagic flux quantification (mean ± SEM, n = 4 independent experiments). **(C)** NLM control-treated neurons and CM-cultured neurons treated with *let-7* mimic both display significant increases in the number of cells with > 5 GFP-LC3 puncta (mean ± SEM, n = 3 independent experiments). *p < 0.05, **p < 0.01; ANOVA with post hoc Tukey test. **(D)** GFP-LC3 primary cortical neurons were cultured in complete media (CM) or nutrient limited media (NLM), and treated with a scrambled miRNA or *let-7* miRNA. NLM treatment or addition of *let-7* miRNA to CM yielded neurons with prominent puncta formation (arrowheads). Scale bars = 20 μm

Let-7 Controls Autophagy Activation Upstream of the mTORC1 Complex

To determine if *let-7*-mediated autophagy activation is upstream to mTORC1 complex repression, we cultured primary cortical neurons under normal CM conditions, infected these neurons with lentivirus encoding the constitutively active Rheb Q64L mutant (Inoki et al., 2003a), and transfected these neurons with the GFP-LC3-mCherry reporter construct, in combination with *let-7* mimic or a scrambled miR. We observed prominent autophagic puncta formation in mock-infected primary neurons treated with *let-7*, comparable to the autophagic puncta formation observed in primary neurons subjected to amino acid starvation (Figures 2.2A-C). However, expression of Rheb-Q64L dramatically suppressed autophagic puncta formation in neurons subjected to amino acid starvation or *let-7* mimic treatment (Figures 2.2A-C), indicating that *let-7* activation is mTORC1-dependent. Immunoblot analysis independently confirmed that *let-7* mediated autophagy activation was markedly blunted in the presence of the Rheb-Q64L mutant (Figure 2.3A, B).

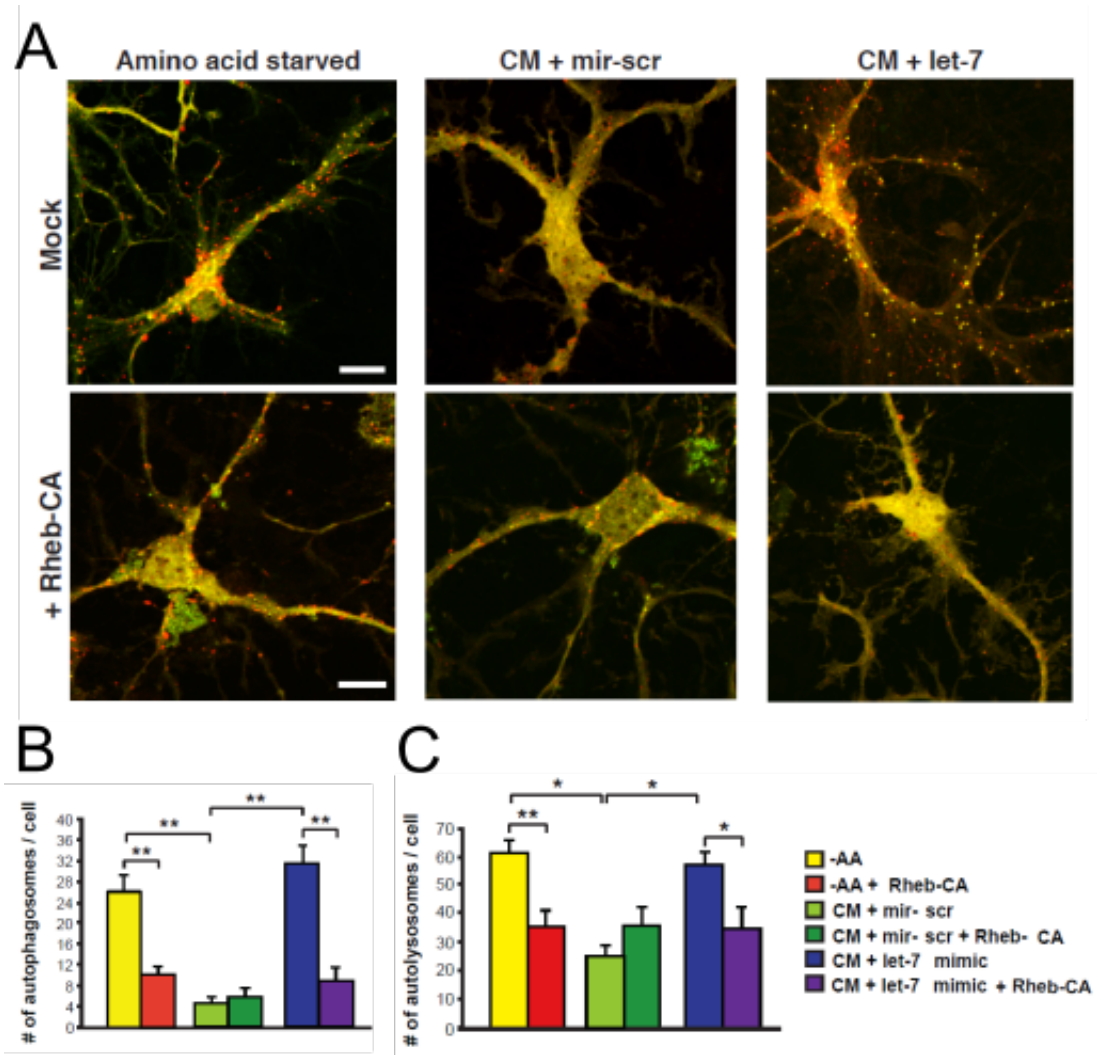

Figure 2.2. *Let-7* Controls Autophagy Activation Upstream of mTORC1. **(A)** Primary cortical neurons were infected with Flag-Rheb-Q64L lentivirus or mock infected, transfected with GFP-LC3-mCherry vector in combination with scrambled miRNA mimic or *let-7* mimic, and then cultured in EBSS media (amino acid starvation) or in CM. Scale bars, 10 mm. **(B)** Average number of autophagosomes/cell (mean ± SEM, n = 3 independent experiments) for primary neurons in (A). **(C)** Average number of autolysosomes / cell (mean ± SEM, n = 3 independent experiments) for primary neurons in (A). *p < 0.05, **p < 0.01; ANOVA with post hoc Tukey test.

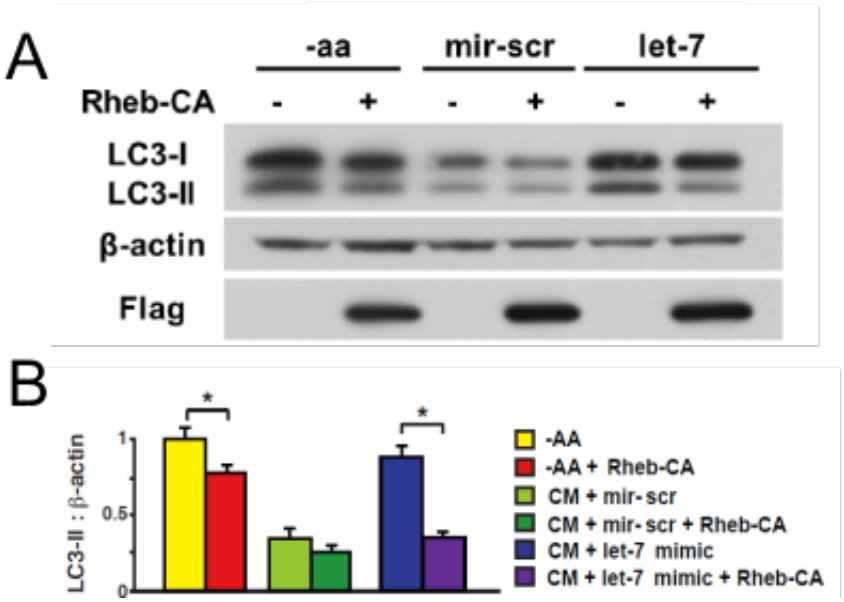

Figure 2.3. *Let-7* Controls Autophagy Activation Upstream of mTORC1. (A) LC3 immunoblot analysis of primary cortical neurons infected with Flag-Rheb-Q64L lentivirus or mock infected, transfected with scrambled miRNA mimic or *let-7* mimic, and then cultured in EBSS media for amino acid starvation (-aa) or in CM. Success of Rheb-Q64L infection was confirmed by immunoblotting for the Flag epitope. (B) Densitometry quantification of LC3-II, normalized to actin, confirms Rheb-Q64L repression of *let-7*-dependent autophagy activation (mean ± SEM, n = 3 independent experiments). *p < 0.05, **p < 0.01; ANOVA with post hoc Tukey test.

The amino acid sensing pathway is coordinately repressed by *let-7*

To determine how *let-7* represses mTORC1 activation in neurons, we considered the targets of *let-7* identified by Ago HITS-CLIP analysis of mouse cortex (Chi et al., 2009), and noted that *Slc7a5* was found to be a *let-7* target (Figure 2.4). Slc7a5 is part of a bidirectional amino acid transporter that exchanges intracellular glutamine for extracellular leucine to promote mTORC1 activation (Nicklin et al., 2009), and has emerged as a key step in the amino acid sensing pathway (Sancak et al., 2008), that strongly regulates the mTORC1 complex at the lysosome (Jewell et al., 2013). TargetScan 6.0 analysis of the 3' UTR regions of 14 genes encoding components of the amino acid sensing pathway yielded predicted *let-7* binding sites for three members of this pathway: Map4k3, RagC, and RagD (Figure 2.4). When compared to the number of predicted *let-7* binding sites called by TargetScan for all annotated genes, the fraction of *let-7* sites predicted by TargetScan for the amino acid sensing pathway represents a significant level of enrichment ($P < 10^{-2}$, $\chi 2$ analysis). TargetScan algorithm prediction is restricted to the 3' UTR, but certain studies underscore the potential role of non-3' UTR sequences in miRNA expression regulation (Chi et al., 2009); hence, we examined mRNAs of amino acid sensing pathway components for *let-7* seed site matches and found putative *let-7* binding sites in 13 of 14 components (Figure 2.5), with many sites falling within coding sequences (Figure 2.4). To evaluate putative *let-7* binding sites as potential direct *let-7* targets, we cloned either 3' UTR sequences or coding sequences downstream of a luciferase cDNA, and then measured luciferase activity off of these 13 luciferase reporter constructs, when individually transfected into HEK293T cells in the presence of mature *let-7* duplex or a scrambled miRNA. We observed significant repression of

luciferase activity by *let-7* for 3'-UTR fragments or coding sequence fragments for 11 of 13 amino acid sensing pathway components, and a trend toward suppression in the remaining two pathway members (Figure 2.6A). We introduced mismatch mutations into predicted seed sites for a subset of *let-7* targets, and found that these binding site substitutions abrogated *let-7* suppression of luciferase activity for all four tested amino acid sensing pathway components (Figure 2.6A). To further assess the physiological significance of *let-7* repression of amino acid sensing pathway gene expression, we generated a lentivirus expression construct encoding *let-7* or a scrambled miRNA, and infected primary cortical neurons with either *let-7* lentivirus or miRscrambled lentivirus. After confirming successful, modest induction of *let-7* expression in infected neurons, we measured expression levels of amino acid sensing pathway genes in neurons infected with *let-7* or the scrambled miRNA, and detected decreased expression for most amino acid sensing pathway genes, with significant reductions noted for a majority of tested genes (Figure 2.6B). These results indicate that *let-7* is directly and coordinately targeting genes that comprise the amino acid sensing pathway, upstream of the mTORC1 complex.

To confirm that *let-7* regulation of amino acid sensing pathway genes occurs at the level of protein expression, we treated Neuro2a cells or primary neurons with a *let-7* anti-miR or a scrambled anti-miR, and observed prominent derepression of putative *let-7* targets upon immunoblotting (Figures 2.7A, C). Quantification of protein expression levels of these *let-7* targets confirmed significant increases, when Neuro2a cells or primary neurons were subjected to anti-*let-7* treatment (Figure 2.7B, D). These findings independently validate the RNA expression level alterations

obtained upon *let-7* treatment, and further demonstrate that *let-7* is regulating amino acid sensing pathway genes.

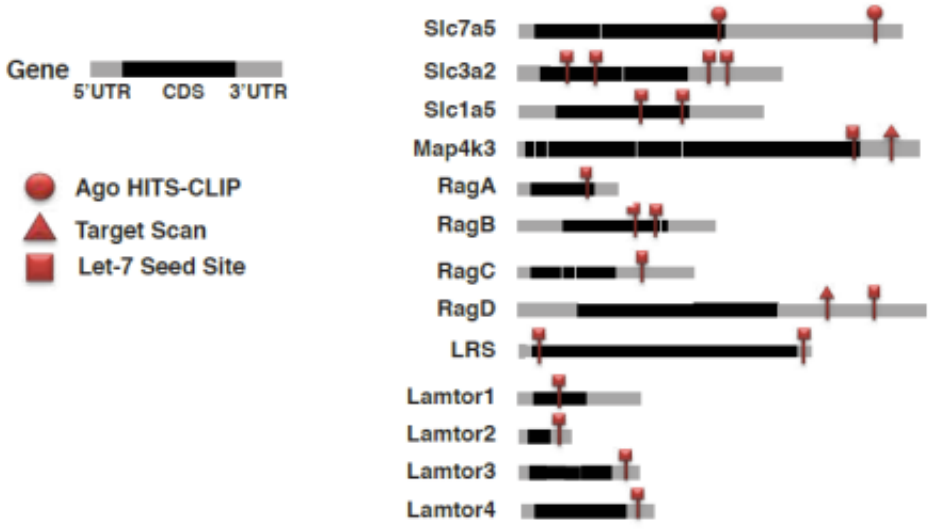

Figure 2.4. Location of *let-7* binding sites within coding regions and 3' UTRs as revealed by argonaute-2 HITS-CLIP (Chi et al., 2009), TargetScan 6.0, or direct scanning for *let-7* seed sites.

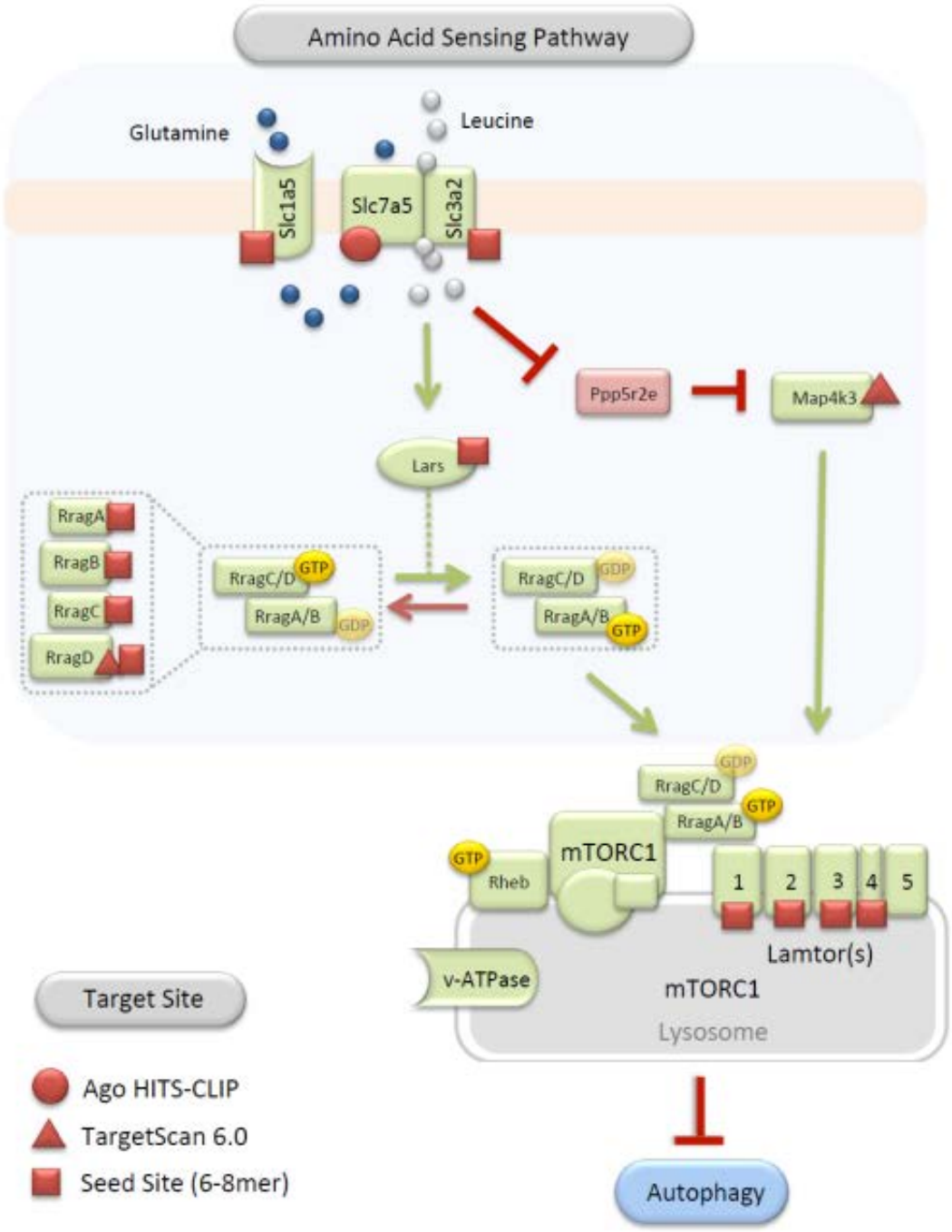

Figure 2.5. *Let-7* targets on the amino acid sensing pathway. This schematic of the amino acid sensing pathway shows positive regulators in green and the negative regulator in red. Thirteen positive regulatory proteins were found to contain target sites for *let-7*, based upon review of published argonaute HITS-CLIP data (Chi et al., 2009), Target Scan 6.0 analysis, or direct inspection of mRNAs for *let-7* seed sequences.

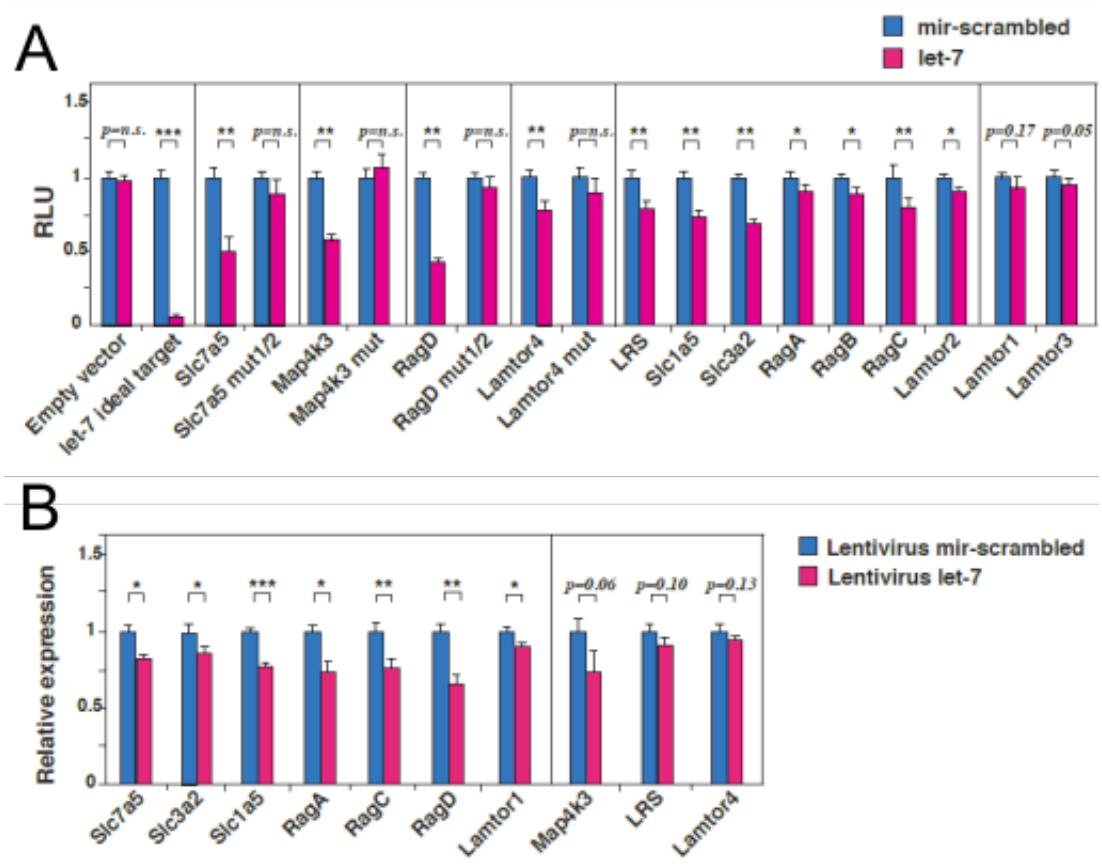

Figure 2.6. *Let-7* Represses Expression of Amino Acid Sensing Pathway Genes. **(A)** Luciferase reporter assays were performed by placing 3' UTR sequences or coding region sequences 3' to the luciferase cDNA in the pGL3 vector, and measuring relative luciferase activity in HEK293T cells upon transfection of *let-7* mimic or scrambled miRNA. Relative luciferase activity is shown for *let-7* mimic normalized to miR-scrambled, and the effect of mutations in seed sequences for a subset of *let-7* targets (Slc7a5, Map4k3, RagD, and Lamtor4) was also measured (mean ± SEM, n = 3 independent experiments). **(B)** RT-PCR quantification of amino acid sensing pathway gene expression in primary cortical neurons infected with either *let-7* lentivirus or miRscrambled lentivirus (mean ± SEM, n = 3 independent experiments).

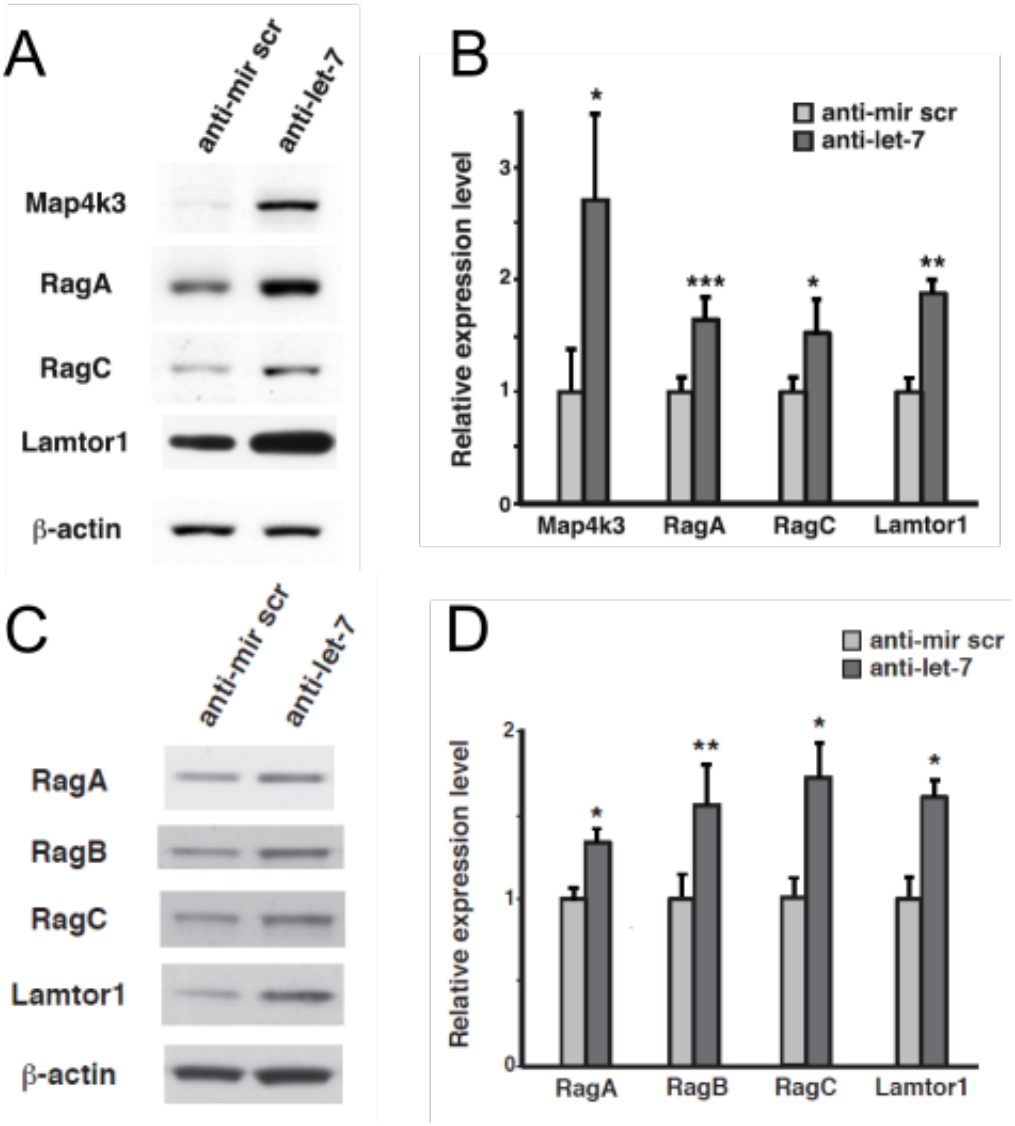

Figure 2.7. *Let-7* Regulation Occurs at the Protein Level. **(A)** Neuro2a cells were transfected with anti-miR scrambled control or with anti-*let-7*, and whole-cell extracts were immunoblotted for the indicated proteins. **(B)** Densitometric quantification of immunoblot analysis shown in (A) (mean ± SEM, n = 3 independent experiments). *p < 0.05, **p < 0.01, ***p < 0.001; t test. **(C)** Primary cortical neurons were transfected with anti-miR scrambled control or with anti-*let-7*, and whole cell extracts were immunoblotted for the indicated proteins. **(D)** Densitometric quantification of immunoblot analysis shown in (C) (mean + s.e.m., n = 3 independent experiments).

Inhibition of MAP4K3, a target of *let-7*, is sufficient to induce autophagy in neurons

The mTORC1 complex is principally responsible for repression of autophagy pathway activation under conditions of abundant nutrients and absence of cell stress. A defining feature of miRNA transcriptional control of biological processes is the coordinate down-regulation of multiple targets on the same pathway (Small and Olson, 2011), and evaluation of *let-7* regulation indicates that *let-7* promotes neuronal autophagy activation through simultaneous downregulation of multiple amino acid sensing pathway targets (Figures 2.4 and 2.5). However, to assess the physiological relevance of identified *let-7* targets for autophagy control in neurons, where amino acid sensing pathway regulation is yet to be studied, we considered the *let-7* family seed site sequence, and determined the extent of *let-7* seed site conservation for genes encoding components of the amino acid sensing pathway. This analysis revealed conservation down to zebrafish or frog respectively for two confirmed *let-7* target sites in the Map4k3 gene, indicating likely regulatory significance; hence, we knocked down MAP4K3 under nutrient replete CM conditions to examine its role in neuronal autophagy regulation. Map4k3 knockdown in GFP-LC3 primary cortical neurons yielded marked induction of autophagy at levels comparable to nutrient deprivation (Figure 2.9). To assure that Map4k3 knock-down resulted in autophagy pathway progression, we performed LC3 immunoblotting analysis on primary neurons transfected with Map4k3 shRNA or control scrambled shRNA, confirmed successful Map4k3 knock-down (Figure 2.8A), and cultured these neurons in the absence or presence of the lysosomal inhibitor ammonium chloride. Characteristic upregulation of autophagic flux was noted for control neurons subjected to nutrient deprivation, and a marked increase in autophagic flux was measured for primary neurons knocked-down

for Map4k3 (Figure 2.10A, B). LC3 Western blot analysis of nutrient replete Neuro2a cells subjected to Map4k3 knock-down similarly resulted in autophagy induction at levels comparable to nutrient deprivation (Figure 2.8B, C), establishing the importance of amino acid sensing pathway regulation for autophagy in neurons.

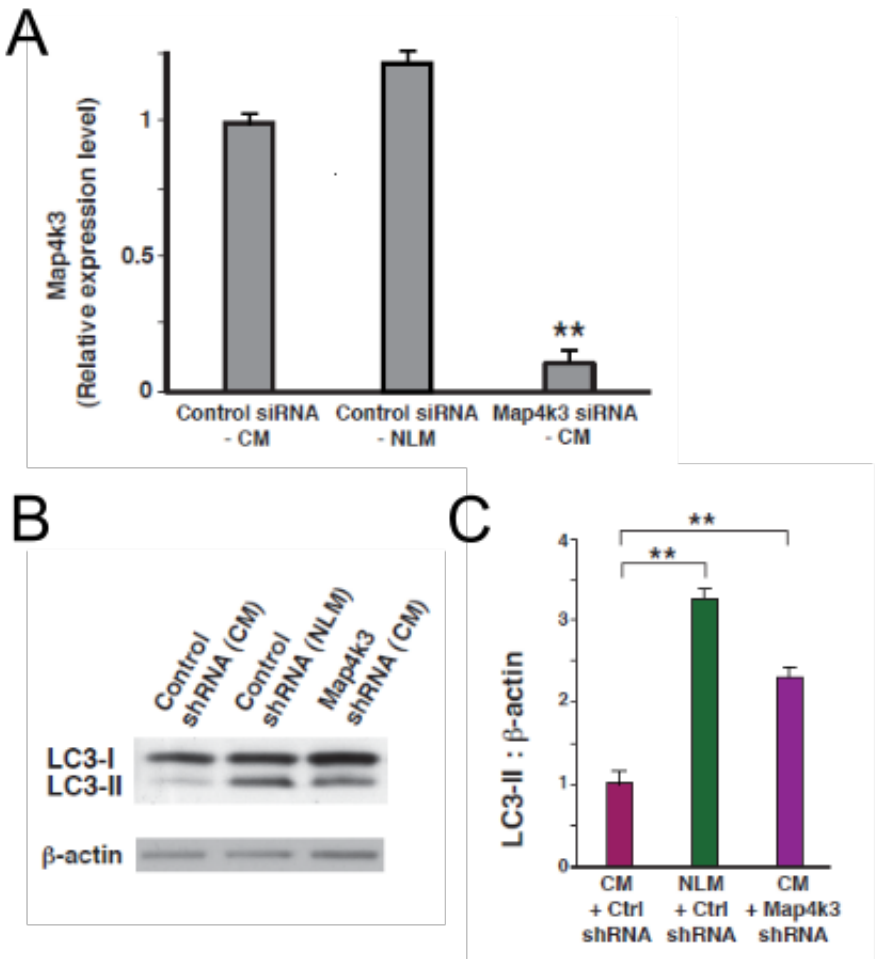

Figure 2.8. Map4k3 knock-down promotes productive neuronal autophagy. **(A)** RT-PCR analysis of Neuro2a cells transfected with the indicated shRNAs, under specified culture conditions (mean + s.e.m., n = 3 independent experiments). **(B)** LC3 immunoblot of Neuro2a cells transfected with the indicated shRNAs, under specified culture conditions. **(C)** Densitometry analysis of LC3 immunoblotting shown in (B). NLM yields a significant increase in LC3-II (to actin), and Map4k3 shRNA knock-down of CM-cultured Neuro2a cells yields a significant increase in LC3-II levels (mean + s.e.m., n = 3 independent experiments). **P < .01; ANOVA with post-hoc Tukey test.

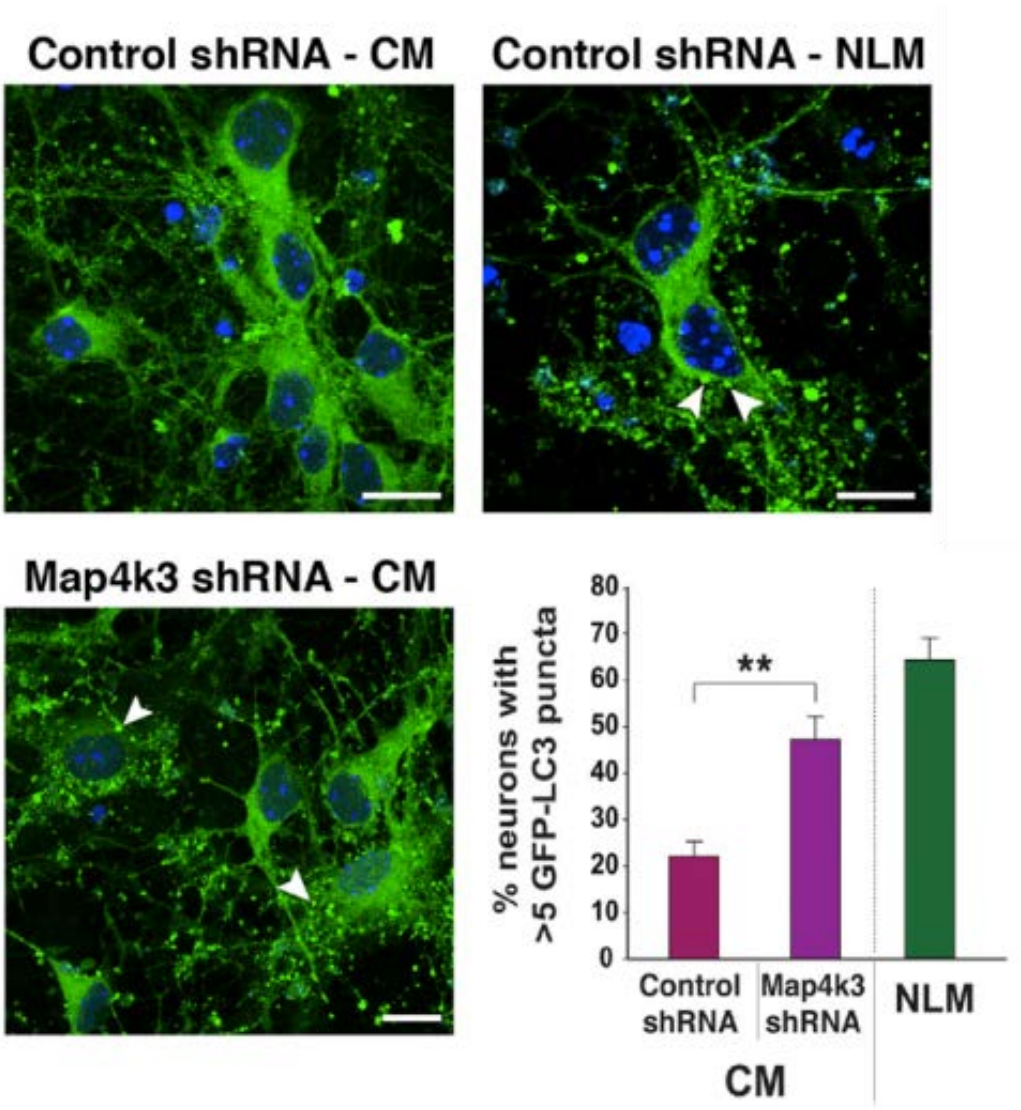

Figure 2.9. Map4k3 knock-down promotes productive neuronal autophagy. GFP-LC3 primary cortical neurons cultured in CM transfected with Map4k3 shRNA exhibit prominent puncta formation (arrowheads), comparable to NLM treatment. Quantification of GFP-LC3 puncta counts/neuron for (F). NLM treatment serves as positive control (mean ± SEM, n = 3 independent experiments). **p < 0.01; ANOVA with post hoc Tukey test. Scale bars, 20 mm.

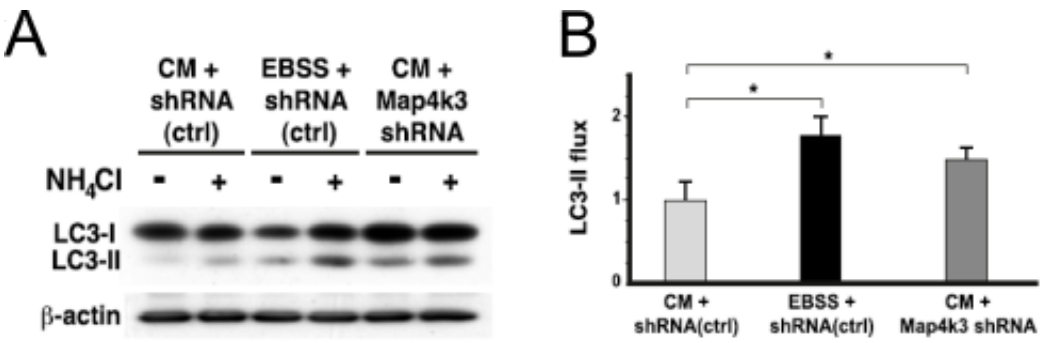

Figure 2.10. Map4k3 knock-down promotes productive neuronal autophagy. **(A)** LC3 immunoblot analysis of primary cortical neurons transfected with control shRNA or Map4k3 shRNA, and cultured under CM or amino acid deprivation (EBSS) conditions, in the absence or presence of the lysosomal inhibitor ammonium chloride. **(B)** Densitometry analysis of LC3 immunoblotting in (A) for autophagic flux quantification (mean ± SEM, n = 3 independent experiments). *p < 0.05, **p < 0.01; ANOVA with post hoc Tukey test.

Discussion

Pathways of nutrient sensing and metabolic regulation have emerged as powerful determinants of lifespan and healthspan in a wide range of model organisms (Lopez-Otin et al., 2013). Hence, it comes as no surprise that the genes comprising these pathways are among the most highly conserved genes found in multicellular organisms. The mTOR signaling pathway is especially well conserved, owing to its central role in the integration of cellular homeostasis, and it is the activation state of the mTOR complexes, mTORC1 and mTORC2, that primarily determine the metabolic disposition of the cell. The mTORC1 complex is principally responsible for dictating whether the cell is in an anabolic or catabolic state, and directly regulates energy metabolism, protein synthesis, lipid synthesis, and the autophagy-lysosome pathway (Laplante and Sabatini, 2012). Of the various inputs to the mTORC1 complex, a deficiency of amino acids can outweigh pro-growth signals coming from mitogen or hormone responsive pathways, resulting in mTORC1 inhibition (Smith et al., 2005). Until recently, components of this amino acid sensing pathway were ill-defined, but over the last decade, the principal factors involved in transmission of amino acid satiety to the mTORC1 complex have been delineated, and include a family of highly conserved Ras-related GTP-binding proteins, known collectively as the Ragulator complex, and a set of five proteins, LAMTOR 1, 2, 3, 4 and 5, that anchor the mTORC1 complex at the lysosome (Bar-Peled et al., 2012; Jewell et al., 2013; Kim et al., 2008a; Yan and Lamb, 2012). Here, we demonstrate that a highly conserved miRNA, *let-7*, regulates the expression and activity of the genes that encode these and other components of the amino acid sensing pathway, thereby establishing *let-7* as a key node in the mTORC1 regulatory circuit.

To define regulatory factors that control autophagy activity in the CNS, we developed a nutrient deprivation protocol in which primary cortical neurons exposed to nutrient-limited media (NLM) were found to undergo autophagy induction in a mTOR and insulin signaling pathway dependent manner (Young et al., 2009). When we interrogated the transcriptomes of primary neurons subjected to NLM treatment, we noted that multiple members of the *let-7* family exhibited marked up-regulation. We then confirmed that *let-7* is sufficient for neuronal autophagy induction in primary neurons transfected with *let-7* mimic.

A recurrent theme in miRNA regulation is the observation that an individual miRNA typically achieves a biological effect by targeting multiple genes along a pathway (Small and Olson, 2011). Our analysis of amino acid sensing pathway component genes revealed evidence for *let-7* modulation of virtually all the genes that we examined. Indeed, we found *let-7* seed site matches in 13 of 14 amino acid sensing pathway genes, and upon direct evaluation of *let-7* repression of a luciferase reporter linked to these putative target sites, we documented significant reductions in luciferase activity for 11 of 13 tested gene sequences, with strong trends evident for the remaining two genes. Mutation of the seed sites for four target sequences abrogated *let-7* repression in this assay. Moreover, we found that a majority of amino acid sensing pathway genes exhibit significant expression reductions in primary neurons infected with *let-7* expressing lentivirus. In these studies, we aimed for modest levels of *let-7* over-expression, with increases of only 20% - 50%, which corresponds closely to physiological *let-7* induction noted upon nutrient deprivation or amino acid starvation. Furthermore, we confirmed that *let-7* regulation of target gene expression occurs at the protein level by performing Western blot analysis on anti *let-*

7-treated neuronal cells. Hence, multiple independent assays corroborate *let-7* regulation of amino acid sensing pathway gene expression.

When we considered the seed site sequences of *let-7* target genes on the amino acid sensing pathway, we noted that seed site sequences within Map4K3 are conserved down to zebrafish or frog. This degree of conservation led us to test if knock-down of Map4K3 would be sufficient to induce neuronal autophagy, and we found that Map4k3 knock-down could promote significant autophagy activation in neurons. While these autophagy pathway effects are consistent with autophagy activation upon Slc1a5 knock-down in non-neuronal cells and autophagy repression by a constitutively active RagA mutant in *Drosophila* and in neonatal mice (Efeyan et al., 2013; Kim et al., 2008a; Nicklin et al., 2009), our results are the first to demonstrate the physiological relevance of amino acid sensing pathway regulation for autophagy modulation in the CNS.

Our discovery of amino acid sensing pathway gene regulation by *let-7* reinforces an emerging view of *let-7* as a predominant regulator of the mTORC1 complex. In a study that examined the regulation of glucose metabolism, *let-7* suppressed the expression of genes encoding components of the insulin signaling pathway in muscle (Zhu et al., 2011). For both the insulin signaling pathway in muscle and the amino acid sensing pathway in neurons, *let-7* regulation yields only modest reductions in expression for individual target genes. Hence, for metabolic pathways, coordinate down-regulation of multiple genes lying on the same pathway likely represents a powerful strategy for achieving a desired metabolic outcome, since network components are often wired into feedback circuit loops. Furthermore, if *let-7* does dictate activity status for the amino acid sensing pathway and the insulin

signaling pathway, then this would facilitate consistency of inputs to the mTORC1 complex through a single master genetic switch, increasing the rapidity and efficiency of mTORC1 signal integration. To establish that *let-7* is acting upstream of mTORC1 to mediate its autophagy regulatory effects, we documented that *let-7* induction of autophagy in neurons can be markedly blunted by co-expression of the constitutively active Rheb-Q64L mutant, which promotes mTORC1 complex activation (Inoki et al., 2003a). As Rag GTPases, which are targeted by *let-7*, were recently found to regulate the mTORC1 complex in response to both glucose and amino acid status (Efeyan et al., 2013), a requirement for *let-7* to permit autophagy induction in response to either glucose deprivation or amino acid starvation is consistent with these recent findings. Indeed, our results, together with studies of *let-7* regulation of the insulin signaling pathway (Zhu et al., 2011), strongly suggest that *let-7* plays a central role in nutrient homeostasis. A complete understanding of this regulatory circuit, including the pathway by which nutrient stress promotes *let-7* activation, will be an important goal for future studies. In light of our results demonstrating *let-7* activation of autophagy, the mechanistic basis of other *let-7* effects also deserve consideration, including *let-7*'s established role as a tumor suppressor (Johnson et al., 2005; Mayr et al., 2007).

One final question worthy of consideration is this: Why would amino acid status serve as a potent signal for autophagy regulation in the CNS? Glutamine and leucine are neutral amino acids subject to uptake by a variety of amino acid transporters in neurons, including the broad specificity uncharged (0) amino acid (B^0AT) family (Zaia and Reimer, 2009). B^0AT3 is a neutral amino acid transporter with a very high affinity for leucine, and localizes to synaptic regions where uptake of

leucine becomes maximal during periods of intense neuronal activity (Zaia and Reimer, 2009). Hence, as full activation of the amino acid sensing pathway occurs when leucine is exchanged for glutamine, which is produced from glutamate and is thus highly abundant in the CNS (McGale et al., 1977), synaptic and metabolic processes may converge in neurons to dictate autophagy pathway levels via mTORC1 activation state, downstream of neutral amino acid inputs. Consequently, *let-7* suppression of amino acid sensing pathway components in neurons could be highlighting synaptic-metabolic crosstalk at work in the neuronal milieu. Indeed, recent studies have shown that glutamine synthetase potently inhibits autophagy by driving the production of glutamine, which prevents the mTORC1 complex from localizing to lysosomes (van der Vos et al., 2012), where its activation by the Ragulator and LAMTOR complexes occurs (Bar-Peled et al., 2012; Sancak et al., 2010). In addition to being coupled to glutamine efflux, synaptic regulation of leucine transporter action may compete with glutamine synthetase to dictate mTORC1 activation state by favoring leucyl-tRNA synthetase activation of mTORC1 via Ragulator and LAMTOR complexes (Han et al., 2012). Delineation of *let-7* targeting of the amino acid sensing pathway has thus uncovered a robust regulatory network that could be amenable to manipulation for therapeutic benefit in diseases affecting both the CNS and peripheral tissues.

Acknowledgements

Chapter 2 is an adaptation of a published manuscript. The full citation is: Dubinsky, A.N., Dastidar, S.G., Hsu, C.L., Zahra, R., Djakovic, S.N., Duarte, S., Esau, C.C., Spencer, B., Ashe, T.D., Fischer, K.M., MacKenna, D.A., Sopher, B.L., Masliah, E., Gaasterland, T., Chau, B.N., Pereira de Almeida, L., Morrison, B.E., and La Spada, A.R. (2014). Let-7 coordinately suppresses components of the amino acid sensing pathway to repress mTORC1 and induce autophagy. Cell metabolism 20, 626-638. The dissertation author was a co-first author of this work.

The authors of the paper would like to thank J.E. Young, T. Bammler, R.P. Beyer, E. Lopez, and S. Mayo for technical assistance. We are grateful to T. Johansen for the gift of the mCherry-GFP-LC3 plasmid, and Z. Yue for providing the GFP-LC3 transgenic mice, with permission from N. Mizushima. This work was supported by grants from the N.I.H. (R01 AG03382 and R01 EY014997 to A.R.L.; T32 AG000216 to A.N.D.; and T32 GM008666 to C.L.H.), and from the Portuguese Foundation for Science and Technology (SFRH/BPD/87552/2012 to S.D. and E-Rare4/0003/2012 to L.P.A.).

CHAPTER 3.

MAP4K3 regulates autophagy induction via phosphorylation of TFEB

Abstract

Autophagy is the major cellular pathway by which macromolecules and organelles are degraded, and is tightly regulated based upon nutrient availability and cell stress. In this paper, we identify MAP4K3 as a critical negative regulator of autophagy through the phosphorylation of transcription factor EB (TFEB). In the presence of amino acids, activated MAP4K3 phosphorylates TFEB at serine 3. This preliminary phosphorylation step is necessary for subsequent mTORC1 phosphorylation of TFEB at serine 211 and sequestration in the cytoplasm by 14-3-3 binding. Loss of MAP4K3 leads to increased TFEB nuclear localization, transcription of TFEB-regulated lysosomal genes, and autophagy induction. The phosphorylation of TFEB at serine 3 is crucial for its interaction with the Rag GTPases and mTORC1 at the lysosome, as well as phosphorylation at serine 211. Our work reveals an exciting novel role for MAP4K3, and provides new insight into the intricate regulation necessary for tight control of autophagy regulation through TFEB.

Introduction

Autophagy is a cellular catabolic pathway necessary for maintaining cellular homeostasis and quality control in response to nutrient availability and cell stress (Shintani and Klionsky, 2004). Autophagy is negatively regulated by the mammalian target of rapamycin complex 1 (mTORC1), a component of the mTOR kinase signaling pathway that coordinates metabolic information, growth factor signaling, and nutrient abundance with cell growth and division (Dazert and Hall, 2011; Laplante and Sabatini, 2012; Ma and Blenis, 2009).

mTORC1 is comprised of the catalytic mTOR subunit, mLST8, DEPTOR, the Tti1–Tel2 complex, Raptor, and PRAS40. In response to amino acid stimulation, mTORC1 is recruited to the cytoplasmic surface of lysosomes via a physical interaction between Raptor and the Rag GTPases, which function as heterodimers wherein the active complex consists of GTP-bound RagA or B complexed with GDP-bound RagC or D (Gao and Kaiser, 2006; Sekiguchi et al., 2001). Importantly, amino acids trigger the GTP loading of RagA/B proteins, thus promoting binding to Raptor and assembly of an activated mTORC1 complex (Kim et al., 2008a; Sancak et al., 2008). In the absence of amino acids, the Rags adopt an inactive conformation (GDP-bound RagA/B and GTP-bound RagC/D), and mTORC1 is inactivated and shuttled back to the cytosol. Bringing mTOR to lysosomes is critical for the activation of its kinase activity by Rheb, a lysosome-enriched GTPase that is regulated via TSC2 by growth factor signaling and energy abundance (Inoki et al., 2003a).

mTORC1 directly represses autophagy by phosphorylating and inhibiting the activity of ULK1/2, members of the Atg family of proteins involved in the earliest step of autophagy induction (Hosokawa et al., 2009a; Hosokawa et al., 2009b). mTORC1

further regulates autophagy by modulating the activity of transcription factor EB (TFEB) (Martina et al., 2012; Roczniak-Ferguson et al., 2012; Settembre et al., 2012). TFEB is a member of the basic helix-loop-helix leucine zipper family of transcription factors that recognizes a 10–base pair motif (GTCACGTGAC) enriched in the promoter regions of numerous lysosomal genes (Sardiello et al., 2009). Activation of TFEB induces expression of genes associated with lysosomal biogenesis and function, and TFEB also stimulates the expression of genes necessary for autophagosome formation, fusion of autophagosomes with lysosomes, and lysosome-mediated degradation of the autophagosomal content (Palmieri et al., 2011; Settembre et al., 2011).

Under nutrient-rich conditions, TFEB interacts with active Rag GTPases, which promote recruitment of TFEB to the lysosomal surface (Martina and Puertollano, 2013). This facilitates mTORC1 phosphorylation of TFEB on several sites, including serine 211 (Ser211) (Martina et al., 2012; Roczniak-Ferguson et al., 2012; Settembre et al., 2012). Phosphorylation of Ser211 creates a binding site for 14-3-3, a cytosolic chaperone that keeps TFEB sequestered in the cytosol. In contrast, under starvation conditions, mTORC1 is inactivated, permitting the TFEB/14-3-3 complex to dissociate, and enabling TFEB to translocate to the nucleus, where it stimulates the expression of its target genes, thus leading to lysosomal biogenesis, increased lysosomal degradation, and autophagy induction (Martina et al., 2012; Roczniak-Ferguson et al., 2012). Therefore, recruitment of TFEB to lysosomes is critical for the proper negative regulation of this transcription factor.

MAP4K3 (also known as germinal center-like kinase) is a member of the Ste20 family of protein kinases that regulates the amino acid sensing pathway

upstream of mTORC1, and is required for maximal mTORC1-dependent S6K/4E-BP1 phosphorylation and regulation of cell growth (Findlay et al., 2007). Knockdown of MAP4K3 in neurons is sufficient to induce autophagy (Dubinsky et al., 2014), but the basis for this MAP4K3-mediated autophagy repression was not known. Here, we demonstrate that MAP4K3 knock-out results in a marked upregulation of TFEB-regulated genes and productive induction of autophagy, and that MAP4K3 absence prevents TFEB association with the mTORC1 regulatory complex at the lysosome. We further find that MAP4K3 directly phosphorylates TFEB at a novel amino-terminal site, and that MAP4K3 phosphorylation of TFEB is required for both the interaction of TFEB with the mTORC1 regulatory complex and for inhibitory phosphorylation of TFEB by mTORC1.

Results

MAP4K3 knock-out cell lines display increased autophagy induction and flux

Although it was previously shown that knockdown of MAP4K3 is sufficient to induce autophagy (Dubinsky et al., 2014), we wished to study the effects of complete MAP4K3 knockout (k.o.) on autophagy regulation. To obtain MAP4K3 k.o. cell lines, we performed CRISPR-Cas9 genome editing with guide sequences targeting two different exon sequences of MAP4K3, resulting in two distinct clones (M1 and M4) with frameshift mutations at either of the two targeted sites. We confirmed complete loss of MAP4K3 protein expression in these two cell lines by immunoblot analysis (Figure 3.1).

Analysis of autophagy activation revealed increased autophagy induction in MAP4K3 k.o. cells, based upon immunostaining quantification of autophagosome formation and LC3 immunoblot measurement of autophagy flux (Figure 3.2 & 3.3). Indeed, MAP4K3 k.o. cells cultured in nutrient rich complete media (CM) displayed increased autophagy activation, comparable to levels seen in starved WT cells. When we analyzed LC3-II levels after treatment with ammonium chloride, a lysosomal inhibitor, we observed a further increase in LC3-II levels in MAP4K3 k.o. cells, indicating an increase in autophagy initiation, rather than a block in autophagosome degradation. To directly assess autophagy flux, we also used the tandem-tagged mCherry-EGFP–LC3 vector, and noted that upon autophagosome formation, LC3 is incorporated into autophagosome membranes, producing yellow puncta in merged images. When autophagosomes fuse with lysosomes, vesicle pH becomes acidic, quenching the EGFP signal so that only mCherry fluorescence remains detectable. This acidification-dependent change in fluorescence emission can be used to monitor

autophagosome maturation. When we monitored autophagic puncta dynamics in MAP4K3 k.o. cells, we observed a marked increase in the number of autophagosomes and autolysosomes per cell in MAP4K3 k.o. cells, when compared to WT control cells (Figure 3.4).

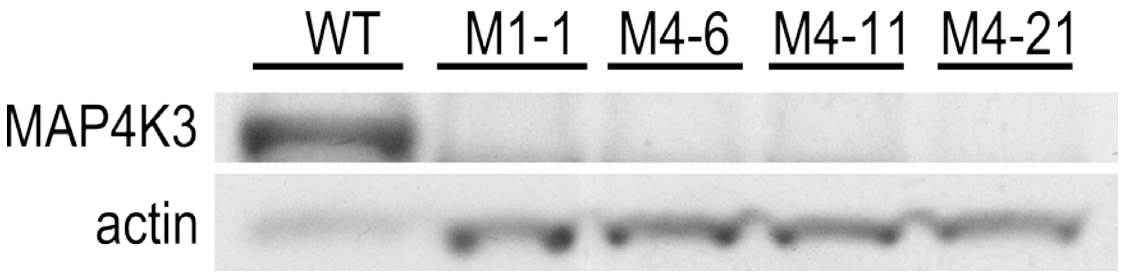

Figure 3.1. Validation of MAP4K3 k.o. cells. Wild type HEK 293A and four different MAP4K3 k.o. clones (M1-1, M4-6, M4-11 and M4-21) were immunoblotted for MAP4K3 to validate MAP4K3 k.o. at the protein level.

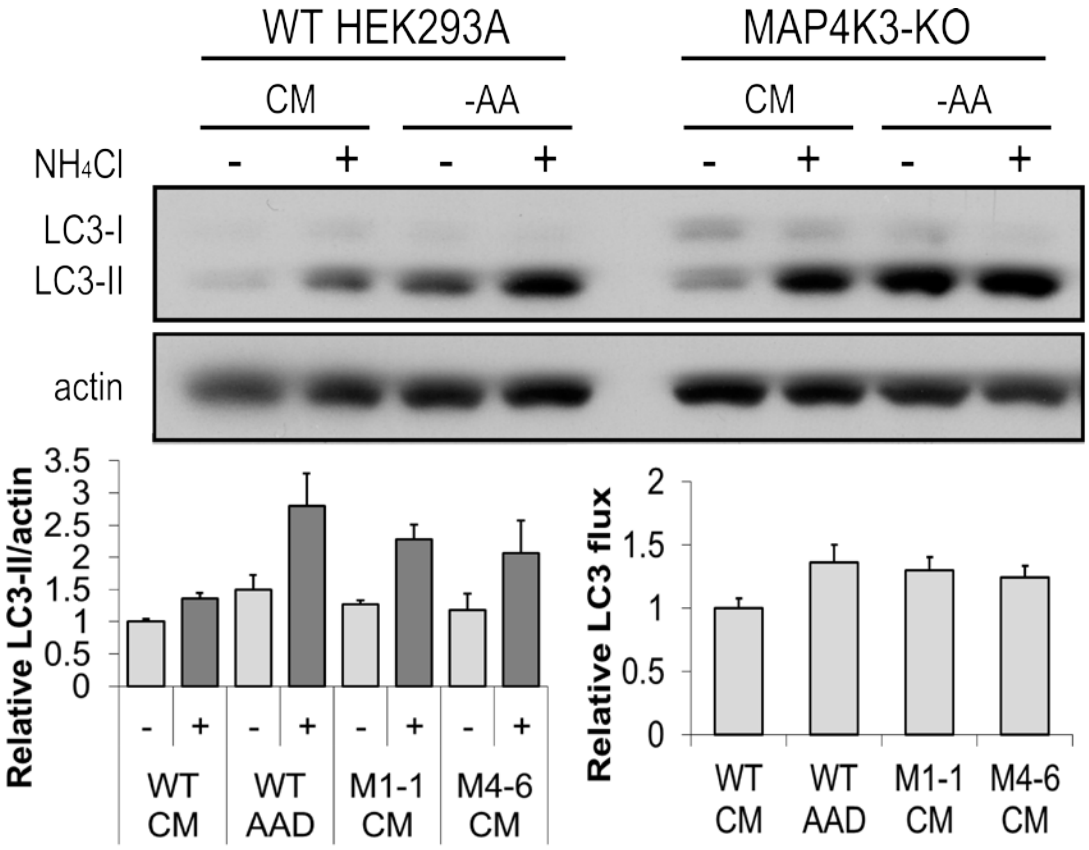

Figure 3.2. Map4k3 knockout promotes autophagy flux. Wild type HEK 293A and MAP4K3 k.o. clone M1-1 were grown in complete media (CM) (DMEM + FBS) or amino acid deprived (EBSS + FBS) conditions, then treated with NH_4Cl to inhibit phagosome-lysosome fusion. Protein lysates were immunoblotted for LC3 and actin. Densitometry analysis was performed of LC3 for autophagic flux quantification.

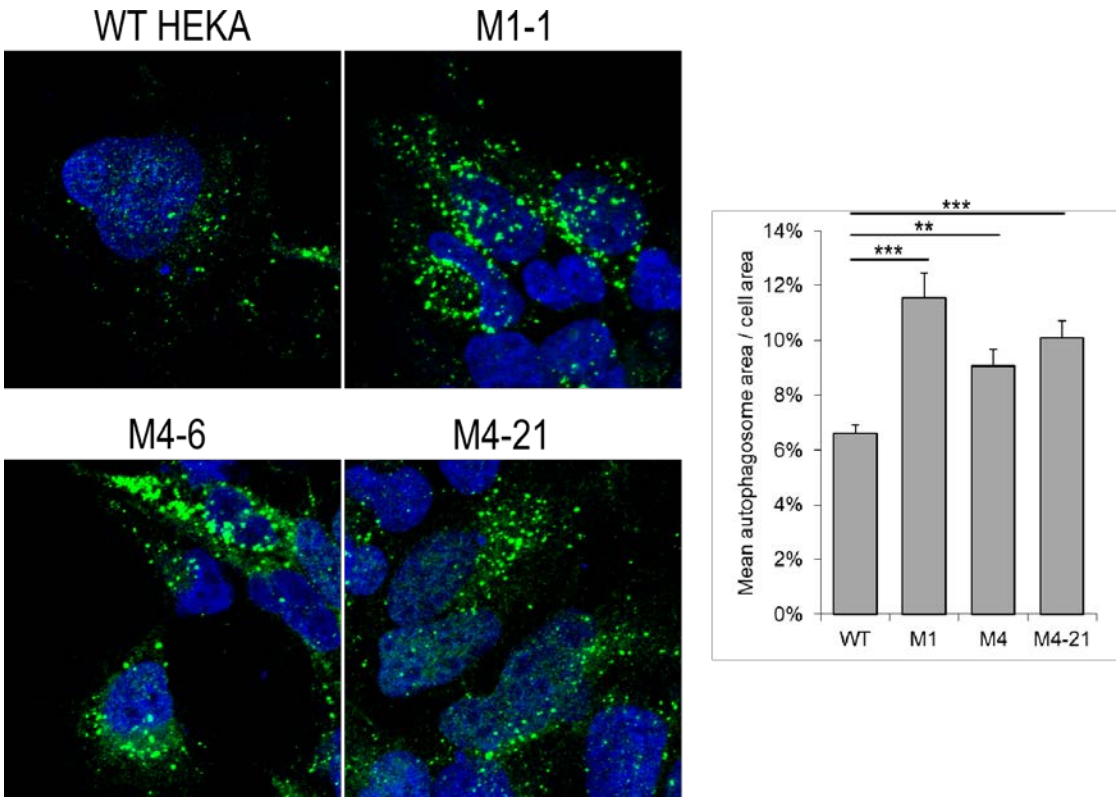

Figure 3.3. MAP4K3 knockout promotes LC3 expression. Wild type HEK293A and MAP4K3 k.o. cells cultured in complete media were fixed, permeabilized with digitonin, and stained for endogenous LC3.

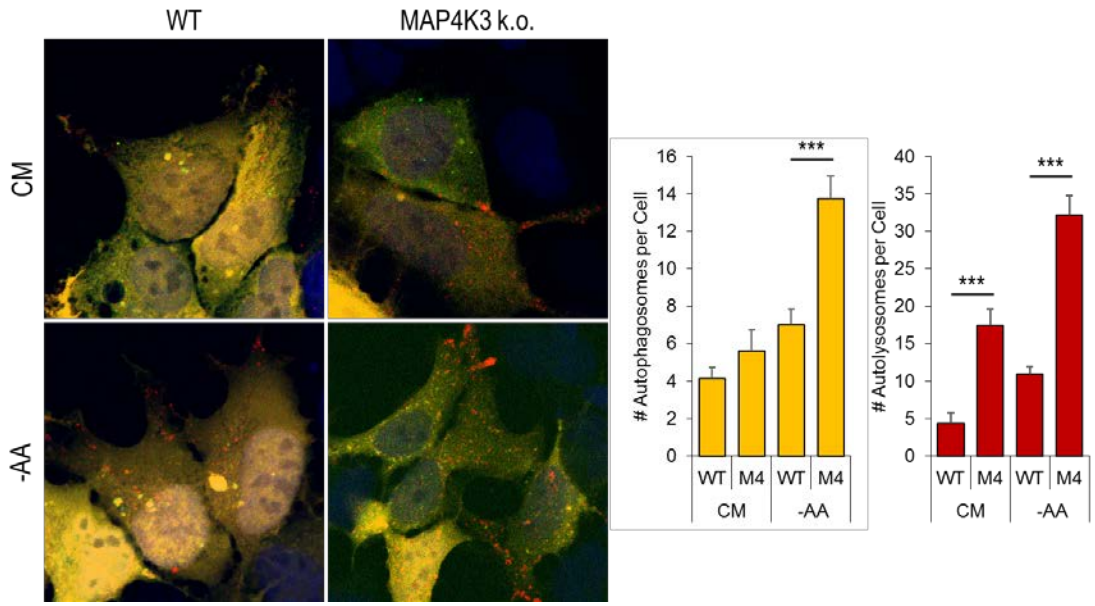

Figure 3.4. MAP4K3 knockout promotes functional autophagy induction. Wild type HEK293A and MAP4K3 k.o. cells cultured in complete media were transfected with mCherry-GFP-LC3 to visualize autophagosomes and autolysosomes.

MAP4K3 knock-out cell lines exhibit increased TFEB nuclear localization and TFEB transcriptional activity, independent of mTORC1 activation state

As TFEB entry into the nucleus is required for transactivation of its target genes, and inhibitory regulation of TFEB by mTORC1 phosphorylation restricts TFEB to the cytosol, we examined the effect of MAP4K3 knock-out on TFEB subcellular localization. MAP4K3 k.o. cells exhibited predominantly nuclear localization of TFEB, regardless of nutrient status (Figure 3.5. To confirm that the difference in TFEB nuclear localization is solely attributable to MAP4K3 k.o., we overexpressed MAP4K3 in MAP4K3 k.o. cells and saw a significant rescue of TFEB localization back to predominantly cytosolic localization (Figure 3.6). The rescue is not complete; this may be attributed to the fact that MAP4K3 induces JNK signaling and caspase-dependent apoptotic cell death when excessively over-expressed.

Consistent with its effect on TFEB nuclear translocation, MAP4K3 k.o. cell lines also displayed significantly higher expression levels of all tested TFEB target genes (Figure 3.7). As MAP4K3 is known to regulate the mTOR signaling pathway (Findlay et al., 2007), we repeated these experiments in the presence of constitutively active Rheb (CA-Rheb) to determine the effect of mTORC1 activation on TFEB transcriptional activity in MAP4K3 k.o. and WT control cell lines. As expected, transfection of CA-Rheb yielded marked repression of TFEB target in WT cells; however, surprisingly, TFEB target gene expression was not repressed in MAP4K3 k.o. cells, but remained at or above the level of expression observed in WT cells at baseline (Figure 3.8). To confirm this finding, we tested whether constitutively active mTOR affects TFEB localization in MAP4K3 k.o. cells. While constitutively active mTOR significantly decreased nuclear localization of TFEB in WT cells treated with

amino acid starvation, constitutively active mTOR only had a minimal effect on starved MAP4K3 k.o. cells (Figure 3.9). To investigate if constitutively active mTOR causes different physiological responses in WT and MAP4K3 k.o. cells, we quantified the number of autophagosomes and autolysosomes produced in both cell types when overexpressing CA-Rheb (Figure in preparation). These results suggest that MAP4K3 regulation of TFEB transactivation may be operating upstream of the mTORC1 complex.

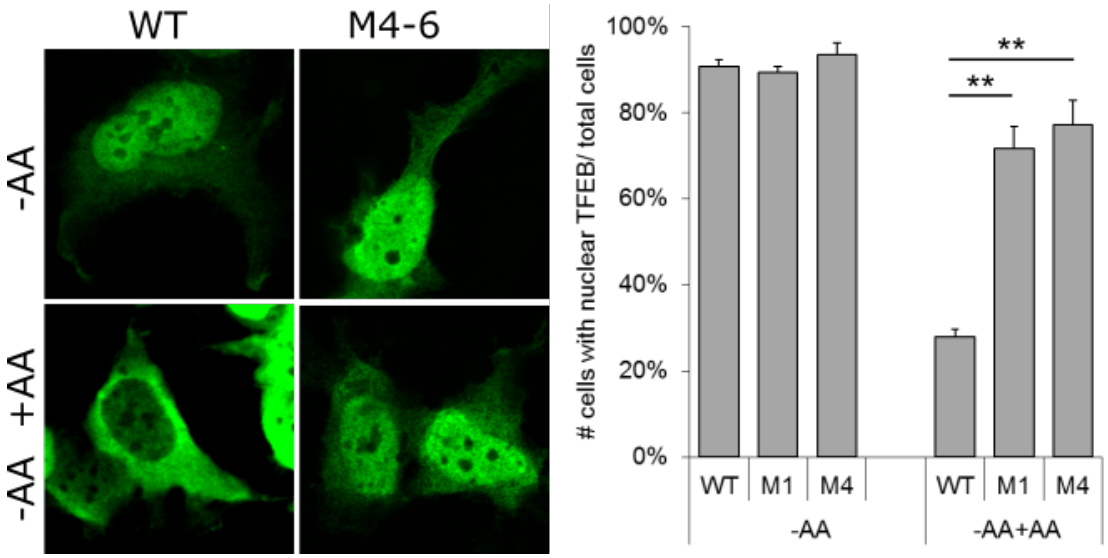

Figure 3.5. MAP4K3 knockout results in increased TFEB nuclear localization. WT and MAP4K3 k.o. cells were transfected with WT-TFEB-FLAG and cultured in complete media and amino acid deprived conditions as indicated. Cells were immunostained with anti-FLAG antibody. Percentages of cells with TFEB predominantly in the nucleus were quantified.

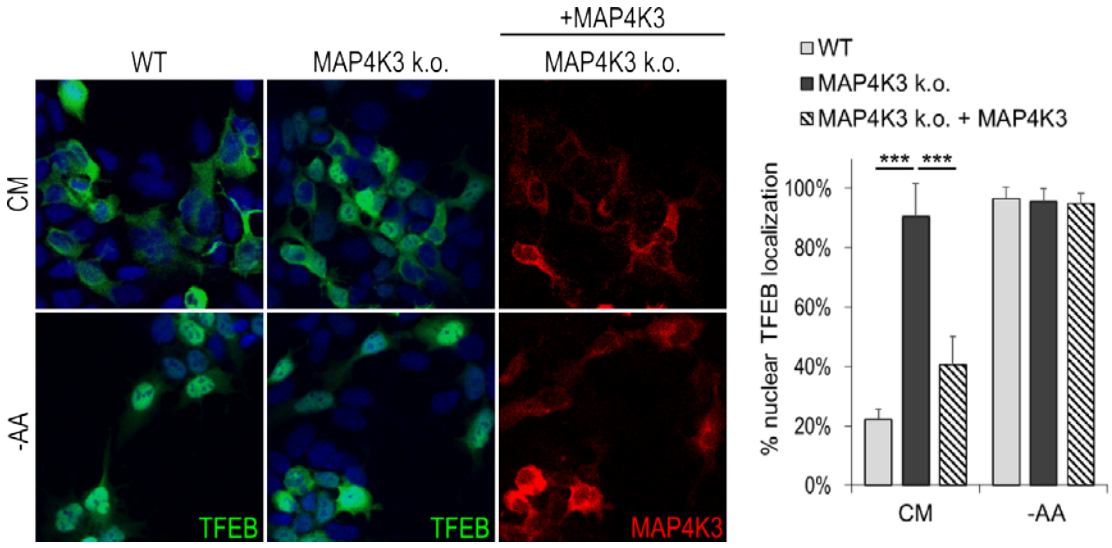

Figure 3.6. Increased TFEB nuclear localization in MAP4K3 knockout cells is rescued by overexpression of MAP4K3. WT and MAP4K3 k.o. cells were transfected with WT-TFEB-FLAG and MAP4K3-mCherry and cultured in complete media and amino acid deprived conditions as indicated. Cells were immunostained with anti-FLAG antibody. Percentages of cells with TFEB predominantly in the nucleus were quantified.

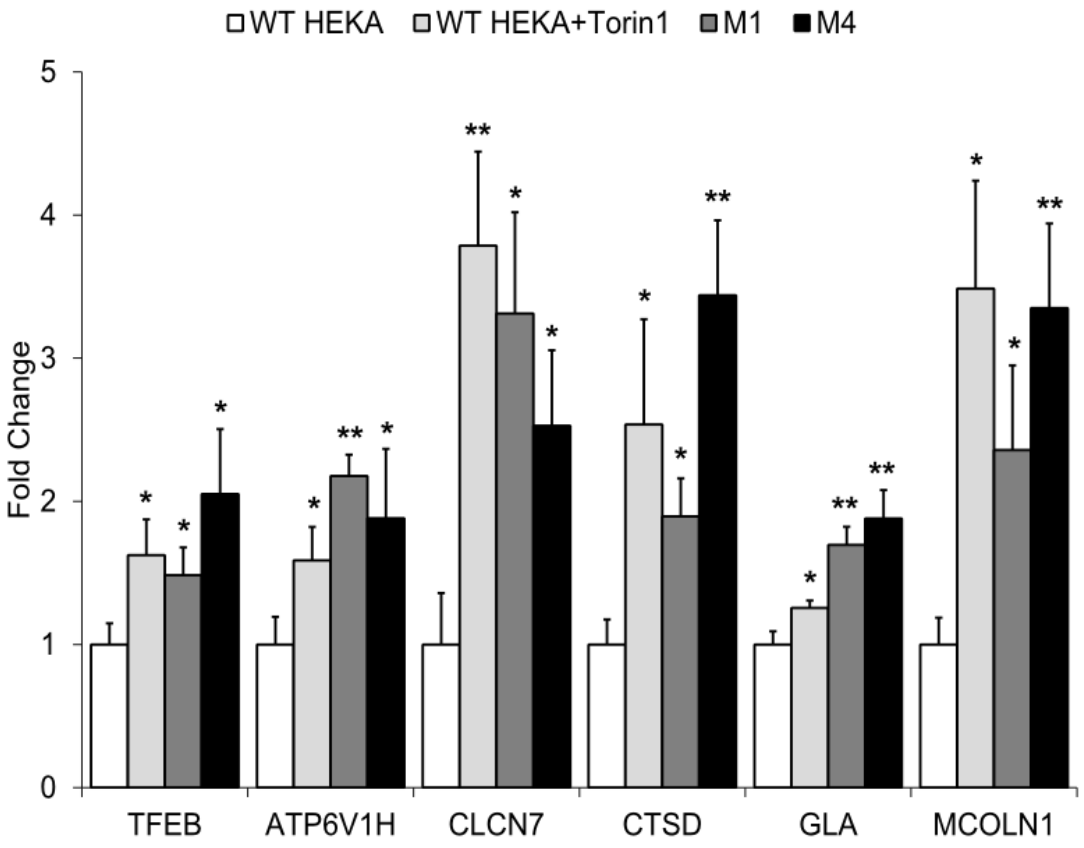

Figure 3.7. MAP4K3 knockout results in increased TFEB transcriptional activity. WT and MAP4K3 k.o. cells were cultured in complete media and treated with Torin1 as indicated. Total RNA was isolated and qRT-PCR was performed for TFEB-regulated genes – TFEB, ATP6V1H, CLCN7, CTSD, CTSF, GLA, and MCOLN1.

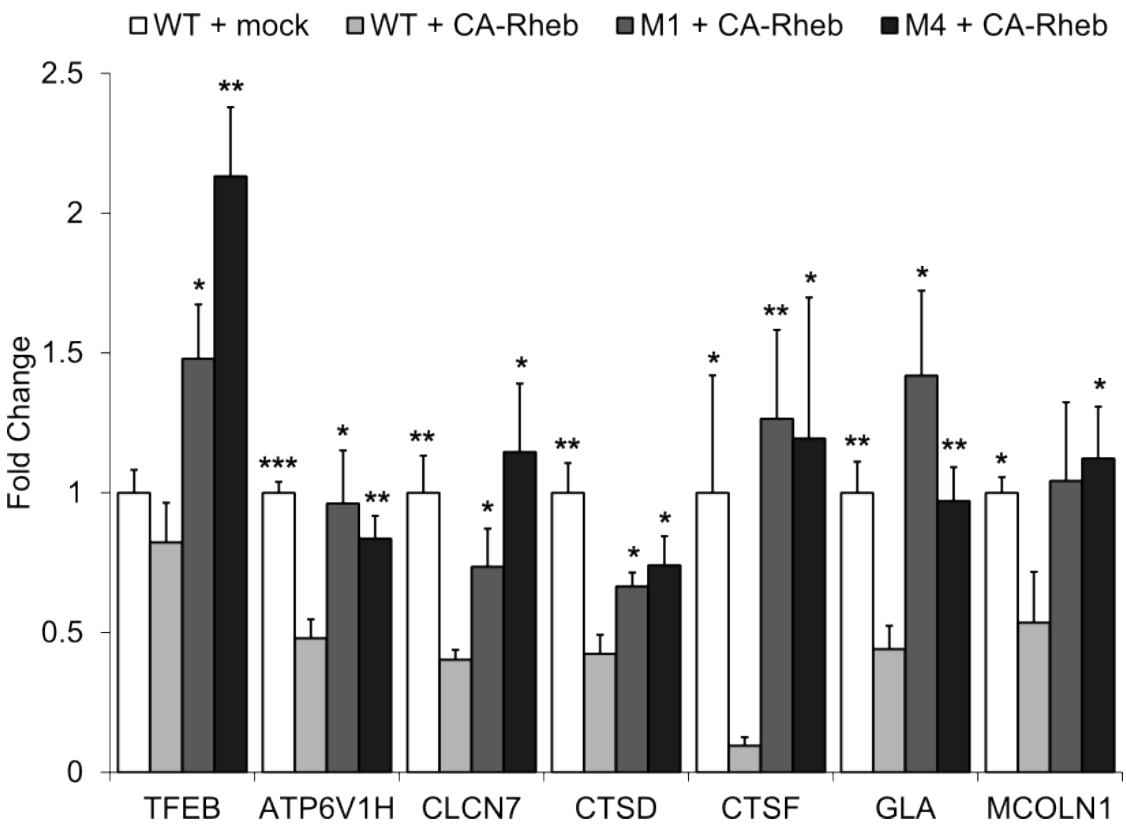

Figure 3.8. MAP4K3 knockout results in increased TFEB transcriptional activity, independent of mTOR activation. WT and MAP4K3 k.o. cells were transfected with constitutively active Rheb for 24 hours. Total RNA was isolated and qRT-PCR was performed for TFEB-regulated genes – TFEB, ATP6V1H, CLCN7, CTSF, and GLA.

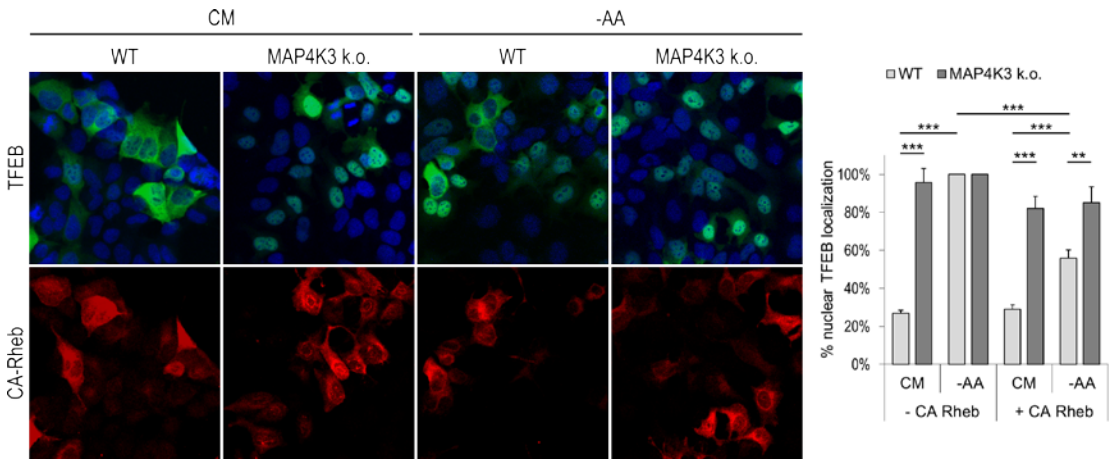

Figure 3.9. MAP4K3 knockout results in increased TFEB nuclear localization, independent of mTOR activation. WT and MAP4K3 k.o. cells were transfected with WT-TFEB-FLAG and constitutively active Rheb-myc and cultured in complete media and amino acid deprived conditions as indicated. Cells were immunostained with anti-FLAG and anti-myc antibody. Percentages of cells with TFEB predominantly in the nucleus were quantified.

MAP4K3 knock-out yields reduces physical interaction of TFEB with mTORC1 and Rag GTPase complex

Retention of TFEB in the cytosol is determined by its phosphorylation status, as phospho-TFEB complexes with 14-3-3, thereby precluding TFEB nuclear entry; whereas dephosphorylated TFEB readily translocates to the nucleus (Roczniak-Ferguson et al., 2012). TFEB interacts with activated Rag GTPases, which promotes recruitment of TFEB to the lysosomal surface, where mTORC1 phosphorylates TFEB on serine 211 to enforce its cytosolic retention and inactivation (Martina and Puertollano, 2013). Previous work has demonstrated that the first 30 amino acids of TFEB are requited for TFEB localization to lysosomes, and documented that mutagenesis of serine 3 and arginine 4 to alanines (S3A/R4A) completely prevents TFEB localization to lysosomes (Martina and Puertollano, 2013). To confirm the importance of the amino-terminal region of TFEB for regulation of its subcellular localization and the specific role of serine 3, we transfected WT HEK293 cells with WT-TFEB-FLAG, and noted interactions of TFEB with Raptor, Rag A, Rag B, and Lamtor1 (Figure 3.10). However, when we transfected WT HEK293 cells with S3A-TFEB-FLAG, or Δ30-TFEB-FLAG, we found that mutation of serine 3 to alanine or deletion of the first 30 amino acids of TFEB prevented its interaction with mTORC1, the Rag GTPases, and the Ragulator complex (Figure 3.10).

The mechanistic basis for serine 3 regulation of TFEB interaction with the mTORC1 complex is yet to be determined. As serine residues are subject to phosphorylation regulation and MAP4K3 is a kinase, we considered the possibility that MAP4K3 regulation of TFEB is occurring through phosphorylation of TFEB. To test this hypothesis, we evaluated the physical interaction of TFEB with mTORC1 and

its associated regulatory proteins in complex with it at the lysosome. While immunoprecipitation of TFEB-FLAG provided evidence for interaction with Raptor, Rag A, and Lamtor1 in WT HEK293 cells, we noted that TFEB-FLAG interaction with these mTORC1 complex components was markedly diminished in the two different MAP4K3 k.o. cell lines (Figure 3.11). Reduced interaction of TFEB-S3A-FLAG was similarly noted in WT HEK293 cells, suggesting that MAP4K3 is required for TFEB interaction with the mTORC1 complex and that mutation of serine 3 to an alanine, which cannot be phosphorylated, also renders TFEB incapable of fully interacting with the mTORC1 complex, highlighting serine 3 as a potential site for MAP4K3 phosphorylation.

Sometimes phenotypes in cell lines derived by CRISPR-Cas9 genome editing stem from an off-target effect. Although our results were obtained in two different MAP4K3 cell lines derived with different guide RNAs, to exclude possible off-target effects, we repeated the TFEB interaction studies in MAP4K3 k.o. cell lines transfected with MAP4K3, and noted that exogenous MAP4K3 expression restored TFEB interaction with Raptor, Rag GTPases, and Lamtor1 in our MAP4K3 k.o. cell lines (Figure 3.12). Furthermore, overexpression of TFEB-S3E, which features a phosphomimetic amino acid substitution of glutamate for serine 3, also partially restored TFEB interaction with these mTORC1 complex components (Figure 3.13). These findings establish a role for MAP4K3 and for serine 3 phosphorylation in the regulation of TFEB interaction with the mTORC1 complex.

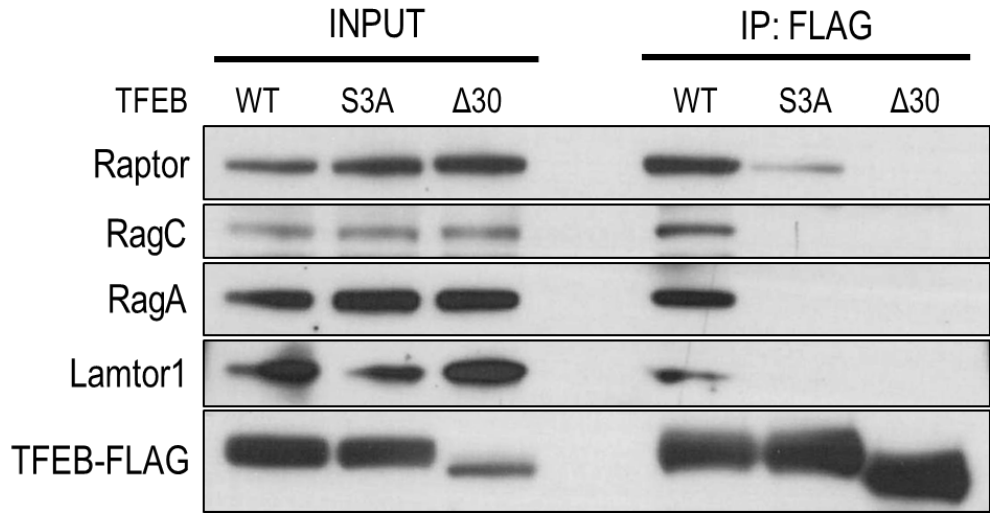

Figure 3.10. TFEB serine 3 is essential for TFEB-mTORC1-Rag GTPase interaction. Wild type HEK 293A cells were transfected with WT-TFEB-FLAG, S3A-TFEB-FLAG, or Δ30-TFEB-FLAG, as indicated. Immunoprecipitation was performed with anti-FLAG antibody, followed by immunoblotting for Raptor, RagA, Lamtor1, and TFEB.

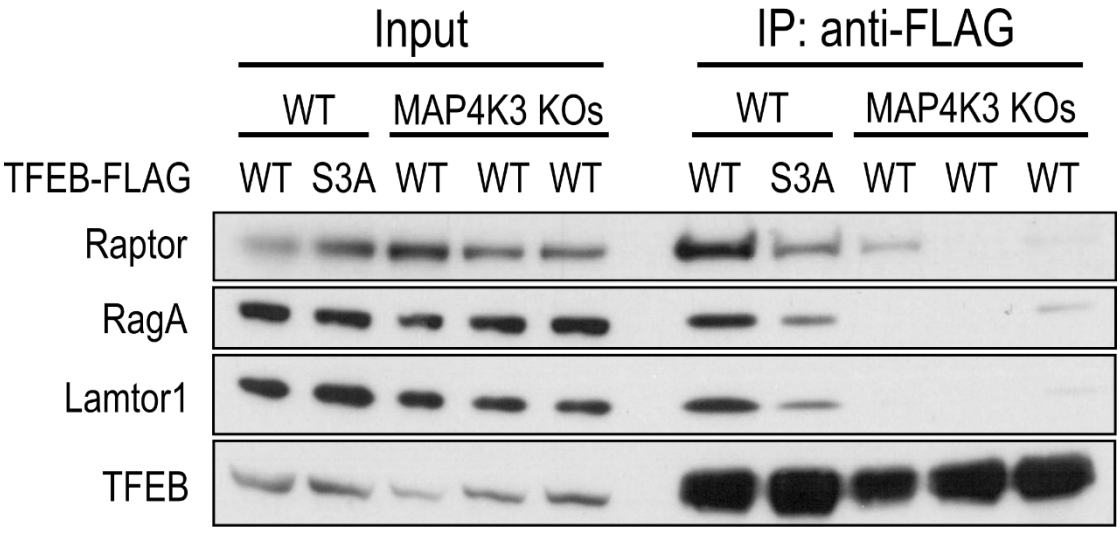

Figure 3.11. MAP4K3 knockout results in reduced TFEB-mTORC1-Rag GTPase interaction, similar to S3A-TFEB. Wild type HEK 293A and MAP4K3 k.o. cells were transfected with WT-TFEB-FLAG or S3A-TFEB-FLAG, as indicated. Immunoprecipitation was performed with anti-FLAG antibody, followed by immunoblotting for Raptor, RagA, Lamtor1, and TFEB.

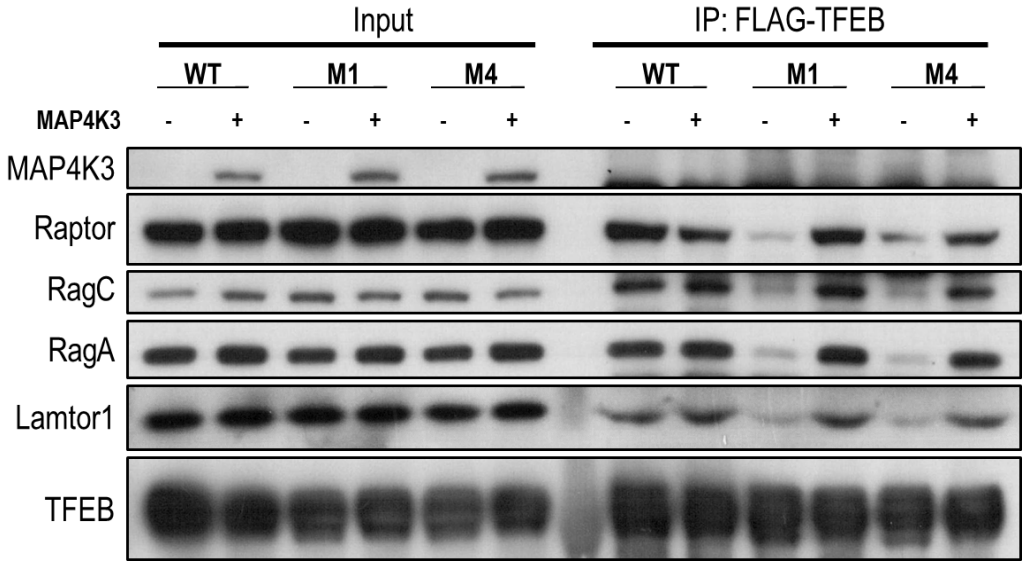

Figure 3.12. TFEB-mTORC1-Rag GTPase interaction in MAP4K3 knockout cells is rescued by MAP4K3 overexpression. Wild type HEK 293A and MAP4K3 k.o. cells were transfected with WT-TFEB-FLAG and MAP4K3 overexpressing constructs, as indicated. Immunoprecipitation was performed with anti-FLAG antibody, followed by immunoblotting for Raptor, RagA, RagC, Lamtor1, and TFEB.

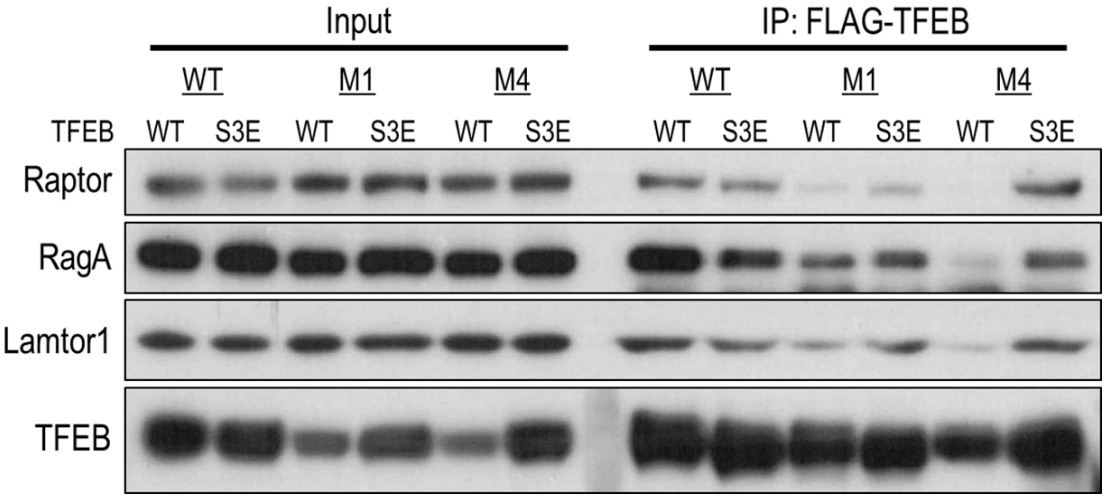

Figure 3.13. TFEB-mTORC1-Rag GTPase interaction in MAP4K3 knockout cells is partially rescued by S3E-TFEB overexpression. Wild type HEK 293A and MAP4K3 k.o. cells were transfected with WT-TFEB-FLAG and S3E-TFEB-FLAG overexpressing constructs, as indicated. Immunoprecipitation was performed with anti-FLAG antibody, followed by immunoblotting for Raptor, RagA, RagC, Lamtor1, and TFEB.

MAP4K3 physically interacts with and phosphorylates TFEB at Serine 3

To determine if MAP4K3 and TFEB interact, we transfected HEK293 cells with either normal MAP4K3 (WT-MAP4K3) or a kinase dead version of MAP4K3 (KD-MAP4K3). When endogenous TFEB was immunoprecipitated and immunoblotted for MAP4K3, we detected a physical interaction between TFEB and MAP4K3, but not between TFEB and a co-transfected negative control protein (HDAC6) (Figure 3.14). Interestingly, the interaction between TFEB and KD-MAP4K3 was significantly stronger than the interaction between TFEB and WT-MAP4K3, suggesting that the kinase activity of MAP4K3 is critical for its interaction with TFEB. To determine if the MAP4K3 – TFEB interaction is direct, we produced *in vitro* translated TFEB protein and performed a pull-down assay with purified FLAG-tagged WT- or KD-MAP4K3, or HDAC6 for negative control. *In vitro* translated WT-TFEB was able to pull down both WT-MAP4K3 and KD-MAP4K3; the pull-down of KD-MAP4K3 was clearly stronger (Figure 3.15). Furthermore, a recombinant GST-TFEB amino-terminal fragment (TFEB: 1-37) was also capable of pulling down WT-MAP4K3 and KD-MAP4K3 equally well (Figure 3.16). These results support a direct interaction between MAP4K3 and TFEB, and indicate that the first 37 amino acids of TFEB are critical for this interaction.

To determine if MAP4K3 can phosphorylate TFEB, we carried out *in vitro* phosphorylation by incubating immunopurified WT-MAP4K3 or KD-MAP4K3 with immunopurified WT-TFEB, S3A-TFEB, or S211A-TFEB in the presence of γ-^{32}P-ATP, and performed two-dimensional phosphopeptide mapping. We did not pursue the use of mass spectrometry, as trypsin digestion of TFEB is predicted to yield a tiny four amino acid N-terminal fragment, which would not be readily detected. A review of the

phosphopeptide maps, revealed a phosphopeptide that was present in the WT-MAP4K3 + WT-TFEB incubation and in the WT-MAP4K3 + S211A-TFEB incubation, but was absent in the WT-MAP4K3 + S3A-TFEB and KD-MAP4K3 + TFEB incubations, for both thermolysin and chymotrypsin digestions (Figure 3.17 and 3.18). Phospho-amino acid analysis (van der Geer and Hunter, 1994) of these peptides confirmed that phosphoserine was specifically decreased in the KD-MAP4K3 + TFEB reaction, in comparison to WT-MAP4K3 + WT-TFEB (Figure 3.19). These results provide compelling evidence that MAP4K3 directly phosphorylates TFEB on the serine 3.

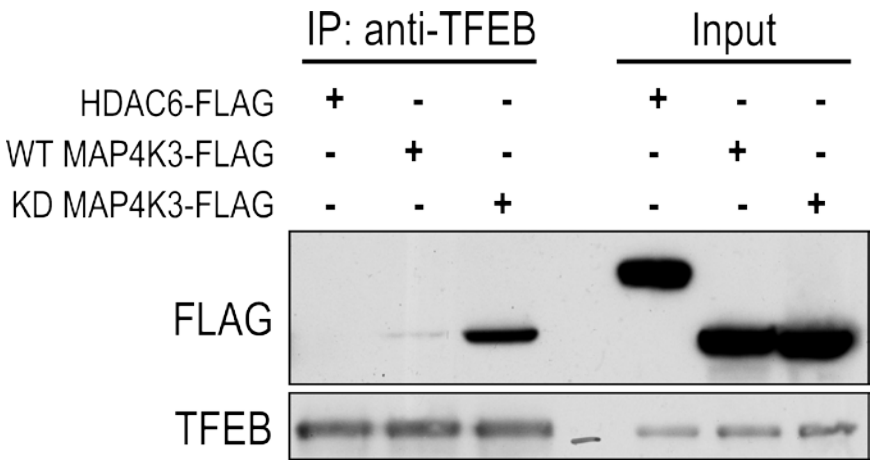

Figure 3.14. MAP4K3 interacts with TFEB. WT HEK293T cells were transfected with HDAC6-FLAG, WT-MAP4K3-FLAG, or kinase dead (KD)-MAP4K3-FLAG. Immunoprecipitation was performed with anti-TFEB antibody, followed by immunoblotting for FLAG and TFEB. HDAC6 was used as negative control.

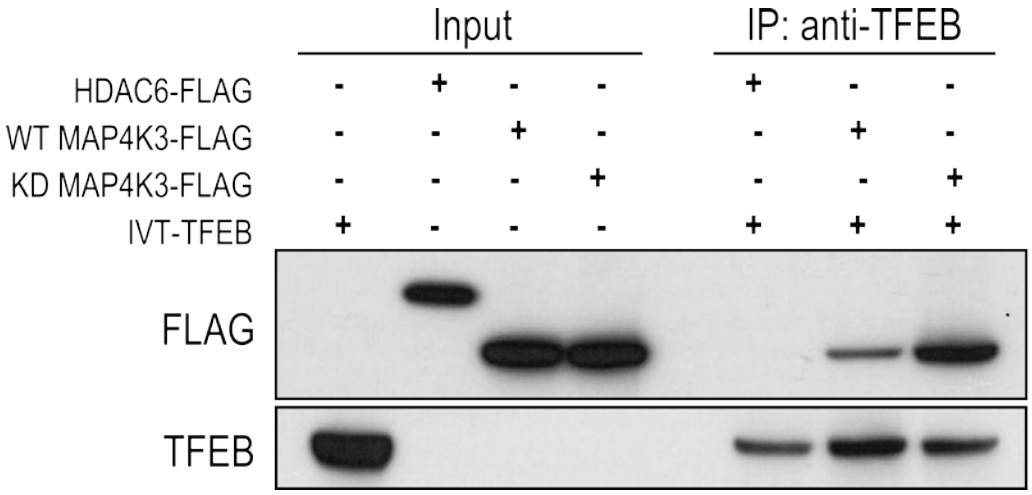

Figure 3.15. MAP4K3 directly interacts with TFEB. WT HEK293T cells were transfected with HDAC6-FLAG, WT-MAP4K3-FLAG, or KD-MAP4K3-FLAG and lysates were immunoprecipitated with anti-FLAG antibody. GST-TFEB protein was in vitro translated using purified HeLa lysates and in vitro pull-down was performed using FLAG-immunoprecipitates.

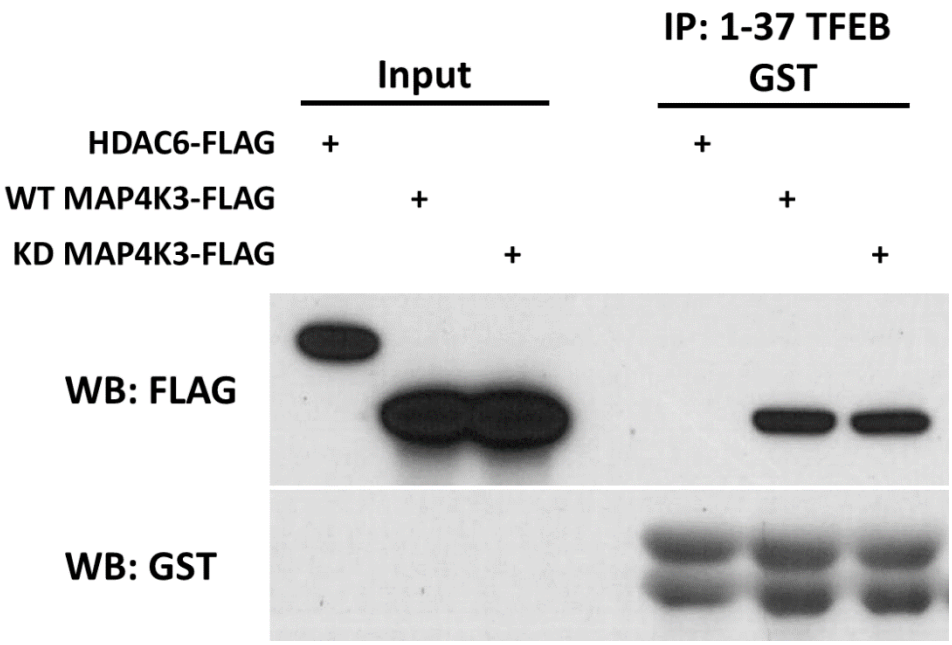

Figure 3.16. MAP4K3 directly interacts with the first 37 amino acids of TFEB. WT HEK293T cells were transfected with HDAC6-FLAG, WT-MAP4K3-FLAG, or KD-MAP4K3-FLAG and lysates were immunoprecipitated with anti-FLAG antibody and eluted with FLAG peptide. Recombinant GST-TFEB protein (aa1-37) was purified from bacteria and immobilized onto GST-beads and in vitro pull-down was performed using eluted FLAG-immunoprecipitates.

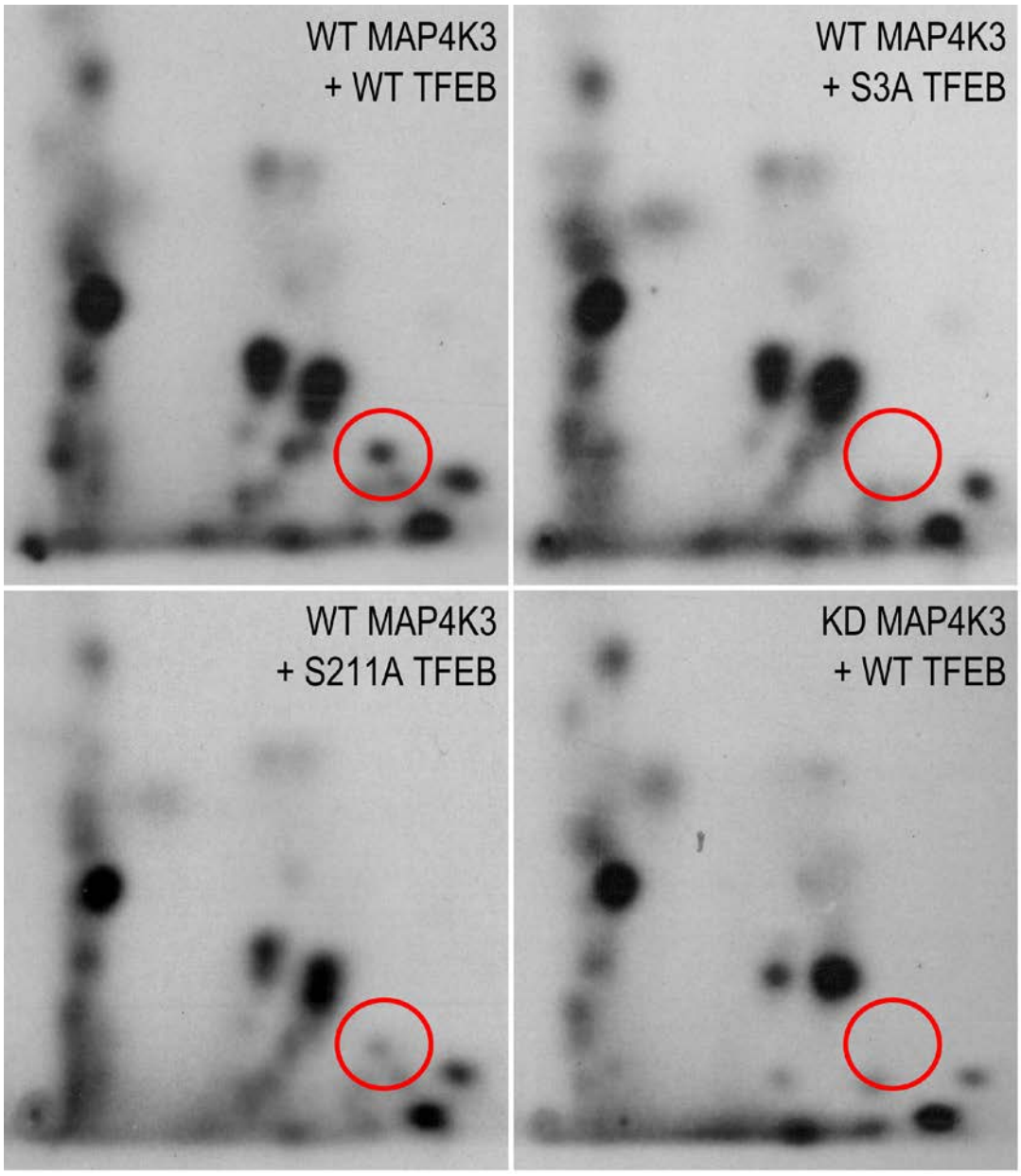

Figure 3.17. MAP4K3 phosphorylates TFEB at serine 3. WT HEK293T cells were transfected with WT-MAP4K3-FLAG, KD-MAP4K3-FLAG, WT-TFEB-FLAG, S3A-TFEB-FLAG, or S211-TFEB-FLAG. Each overexpressed protein was purified by immunoprecipitation using anti-FLAG antibody. In-vitro kinase reaction was performed by mixing MAP4K3 and TFEB proteins, as indicated, with P32-gamma ATP. Phospho-peptide mapping was performed using the thermolysin enzyme and autoradiography was performed to detect phosphorylated peptides on TFEB.

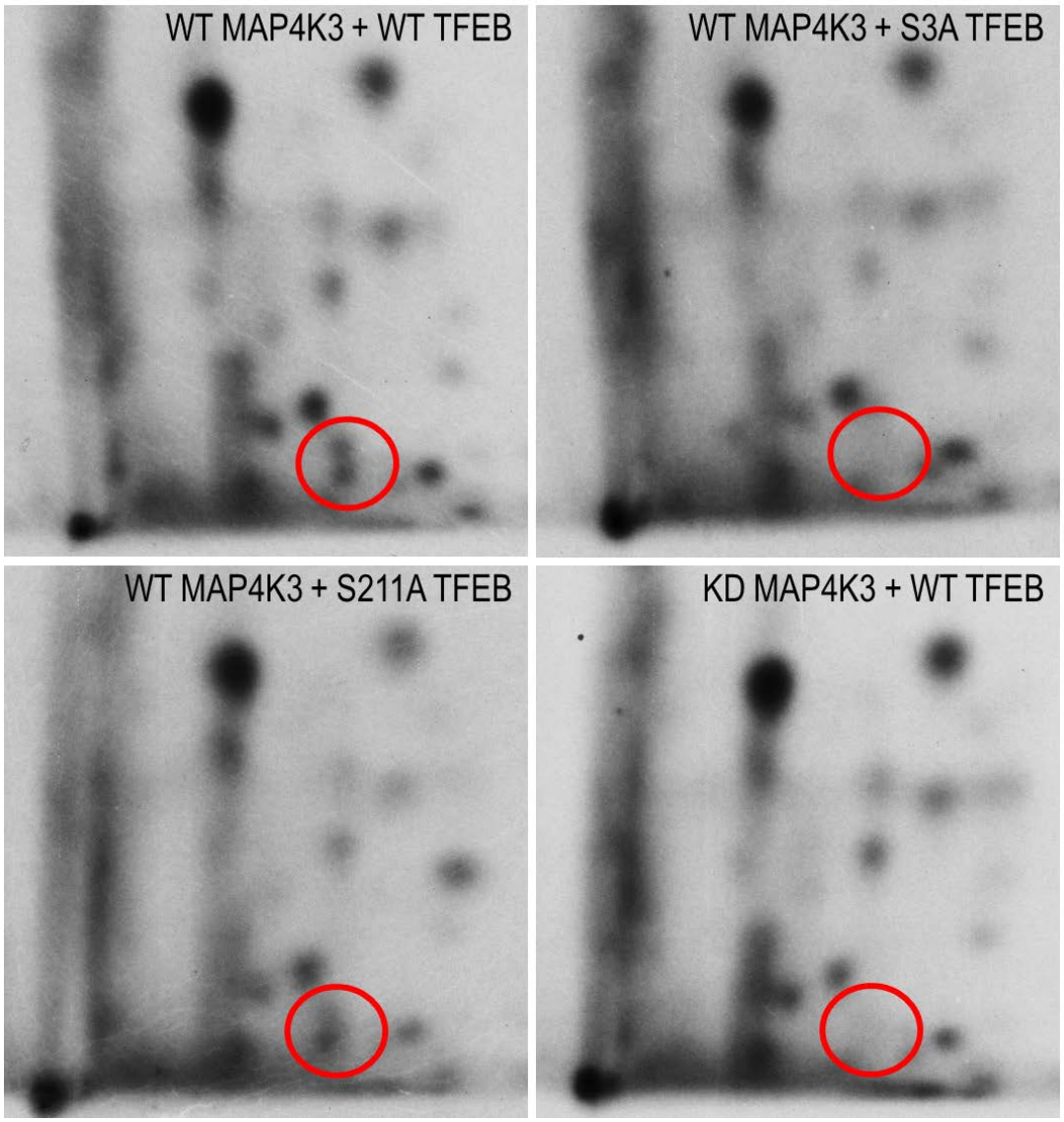

Figure 3.18. MAP4K3 phosphorylates TFEB at serine 3. In-vitro kinase reaction was performed as in Figure 3.17, and phospho-peptide mapping was performed using the trypsin enzyme and autoradiography was performed to detect phosphorylated peptides on TFEB.

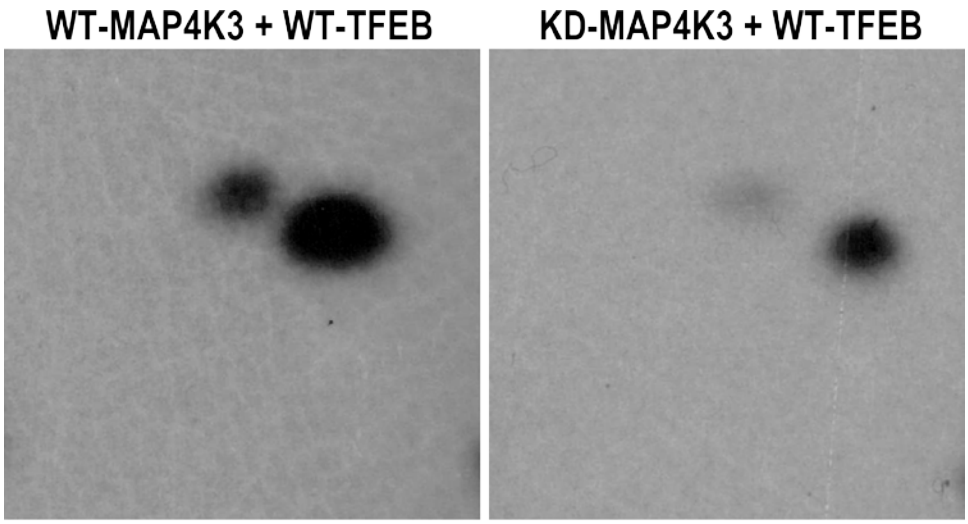

	p-Ser	p-Thr	p-Ser/p-Thr	p-Ser/Total
WT+ WT	24545.08	68306.28	0.359339	0.264348
KD+ WT	7758.966	30850.44	0.251503	0.200961

Figure 3.19. Kinase assay with KD-MAP4K3 and TFEB shows less phospho-serine than WT-MAP4K3 and TFEB. Phospho-amino acid analysis was performed after in-vitro kinase reaction was performed as in Figure 3.17. Relative levels of phospho-serine and phospho-threonine were quantified by densitometry analysis.

MAP4K3 phosphorylation of TFEB at Serine 3 is required for subsequent mTORC1 phosphorylation of TFEB at Serine 211

The phosphorylation of TFEB by mTORC1 at serine 211 has been established as a crucial regulatory event in the repression of TFEB activity (Martina et al., 2012; Roczniak-Ferguson et al., 2012). To determine the relationship between MAP4K3 phosphorylation of TFEB at serine 3 and mTORC1 phosphorylation of TFEB at serine 211, we examined the effect of TFEB serine 3 status upon phosphorylation at serine 211 by immunoblotting analysis with phospho-specific anti-pSer211 antibodies. When we compared WT-TFEB with S3A-TFEB upon transfection in WT HEK293 cells, we observed a dramatic reduction in serine 211 phosphorylation of S3A-TFEB that was comparable to the reduction in WT-TFEB serine 211 phosphorylation after Torin-1 treatment (Figure 3.20). We then evaluated the effect of MAP4K3 upon mTORC1-mediated TFEB phosphorylation by immunoblotting for TFEB serine 211 phosphorylation in MAP4K3 k.o. cells transfected with either WT-TFEB, S3A-TFEB, or S3E-TFEB (you need to describe S3A and S3E-TFEB). TFEB serine 211 phosphorylation of WT-TFEB or S3A-TFEB was undetectable in MAP4K3 k.o. cells, while TFEB serine 211 phosphorylation of S3E-TFEB did occur in the MAP4K3 k.o. cells. This indicates that serine 3 phosphorylation precedes serine 211 phosphorylation, and places MAP4K3 phospho-regulation of TFEB upstream of mTORC1 phospho-regulation.

To confirm that the decrease in mTORC1-mediated TFEB phosphorylation at serine 211 is the result of MAP4K3 k.o., we attempted to rescue the effect by overexpressing WT or kinase-dead MAP4K3 in the two cell types. In WT cells, overexpression of WT MAP4K3 had no effect on TFEB serine 211 phosphorylation,

while KD MAP4K3 overexpression diminished TFEB serine 211 phosphorylation slightly (Figure 3.21). Because MAP4K3 requires transautophosphorylation at serine 170 within its kinase activation domain in order for its activation (Yan et al., 2010), overexpression of kinase dead MAP4K3 may cause a constitutively inactivating effect on endogenous MAP4K3. In MAP4K3 k.o. cells, overexpression of WT MAP4K3 was sufficient to partially rescue TFEB serine 211 phosphorylation, while overexpression of KD MAP4K3 resulted in no difference in TFEB serine 211 phosphorylation from baseline MAP4K3 k.o. levels (Figure 3.21). These data support that MAP4K3 kinase activity both precedes and is necessary for TFEB serine 211 phosphorylation.

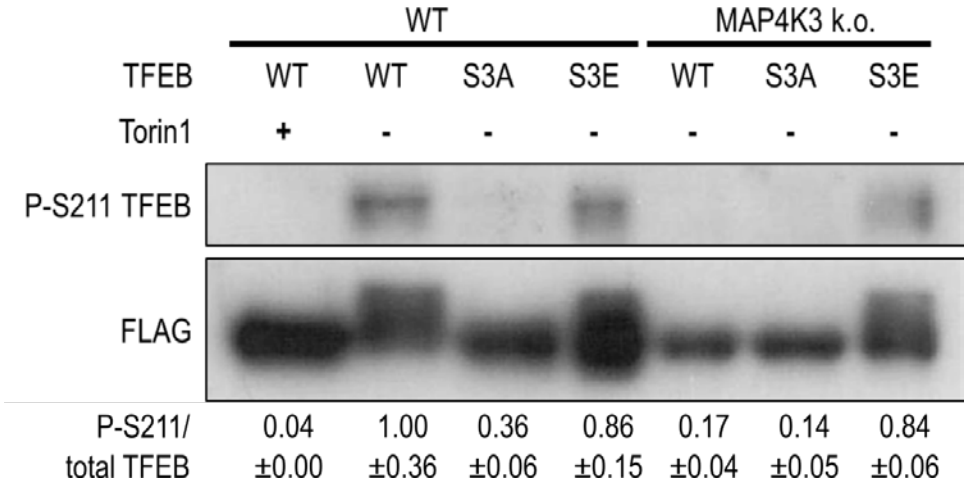

Figure 3.20. MAP4K3 phosphorylation of TFEB at serine 3 is necessary for mTOR phosphorylation at serine 211. WT HEK293T cells were transfected with WT-TFEB-FLAG, S3A-TFEB-FLAG, or S3E-TFEB-FLAG and Torin1 treatment was used as a negative control. Immunoprecipitation was performed with anti-FLAG antibody, followed by immunoblotting for phospho-serine 211 TFEB and FLAG.

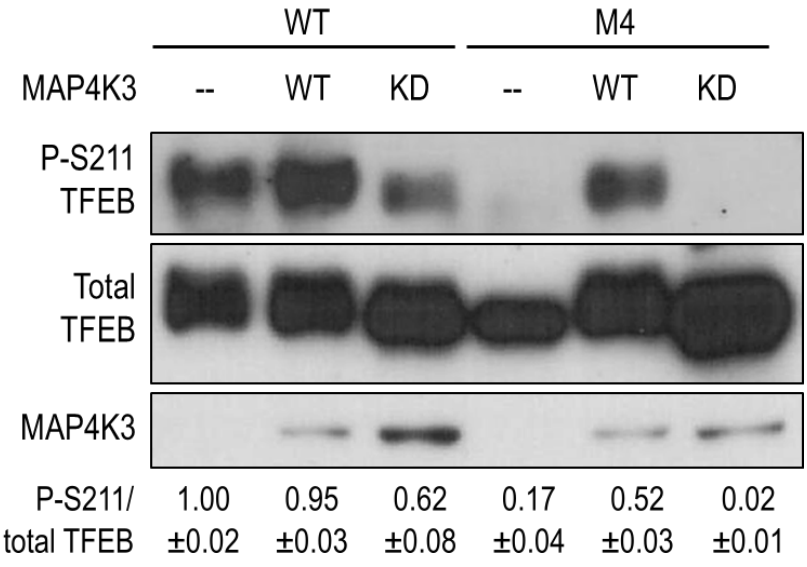

Figure 3.21. MAP4K3 phosphorylation of TFEB is necessary for mTOR phosphorylation at serine 211. WT HEK293T cells were untransfected or transfected with WT or kinase-dead MAP4K3. Immunoprecipitation was performed with anti-FLAG antibody, followed by immunoblotting for phospho-serine 211 TFEB and FLAG. Quantification of relative phosphorylation of TFEB serine 211 was performed by densitometry for n=3.

Discussion

Autophagy is a fundamentally important pathway that requires tight regulation based upon nutrient availability and cell stress. Our study is the first to identify MAP4K3 as a direct regulator of autophagy through phosphorylation of TFEB at serine 3. MAP4K3 phosphorylation of TFEB at serine 3 is necessary for mTOR phosphorylation of TFEB at serine 211, which results in TFEB binding to 14-3-3 and sequestration in the cytoplasm (Figure 3.22) (Martina et al., 2012; Roczniak-Ferguson et al., 2012; Settembre et al., 2012)(Martina et al., 2012; Roczniak-Ferguson et al., 2012; Settembre et al., 2012)(Martina et al., 2012; Roczniak-Ferguson et al., 2012; Settembre et al., 2012).

Previous studies have identified MAP4K3 to be required for maximal mTORC1 activation and cell growth (Findlay et al., 2007; Yan et al., 2010). However, other studies have also identified MAP4K3 as a pro-apoptotic kinase that activates apoptosis through the mTORC1 and JNK pathways (Lam et al., 2009). Indeed, we have also noted increased cell death due to high overexpression of MAP4K3. The exact mechanism that allows MAP4K3 to either promote cell growth or cell death in different conditions is unclear. It is possible that the trans-autophosphorylation of MAP4K3 at serine 170 is necessary for its activation of mTORC1 in response to the presence of amino acids, while a different post-translational modification on MAP4K3 leads to translational upregulation of PUMA and BAD to promote apoptosis. The dual roles of MAP4K3 may explain why overexpression of MAP4K3 may not be sufficient for a complete rescue of all phenotypes seen in MAP4K3 k.o. cells.

The first 30 N-terminal amino acids of TFEB are both necessary and sufficient for lysosomal localization of TFEB and binding to the Rag GTPases (Roczniak-

Ferguson et al., 2012). Additionally, mutagenesis of serine 3 and arginine 4 to alanines (S3A/R4A) completely prevents TFEB localization to lysosomes (Martina and Puertollano, 2013). We also found that mutation of serine 3 to alanine or deletion of the first 30 amino acids of TFEB prevented its interaction with mTORC1, the Rag GTPases, and the Ragulator complex (Figure 3.10). However, deletion of the first 30 amino acids consistently led to decreased TFEB interaction with the mTORC1, the Rag GTPases, and the Ragulator complex than mutation of serine 3 to alanine alone. This raises the possibility that phosphorylation of TFEB on serine 3 by MAP4K3 is not the sole regulatory post-translational modification that occurs in the first 30 amino acids of TFEB. However, serine 3 is the only phosphorylate-able residue in the first 30 amino acids of TFEB.

Here, we have elucidated the role of MAP4K3 activity in autophagy induction and identified a novel route by which TFEB localization is regulated. By phosphorylating TFEB at serine 3, MAP4K3 primes TFEB for phosphorylation by mTOR at serine 211, resulting in its binding of 14-3-3 and cytosolic sequestration. MAP4K3 emerges as an important regulator of autophagy; knockout of MAP4K3 not only indirectly induces autophagy through downregulation of mTORC1 activity, but also directly induces autophagy through the phosphorylation of TFEB. This two-step regulation is unsurprising for a biological process that requires tight regulation to balance cellular homeostasis.

Upregulation of TFEB and resulting lysosomal enhancement has been shown to improve clearance of aggregates and ameliorate progression of lysosomal storage diseases (Spampanato et al., 2013) and neurodegenerative diseases (Kilpatrick et al., 2015; Polito et al., 2014; Xiao et al., 2015). Better understanding of TFEB

regulation is critical for the development of therapies that can specifically upregulate autophagy in areas where it is necessary, rather than systemically, as TFEB overexpression has been shown to have negative effects in some organ systems (Kim et al., 2014). Further, while inhibition of mTORC1 has been known to upregulate TFEB, mTORC1 is not an ideal drug target due to its central role in regulating cell growth and macromolecule synthesis. Indeed, long-term mTORC1 inhibition results in immunosuppression and wound healing (Lamming et al., 2013). Therefore, identification of MAP4K3 as an mTOR-independent regulator of TFEB activity offers a novel target for TFEB-mediated therapeutic enhancement of cellular clearance.

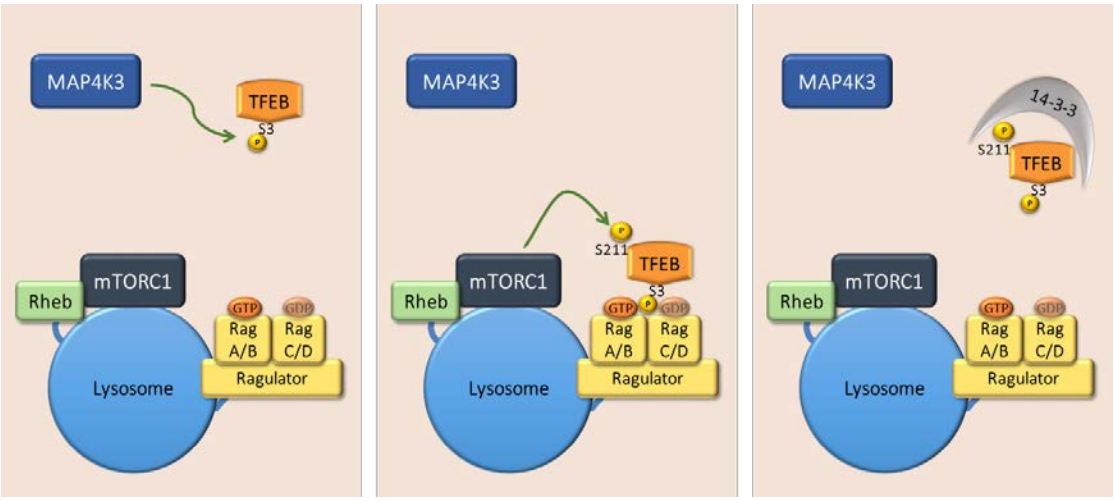

Figure 3.22. Model representing the mechanism of MAP4K3 regulation of TFEB in response to amino acids. First, the presence of amino acids activates MAP4K3, which phosphorylates TFEB at serine 3. This enhances TFEB interaction with the Rag GTPases and mTORC1 complex at the lysosomes and facilitates mTORC1 phosphorylation of TFEB at serine 211. This two-step phosphorylation process is necessary for TFEB binding to 14-3-3 and TFEB sequestration in the cytoplasm. Loss of MAP4K3 leads to decreased TFEB binding to 14-3-3 and increased TFEB nuclear localization.

Acknowledgements

Chapter 3 is an original document describing scientific work that is currently being prepared as a manuscript for submission. Hsu, C.L., Lee, E.X., Meisenhelder, J., Gordon, K.L., Hunter, T., and La Spada, A.R. “MAP4K3 regulates autophagy induction via direct phosphorylation of TFEB.” The dissertation author is the principal author of this work.

CHAPTER 4.

MAP4K3 distinctly regulates mTORC1 activity via AMPK and mTORC1 localization via GATOR1

Abstract

The mammalian target of rapamycin complex 1 (mTORC1) is the central node of an essential signaling pathway that integrates a complex variety of environmental stimuli, such as nutrient status and cell stress, to regulate cellular processes, such as cell growth, protein synthesis, autophagy, and lipid metabolism. In this paper, we elucidate the mechanism by which MAP4K3 separately regulates mTORC1 activity and localization. In MAP4K3 k.o. cells, we show that mTORC1 is unable to be activated in the presence of amino acids, while simultaneously exhibiting increased lysosomal localization in the absence of amino acids, two seemingly contradictory phenotypes. We hypothesize that MAP4K3 is critical for the activation of mTORC1 through the inhibition of AMPK and TSC2, upstream inhibitors of mTORC1, in the presence of amino acids. Subsequent to mTORC1 activation, MAP4K3 then activates the GATOR1 complex, which represses Rag GTPase activity in order to mobilize mTORC1 off the lysosome to phosphorylate and activate its substrates. We hypothesize that the mechanism for MAP4K3 inhibition of AMPK is through the phosphorylation and inhibition of SIRT1, which leads to increased acetylation of LKB1

and inhibition of its kinase activity towards AMPK. Through this complex mechanism, MAP4K3 exhibits tight control over the activity and subcellular localization of mTORC1, allowing for precise regulation of cell cycle and metabolism in the presence of amino acids.

Introduction

The mammalian target of rapamycin complex 1 (mTORC1) is the central node of an essential signaling pathway that integrates a complex variety of environmental stimuli, such as nutrient status and cell stress, to regulate cellular processes, such as cell growth, protein synthesis, autophagy, and lipid metabolism (Howell and Manning, 2011; Laplante and Sabatini, 2012). Deregulation of mTORC1 signaling can be found in a myriad of human disorders, including neurodegeneration, cancer, and metabolic diseases.

In response to the presence of amino acids, mTORC1 is recruited to the cytoplasmic surface of lysosomes via a physical interaction between Raptor and the Rag GTPases. The Rag GTPases belong to the RAS superfamily of GTPases and function as heterodimers wherein the active complex consists of GTP-bound RagA or B complexed with GDP-bound RagC or D (Gao and Kaiser, 2006; Sekiguchi et al., 2001). Importantly, amino acids trigger the GTP loading of RagA/B proteins, thus promoting binding to Raptor and assembly of an activated mTORC1 complex (Kim et al., 2008a; Sancak et al., 2008). In the absence of amino acids, the Rags adopt an inactive conformation (GDP-bound RagA/B and GTP-bound RagC/D), and mTORC1 is inactivated and shuttled back to the cytosol. The activation of Rag GTPases is tightly regulated by GEF and GAP proteins. The lysosomal Ragulator complex functions as a GEF for RagA/B in response to amino acid stimulation (Bar-Peled et al., 2012). The GATOR1 complex, a trimeric complex consisting of NPRL2, NPRL3, and DEPDC5, acts as a GAP for RagA/B and negatively regulates mTORC1 activation by promoting the GTPase activity of RagA/B (Bar-Peled et al., 2013).

Bringing mTOR to lysosomes is critical for the activation of its kinase activity by Rheb, a lysosomally localized GTPase that is regulated by growth factor signaling, energy abundance, and stress (Inoki et al., 2003a). Rheb is required for amino acid induction of mTORC1 activation, as amino acids fail to activate mTORC1 in Rheb knockout cells (Hara et al., 1998; Long et al., 2005). Upstream of Rheb is the TSC-TBC complex, formed by Tuberous sclerosis complex protein 1 and 2 (TSC1 and TSC2) and TBC1D7. The C terminal domain of TSC2 acts as a GAP for Rheb, while complex formation with TSC1 and TBC1D7 stabilizes TSC2 and enhances its GAP activity (Garami et al., 2003; Inoki et al., 2003a; Tee et al., 2003; Zhang et al., 2003). Loss of function of the TSC-TBC complex leads to constitutive mTORC1 activation that is unresponsive to changes in cellular growth conditions (Jaeschke et al., 2002; Kwiatkowski et al., 2002).

Many signals regulate mTORC1 and Rheb through the TSC-TBC complex. For example, growth factors and cytokines activate mTORC1 via Akt-dependent inhibitory phosphorylation of TSC2 (Inoki et al., 2002; Manning et al., 2002; Potter et al., 2002) and energy stress inhibits mTORC1 through an AMPK-mediated activating phosphorylation on TSC2 (Inoki et al., 2003b; Shaw et al., 2004). AMPK is a serine/threonine kinase composed of a catalytic (α) and two regulatory (β and γ) subunits activated by increases in cellular AMP or ADP levels. Under nutrient starvation conditions, AMPK is phosphorylated at threonine 172 by liver kinase B1 (LKB1), a tumor suppressor gene mutated in Peutz–Jeghers syndrome. Then, the γ subunit of AMPK binds to AMP and ADP, enforcing a conformational change that blocks de-phosphorylation of AMPK to keep it in an activated state. The phosphorylation of AMPK at threonine 172 in the activation loop is essential for its

activation. Once active, AMPK phosphorylates TSC2 at serine 1387, which acts as a primer for the phosphorylation and activation of TSC2 by glycogen synthase kinase (GSK)3-β (Inoki et al., 2006), resulting in mTORC1 inactivation.

LKB1 is allosterically activated through its interaction with STE20-related adapter (STRAD) and the adaptor protein mouse protein 25 (MO25) (Boudeau et al., 2003). When active, LKB1 is predominantly in the cytoplasm; however, when not associated with other proteins, LKB1 is located predominantly in the nucleus due to its N-terminal nuclear localization signal. Lan and colleagues showed that overexpression of SIRT1, a class III NAD+-dependent histone/protein deacetylase, led to increased LKB1 deacetylation at lysine 48, cytoplasmic localization of LKB1, and kinase activity against targets AMPK and MARK1 (Lan et al., 2008).

SIRT1 is the most well-studied member of the sirtuin family of proteins, which act as energy sensors and metabolic regulators in multiple tissue types. SIR2 protein is the sirtuin homologue in Saccharomyces cerevisiae, and over-expression of SIR2 extends replicative life-span in yeast, and orthologues of SIR2 extend organismal life-span in both worms and flies (Kaeberlein et al., 1999; Tissenbaum et al., 2000). SIRT1 activity can be regulated post-transcriptionally by several mechanisms, including through interactions with proteins such as DBC1 (deleted in breast cancer 1) (Escande et al., 2010; Kim et al., 2008b), changes in NAD+ levels (Lin et al., 2000), and phosphorylation. Interestingly, AMPK has been shown to activate SIRT1 by upregulating the gene encoding the NAD+ synthetic enzyme nicotinamide phosphoribosyltransferase (NAMPT) (Canto et al., 2009; Fulco et al., 2008), comprising a positive feedback loop.

Previously, MAP4K3 was identified as a Ste20 kinase that regulates the activity of mTORC1 in response to amino acids, but not insulin or rapamycin (Findlay et al., 2007). Additionally, MAP4K3 has been shown to regulate autophagy, both indirectly through mTORC1 and directly through phosphorylation of TFEB (Dubinsky et al., 2014). Here, we demonstrate that in MAP4K3 k.o. cells, mTORC1 is unable to be activated in the presence of amino acids, while simultaneously exhibiting increased lysosomal localization in the absence of amino acids, two seemingly contradictory phenotypes. We hypothesize that MAP4K3 is critical for the activation of mTORC1 through the inhibition of AMPK and TSC2, upstream inhibitors of mTORC1, in the presence of amino acids. Subsequent to mTORC1 activation, MAP4K3 then activates the GATOR1 complex, which represses Rag GTPase activity in order to mobilize mTORC1 off the lysosome to phosphorylate and activate its substrates. We hypothesize that the mechanism for MAP4K3 inhibition of AMPK is through the phosphorylation and inhibition of SIRT1, which leads to increased acetylation of LKB1 and inhibition of its kinase activity towards AMPK. Through this complex mechanism, MAP4K3 exhibits tight control over the activity and subcellular localization of mTORC1, allowing for precise regulation of cell cycle and metabolism in the presence of amino acids.

Results

MAP4K3 is critical for mTORC1 activation in the presence of amino acids

To evaluate the importance of MAP4K3 to mTORC1 activation, we generated two clonal MAP4K3 k.o. cell lines (M1 and M4) using CRISPR-Cas9 genome editing (see Chapter 2). We found that loss of MAP4K3 in HEK293A cells resulted in inhibited cell growth (Figure 4.1) and reduced cell size (Figure 4.2). Next, we tested mTORC1 activation in WT and MAP4K3 k.o. cells in response to various nutrient stimuli by probing for phosphorylation of downstream phosphorylation targets of mTORC1, S6 kinase (S6K) and eIF4E (eukaryotic initiation factor 4E)-binding protein 1 (4E-BP1), as well as the phosphorylation target of S6K, ribosomal protein S6. In response to amino acid starvation, WT cells exhibited consistent reduction in phosphorylation of mTORC1 downstream targets and a rapid increase in phosphorylation after only ten minutes of amino acid stimulation (Figure 4.3). While there is no difference in the effect of amino acid starvation on mTORC1 activity in MAP4K3 k.o. cells, there is a striking difference after amino acid stimulation. In MAP4K3 k.o. cells, there is little to no phosphorylation of S6K, S6, or 4E-BP1 in response to amino acid stimulation. In contrast, stimulation of WT and MAP4K3 k.o. cells with insulin yielded comparable activation of mTORC1 in both cell types. This supports that MAP4K3 plays a critical role in activating mTORC1 specifically in the presence of amino acids.

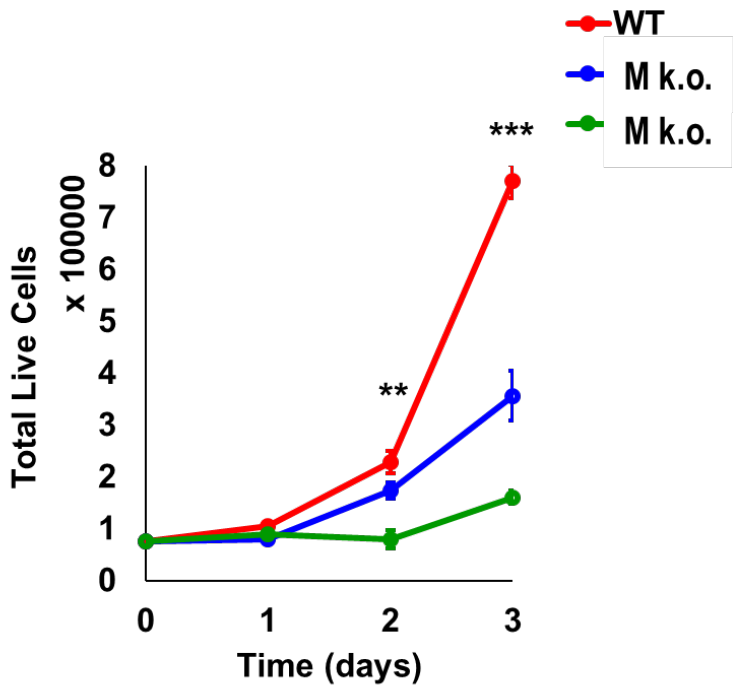

Figure 4.1. MAP4K3 is important for maintaining cellular growth. Cells were grown in normal media conditions

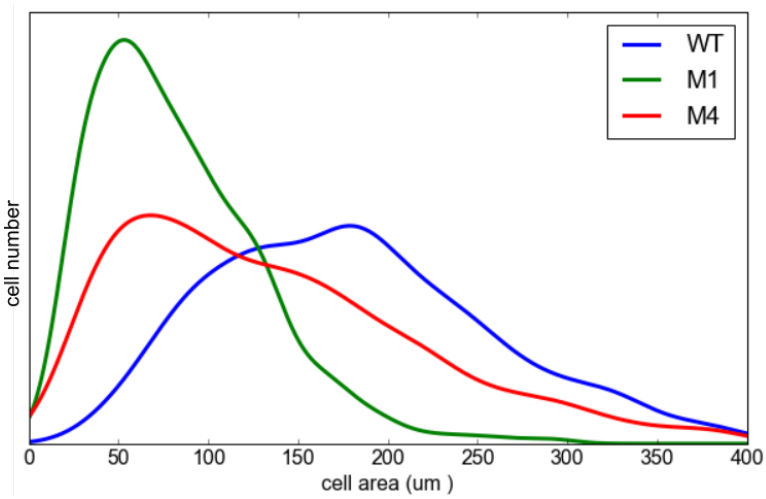

Figure 4.2. MAP4K3 is important for maintaining cell size. Kernel density plot of cell size of WT cells and two MAP4K3 k.o. cell lines grown in complete media.

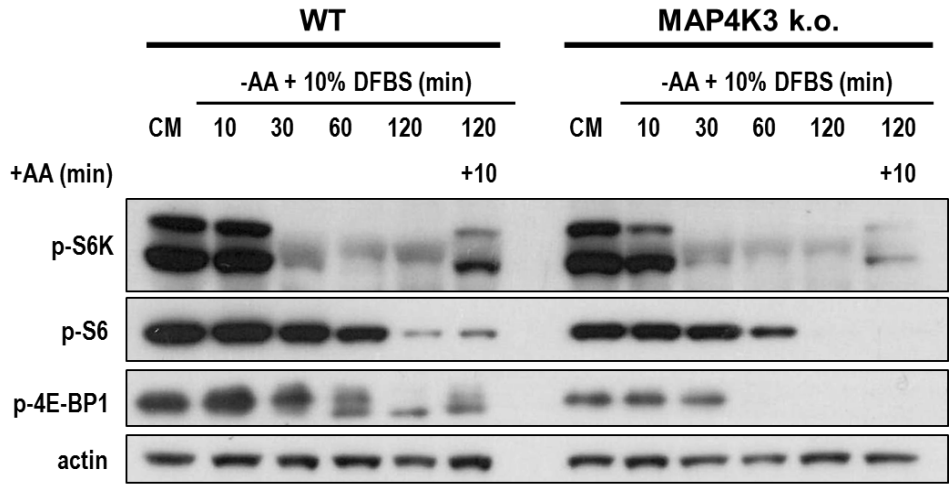

Figure 4.3. MAP4K3 is necessary for the regulation of the mTORC1 signaling pathway by amino acids. WT and MAP4K3 k.o. cells were starved for 10, 30, 60, and 120 minutes, then re-stimulated with amino acids for 10 minutes. Cell lysates were immunoblotted for the phosphorylation state of S6K1, S6, and 4E-BP1. MAP4K3 k.o. inhibits amino acid-induced phosphorylation of S6K1, S6, and 4E-BP1.

MAP4K3 is an important regulator of mTORC1 lysosomal localization through the GATOR1 complex

mTORC1 is recruited to the lysosomes by active Rag GTPases in the presence of amino acids (Kim et al., 2008a; Sancak et al., 2008). In the absence of amino acids, we observed diffuse mTOR localization in WT cells, followed by mTOR recruitment to the lysosomal surface following amino acid stimulation (Figure 4.4A). Surprisingly, mTOR was significantly more localized to the lysosomes in MAP4K3 k.o. cells during amino acid starvation compared to WT cells, and there was no significant difference in mTOR localization once amino acids were added to the culture media (Figure 4.4A-C). These results suggest that mTOR localization can be uncoupled from its activation.

Because mTORC1 lysosomal recruitment depends on active Rag GTPases, specifically GTP-bound RagA or B complexed with GDP-bound RagC or D, we evaluated the ability of constitutively inactive GDP-bound RagA (RagA T21N) to reverse the lysosomal localization of mTOR seen in amino acid-starved MAP4K3 k.o. cells. Indeed, overexpression of RagA-GDP was sufficient to reverse the lysosomal localization of mTOR seen in both amino acid-starved and re-stimulated MAP4K3 k.o. cells (Figure 4.6). Further, because the GATOR1 complex acts as a GAP for RagA/B (Bar-Peled et al., 2013), we evaluated the ability of GATOR1 overexpression to reverse the increased mTOR lysosomal localization seen in MAP4K3 k.o. cells. Overexpression of DEPDC5, one component of the GATOR1 complex, was sufficient to prevent mTOR lysosomal localization in all cells, including MAP4K3 k.o. cells (Figure 4.7). These findings suggest that MAP4K3 regulation of mTORC1 localization is upstream of the GATOR1 complex. To determine if MAP4K3 interacts with

components of the GATOR1 complex, we transfected HEK293 cells with normal MAP4K3 (WT-MAP4K3) or a kinase dead version of MAP4K3 (KD-MAP4K3) along with DEPDC5, NPRL2, and NPRL3. We then immunoprecipitated overexpressed MAP4K3 and when we immunoblotted for the GATOR1 components, we found evidence for a physical interaction between GATOR1 and MAP4K3 (Figure 4.8). This evidence supports the possibility that MAP4K3 could be acting through GATOR1 to affect mTORC1 subcellular localization. Specifically, MAP4K3 could be inhibiting GATOR1, which leads to an increase in active Rag GTPases and recruitment of mTORC1 to the lysosomes.

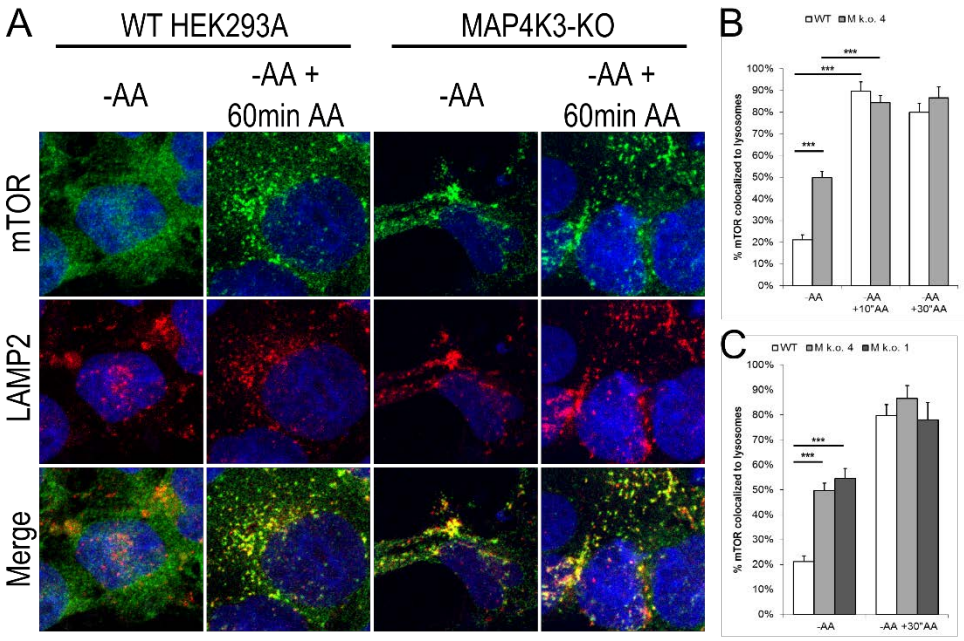

Figure 4.4. MAP4K3 regulates mTORC1 localization to the lysosomal surface. **(A)** WT and MAP4K3 k.o. cells were starved with amino acids for three hours or starved and re-stimulated with amino acids for 60 minutes before co-immunostaining for mTOR (green) and Lamp2 (red). **(B, C)** Quantification performed using CellProfiler of the percentage of LAMP2 puncta that are superimposed by mTOR puncta in WT and two MAP4K3 k.o. cell lines undergoing amino acid starvation or starvation and re-stimulation with amino acids for the specified times.

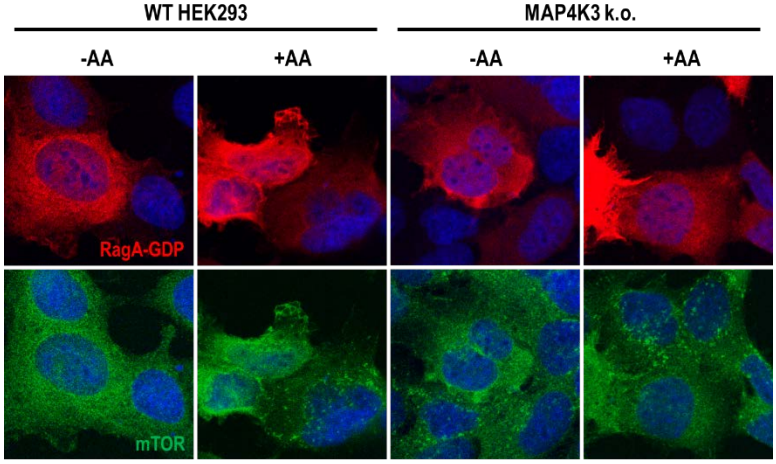

Figure 4.6. MAP4K3 regulates mTORC1 localization to the lysosomal surface upstream of Rag GTPases. WT and MAP4K3 k.o. cells were transfected with constitutively inactive GDP-bound RagA-FLAG, then starved with amino acids for three hours or starved and re-stimulated with amino acids for 30 minutes before co-immunostaining for mTOR (green) and RagA-FLAG (red).

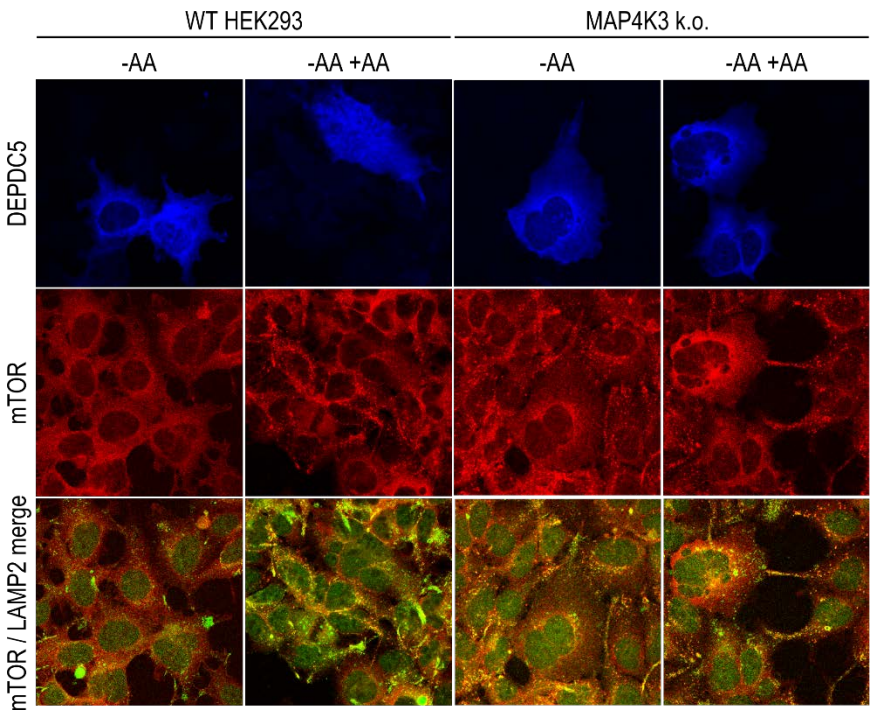

Figure 4.7. MAP4K3 regulates mTORC1 localization to the lysosomal surface upstream of GATOR1. WT and MAP4K3 k.o. cells were transfected with DEPDC5, then starved with amino acids for three hours or starved and re-stimulated with amino acids for 30 minutes before co-immunostaining for mTOR (red), Lamp2 (green), and DEPDC5 (blue).

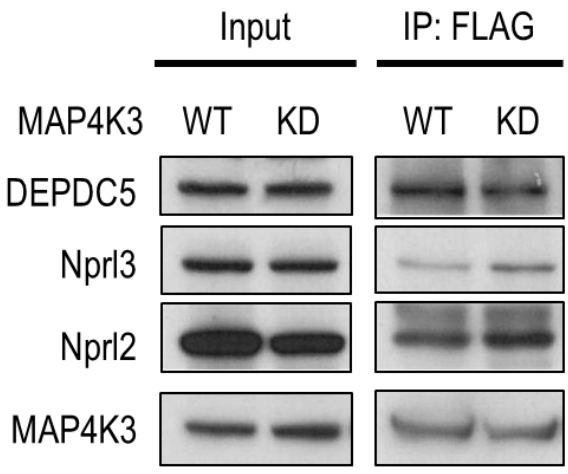

Figure 4.8. MAP4k3 interacts with all components of the GATOR1 complex. HEK293T cells were transfected with expression vectors of WT- or KD-MAP4K3, DEPDC5, Nprl2, and Nprl3, lysates were prepared and immunoprecipitated with FLAG antibody, followed by immunoblotting for the indicated proteins.

MAP4K3 regulates mTORC1 activity through Rheb GTPase activation

However, bringing mTOR to lysosomes is critical for its activation by the Rheb GTPase. In seeming contradiction, increased mTOR lysosomal localization is not accompanied by increased mTORC1 activity in MAP4K3 k.o. cells, but rather decreased mTORC1 activity. To investigate this phenomenon further, we evaluated Rheb activity in MAP4K3 k.o. cells. Overexpression of the constitutively active Rheb Q64L mutant was sufficient to constitutively activate mTORC1 signaling in both WT and MAP4K3 k.o. cells, regardless of amino acid status (Figure 4.9). This finding suggests that MAP4K3 may normally activate mTORC1 through activation of Rheb. Rheb activity is regulated by TSC2, which acts as a GAP for Rheb (Garami et al., 2003; Inoki et al., 2003a; Tee et al., 2003; Zhang et al., 2003). Consistent with the binding preference of many GAPs for the GTP-loaded state of target GTPases, TSC2 preferentially interacts with GTP-bound Rheb (Carroll et al., 2016). We observed that the interaction between endogenous TSC2 and Rheb in WT cells was much stronger than in MAP4K3 k.o. cells (Figure 4.10). This suggests that there is a significantly higher proportion of GDP-bound Rheb in MAP4K3 k.o. cells as compared to WT cells.

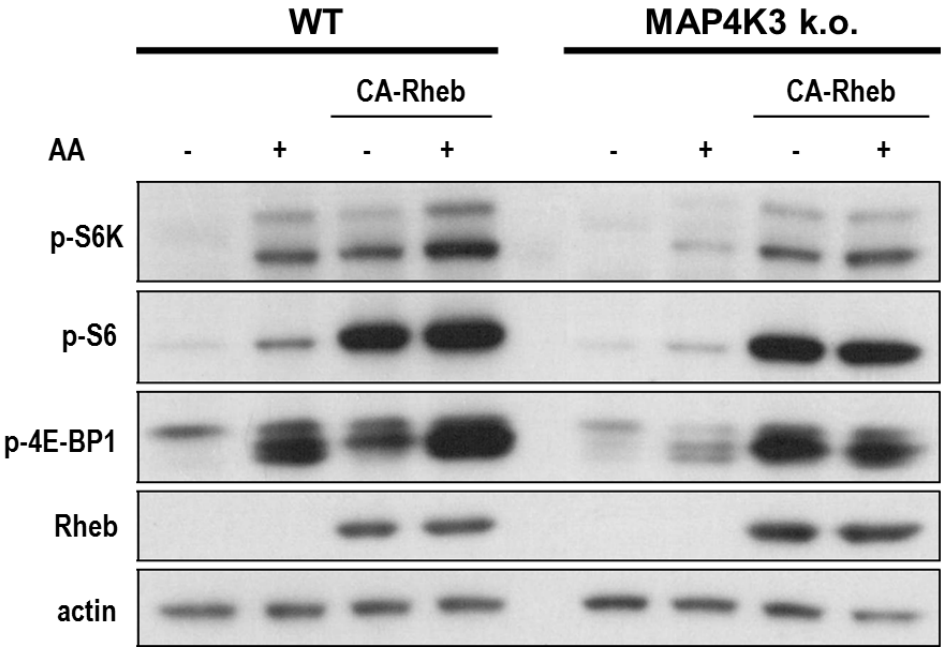

Figure 4.9. MAP4K3 regulates mTORC1 activation upstream of Rheb GTPase. WT and MAP4K3 k.o. cells were transfected with constitutively active Rheb where indicated and starved of amino acids for 3 hours or starved and re-stimulated with amino acids for 10 minutes. Lysates were prepared and immunoblotted for the indicated proteins.

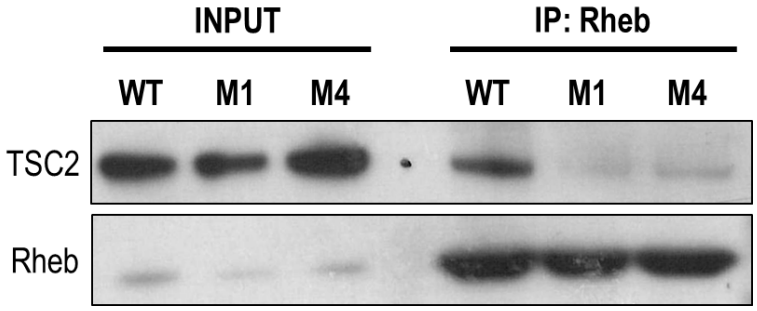

Figure 4.10. Loss of MAP4K3 leads to a decrease in endogenous GTP-bound Rheb. Lysate were prepared from WT and two MAP4K3 k.o. cell lines and immunoprecipitated with Rheb antibody for endogenous TSC2.

MAP4K3 regulates Rheb GTP-loading via the LKB1-AMPK axis

Many signals, such as growth factors, cytokines, and energy stress, regulate mTORC1 and Rheb through TSC2. Of the known upstream regulators of TSC2, AMPK was revealed to also interact with MAP4K3 through mass spectrometry. Following increased cellular AMP or ADP levels, active AMPK phosphorylates and activates TSC2, which is required for translation regulation and cell size control in response to energy deprivation (Inoki et al., 2003b). After confirming interaction between MAP4K3 and AMPK by co-immunoprecipitation, we determined whether MAP4K3 acts upstream of AMPK to activate mTOR by making MAP4K3/AMPK double k.o. cells using CRISPR/Cas9 genome editing. While MAP4K3 k.o. cells exhibited blunted mTORC1 signaling in response to amino acid stimulation, MAP4K3 – AMPK double k.o. cells reversed mTORC1 signaling back to WT levels (Figure 4.11). Consistent with rescued mTORC1 signaling, AMPK k.o. on top of the MAP4K3 k.o. background also rescued the smaller cell size phenotype and slower cell growth seen in MAP4K3 single k.o. cells (Figure 4.12). Because LKB1 is the kinase responsible for phosphorylating and activating AMPK following energy deprivation (Hawley et al., 2003; Lizcano et al., 2004; Shaw et al., 2004), we investigated whether MAP4K3 acts upstream of LKB1 by making MAP4K3/LKB1 double k.o. cells using CRISPR/Cas9 genome editing. Similar to our results with MAP4K3/AMPK double k.o. cells, MAP4K3/LKB1 double k.o. cells also rescued mTORC1 inactivation phenotypes observed in MAP4K3 single k.o. cells (Figure 4.13 and 4.14). These results indicate that MAP4K3 is acting upstream of the LKB1-AMPK axis to ultimately activate mTORC1.

LKB1 activity is dictated by its subcellular localization; LKB1 is inactive in the nucleus, but becomes activated in the cytoplasm by forming a complex with STRAD and MO25 (Boudeau et al., 2003). When we assayed LKB1 subcellular localization in WT and MAP4K3 k.o. cells, we found that while LKB1 was predominantly localized in the nucleus of WT cells following amino acid stimulation, LKB1 remained localized in the cytoplasm in MAP4K3 k.o. cells (Figure 4.15). Lan and colleagues showed that deacetylation of LKB1 at lysine 48 led to increased cytoplasmic localization and activity (Lan et al., 2008). Consistent with our previous results showing increased LKB1 cytoplasmic localization in MAP4K3 k.o. cells, we also found that LKB1 was more acetylated in MAP4K3 k.o. cells, using an antibody to detect pan- acetylation on lysine (Figure 4.16). This suggests that LKB1 is more active in MAP4K3 k.o. cells than in WT cells, leadings to increased AMPK and TSC2 activation and decreased mTORC1 activity.

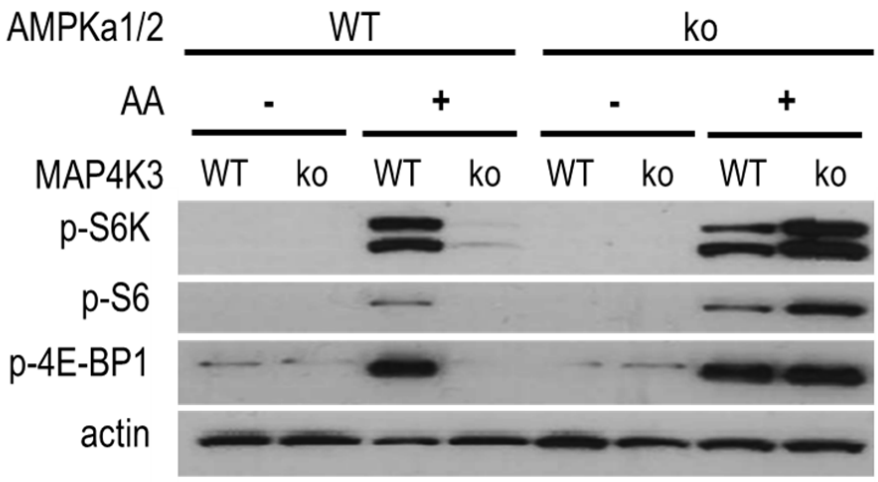

Figure 4.11. MAP4K3 regulates mTORC1 activation upstream of AMPK. WT, MAP4K3 single k.o., AMPK single k.o., and MAP4K3/AMPK double k.o. cells were amino acid starved for 3 hours or starved and re-stimulated with amino acids for 30 minutes. Lysates were prepared and immunoblotted for the indicated proteins.

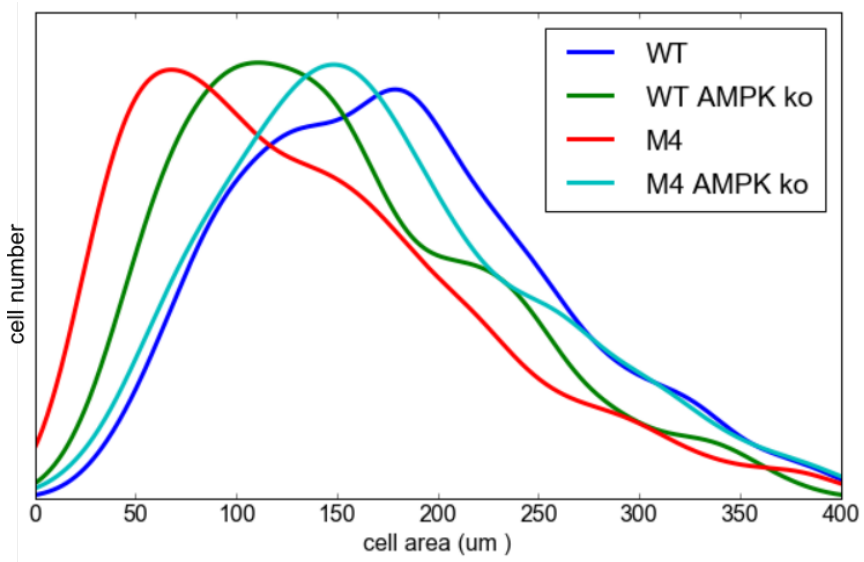

Figure 4.12. MAP4K3 regulates mTORC1 activation upstream of AMPK. Kernel density plot of cell size of WT, MAP4K3 single k.o., AMPK single k.o., and MAP4K3/AMPK double k.o. cell lines grown in complete media.

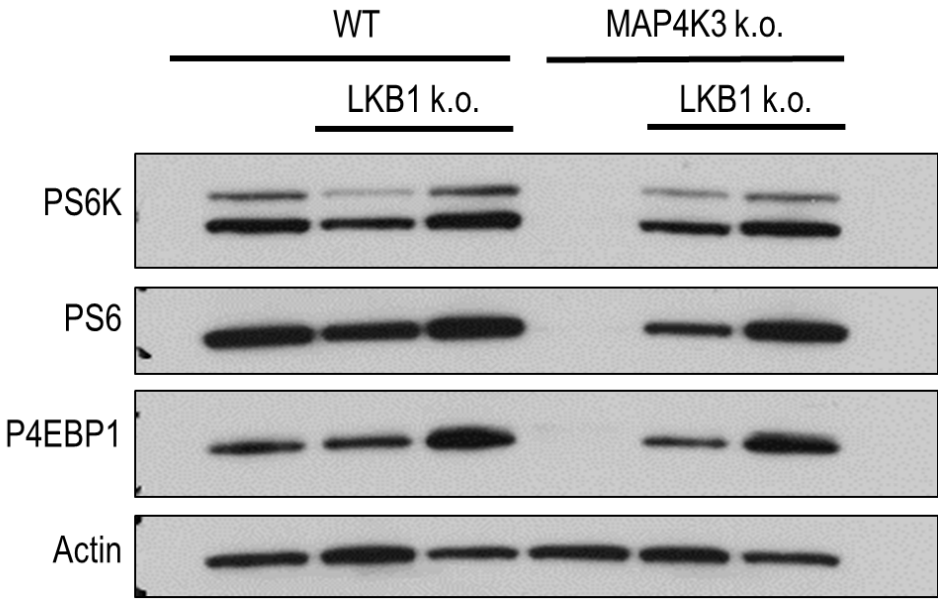

Figure 4.13. MAP4K3 regulates mTORC1 activation upstream of LKB1. WT, MAP4K3 single k.o., LKB1 single k.o., and MAP4K3/LKB1 double k.o. cells were amino acid starved for 3 hours or starved and re-stimulated with amino acids for 30 minutes. Lysates were prepared and immunoblotted for the indicated proteins.

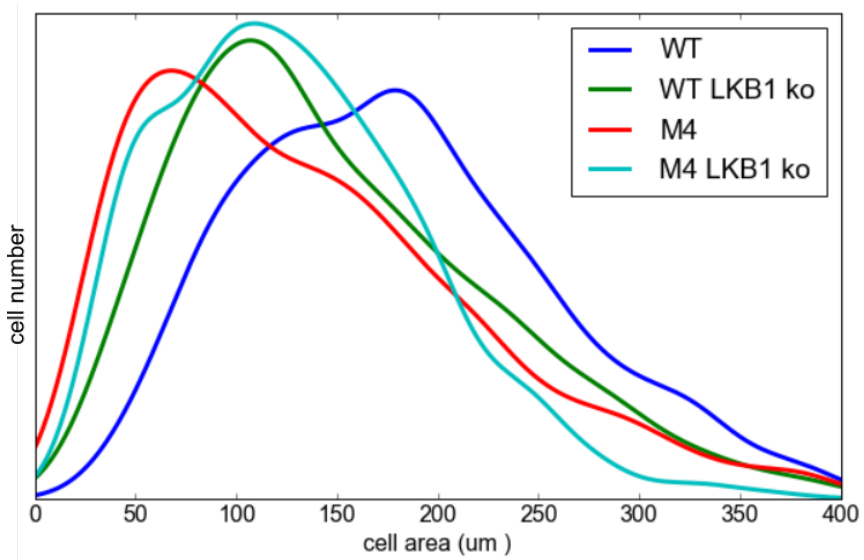

Figure 4.14. MAP4K3 regulates mTORC1 activation upstream of LKB1. Kernel density plot of cell size of WT, MAP4K3 single k.o., LKB1 single k.o., and MAP4K3/LKB1 double k.o. cell lines grown in complete media.

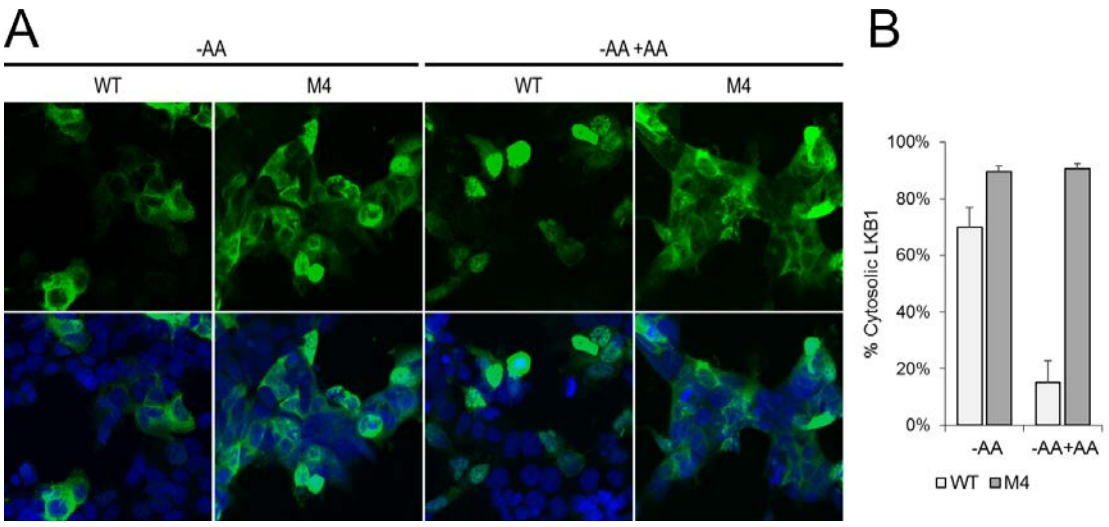

Figure 4.15. MAP4K3 regulates LKB1 subcellular localization. (A) WT and MAP4K3 k.o. cells were transfected with LKB1-FLAG, then amino acid starved for 3 hours or starved and re-stimulated with amino acids for 30 minutes, before immunostaining for LKB1-FLAG (green) and DAPI (blue). **(B)** Quantification of the percentage of LKB1 that is localized in the cytosol in (A).

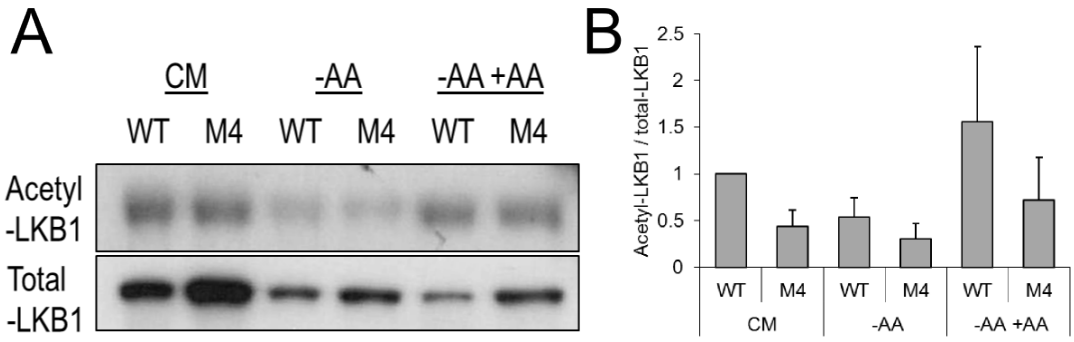

Figure 4.16. MAP4K3 regulates LKB1 acetylation. (A) WT and MAP4K3 k.o. cells were transfected with LKB1-FLAG, then amino acid starved for 3 hours or starved and re-stimulated with amino acids for 30 minutes. Lysates were prepared and immunoprecipitated with FLAG for overexpressed LKB1, then immunoblotted for pan-acetyl lysine and FLAG for total immunoprecipitated LKB1. **(B)** Quantification of the ratio of acetylation on LKB1 to total LKB1 in (A). n=2

MAP4K3 inhibits SIRT1 via phosphorylation

Overexpression of SIRT1, a class III NAD+-dependent histone/protein deacetylase, leads to increased LKB1 deacetylation, cytoplasmic localization of LKB1, and kinase activity against targets AMPK and MARK1 (Lan et al., 2008). SIRT1 itself can be regulated through phosphorylation. We hypothesized that MAP4K3 might act upon LKB1 and AMPK through SIRT1, which was also revealed to interact with MAP4K3 through mass spectrometry interactome screen that we performed. MAP4K3 interaction with SIRT1 was confirmed by co-immunoprecipitation (Figure 4.17). Interestingly, the interaction between SIRT1 and KD-MAP4K3 was significantly stronger than the interaction between SIRT1 and WT-MAP4K3, suggesting that the kinase activity of MAP4K3 is critical for its interaction with SIRT1. To determine if the MAP4K3 – SIRT1 interaction is direct, we produced in vitro translated SIRT1 protein and performed a pull-down assay. In vitro translated SIRT1 was able to pull down both WT-MAP4K3 and KD-MAP4K3 (Figure 4.18). To narrow down the domain that is critical for MAP4K3 binding and phosphorylation of SIRT1, we performed co-immunoprecipitations using three N-terminal and two C-terminal deletion constructs of SIRT1 with MAP4K3. WT and KD-MAP4K3 bind differentially to full-length and 142-747 SIRT1, but equally to 1-698 SIRT1 (Figure 4.19). Phosphorylation of a substrate by its kinase often leads to changes in charge and conformation of the substrate, causing dissociation of the kinase from its substrate. Hence, our findings suggests that MAP4K3 phosphorylates SIRT1 at a residue in the region of SIRT1 from 698-747aas, as the binding strength between WT and KD MAP4K3 becomes equal once this domain is lost. Additionally, MAP4K3 binds to full-

length and 142-747 SIRT1, but not to 465-747 SIRT1, which suggests that the region of 142-465aas of SIRT1 is necessary for MAP4K3 binding to SIRT1.

To investigate if MAP4K3 directly phosphorylates SIRT1, we performed *in vivo* kinase assays by overexpressing SIRT1 in WT and MAP4K3 k.o. cells, then feeding the cells with P32-orthophosphate, in the presence or absence of amino acids. The ratio of P32 incorporation into SIRT1 in the presence versus the absence of amino acids was much higher in WT cells compared to MAP4K3 k.o. cells (Figure 4.20), suggesting that MAP4K3 is critical for phosphorylating SIRT1 in the presence of amino acids. We then performed two-dimensional phosphopeptide mapping on the phosphorylated SIRT1 protein. We found that SIRT1 isolated from WT cells stimulated with amino acids contained residues that were uniquely phosphorylated compared to both WT cells without amino acid stimulation and MAP4K3 k.o. cells, both with and without amino acids (Figure 4.21). These phosphorylated residues must be specific to MAP4K3 activated by amino acid stimulation. With these findings, we propose the hypothesis that MAP4K3 phosphorylates and inactivates SIRT1 in the presence of amino acids, dampening LKB1, AMPK, and TSC2 activity, leading to increased GTP-bound Rheb and mTORC1 activity.

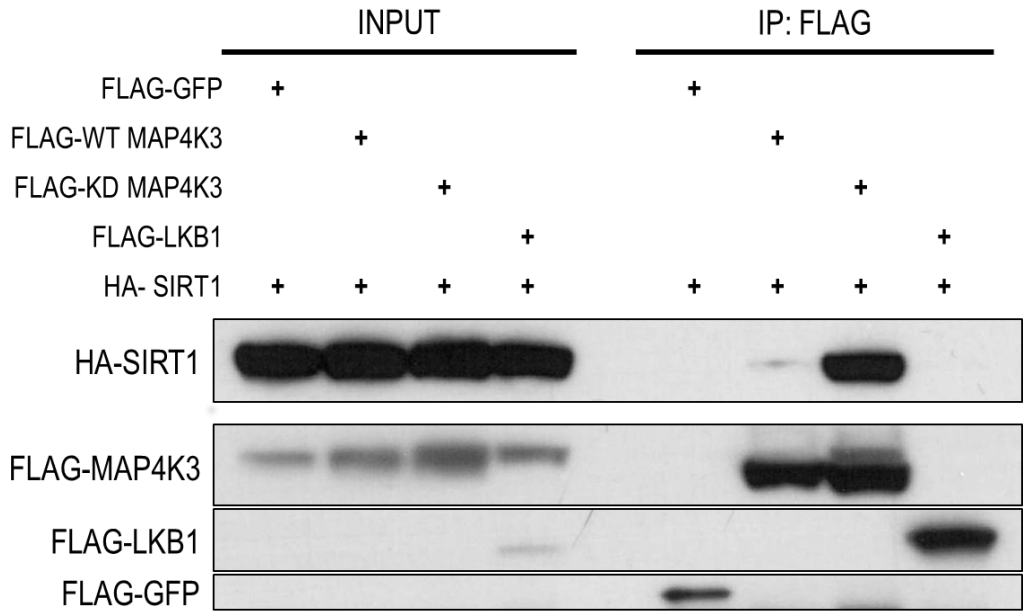

Figure 4.17. MAP4K3 interacts with SIRT1. HEK293A cells were transfected with HA-SIRT1 and WT- or KD- MAP4K3-FLAG or FLAG-GFP or FLAG-LKB1 for negative controls. Lysates were prepared and immunoprecipitated with FLAG antibody, then immunoblotted for the indicated proteins.

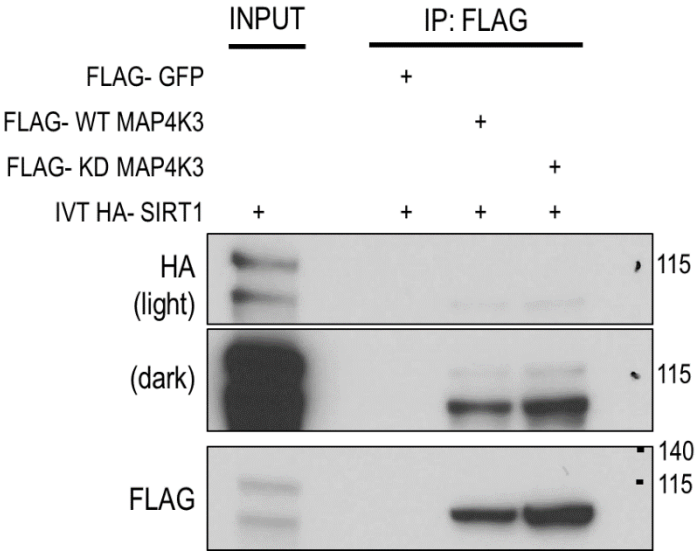

Figure 4.18. MAP4K3 interacts directly with SIRT1. *In vitro* translated HA-SIRT1 was produced and mixed with immunoprecipitated WT- or KD-MAP4K3-FLAG, then pulled-down with FLAG antibody and immunoblotted for MAP4K3 and SIRT1.

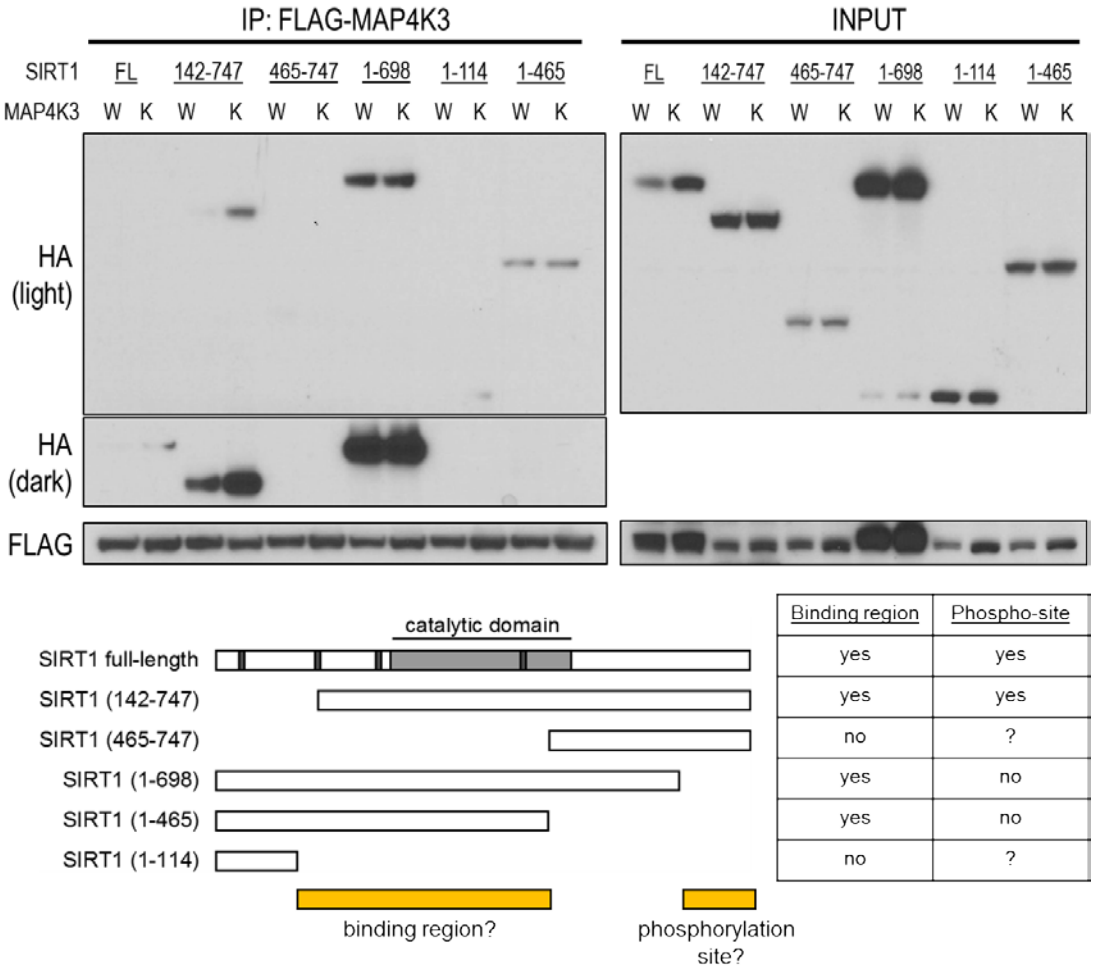

Binding region	Phospho-site
yes	yes
yes	yes
no	?
yes	no
yes	no
no	?

Figure 4.19. MAP4K3 most likely phosphorylates SIRT1 in the C-terminal fifty amino acids of SIRT1. Various deletion constructs of SIRT1 were co-transfected with WT- or KD- MAP4K3-FLAG, then immunoprecipitated with FLAG antibody and immunoblotted for MAP4K3 and SIRT1.

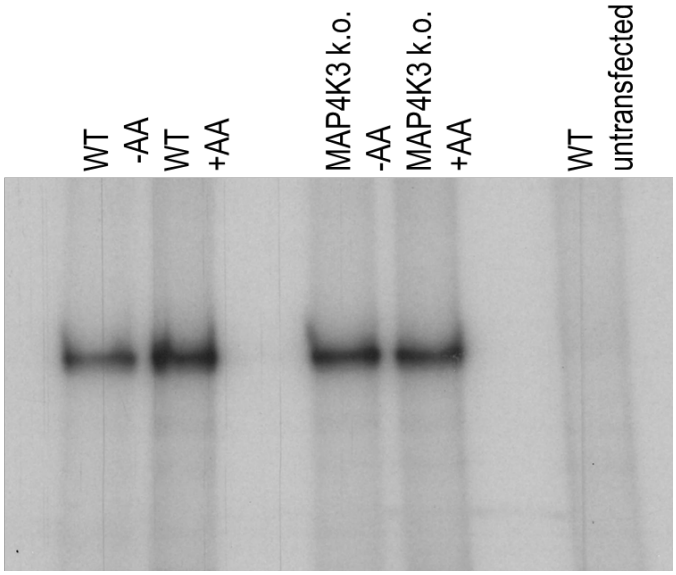

Figure 4.20. MAP4K3 regulates phosphorylation of SIRT1 *in vivo.* HA-SIRT1 was overexpressed in WT and MAP4K3 k.o. cells that were fed P32 orthophosphate, then starved or stimulated with amino acids for 30 minutes. Lysates were prepared, immunoprecipitated with HA antibody for SIRT1 protein, and analyzed by SDS-PAGE and autoradiography of P32 incorporation into SIRT1.

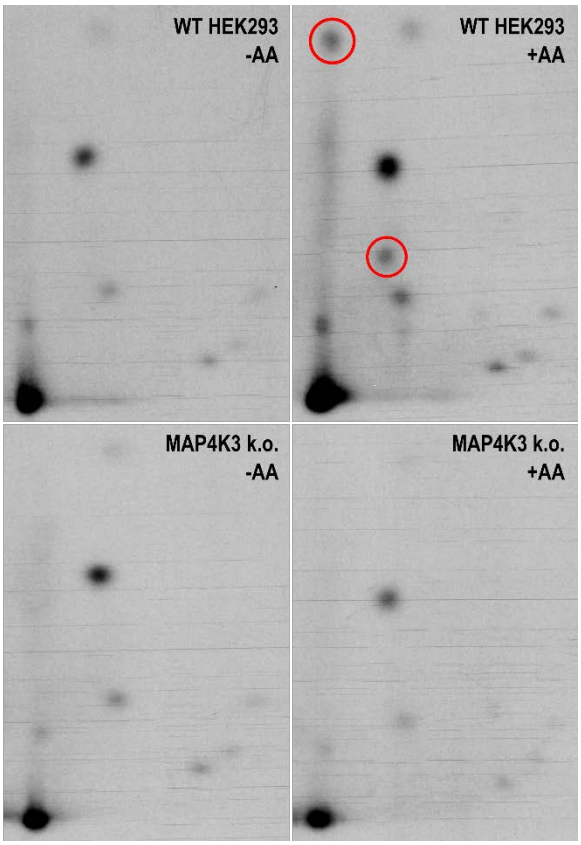

Figure 4.21. MAP4K3 regulates phosphorylation of SIRT1 *in vivo.* HA-SIRT1 was extracted (from Figure 4.20) and phosphopeptide mapping was performed, with cleavage from glutamate endopeptidase. Unique phosphopeptides in SIRT1 overexpressed in WT cells stimulated with amino acids are circled in red.

Discussion

The mTORC1 signaling pathway is a tightly regulated process that integrates an array of environmental stimuli to control cell growth and metabolism. While MAP4K3 has been shown to activate mTORC1 signaling in response to amino acids (Findlay et al., 2007), the exact mechanism has yet to be elucidated. Additionally, mTORC1 activity has been tied to its localization to lysosomes (Sancak et al., 2010). Here we reveal that MAP4K3 regulates mTORC1 activity via phosphorylation of SIRT1 and inactivation of the LKB1-AMPK axis, while simultaneously regulating mTORC1 localization via the GATOR1 complex (Figure 4.22). This suggests that mTORC1 localization does not always dictate its activity, and further, that once mTORC1 is activated at the lysosome, it must leave the lysosome in order to carry out its kinase activities. We hypothesize that MAP4K3 may activate mTORC1 at the lysosomes, then subsequently mobilize mTORC1 away from the lysosome, once it has been activated. In MAP4K3 k.o. cells, neither function of MAP4K3 is performed; therefore, we observe both mTORC1 inactivation and increased mTORC1 localization to lysosomes, two seemingly contradictory phenotypes. Further analysis is necessary to better understand the temporal qualities of MAP4K3 regulation of mTORC1 activity and localization, which are currently stunted by lack of reagents for *in vivo* time-lapse microscopy of mTORC1. Also, more work will need to be done to fully understand whether and how SIRT1 regulates LKB1 and AMPK activity.

In this study, we also investigate the interplay between SIRT1 and AMPK activity, which is currently proposed to comprise a positive feedback loop. Multiple studies show SIRT1 regulating LKB1 and AMPK activity. For example, Lan et al., demonstrated that overexpression of SIRT1 diminishes LKB1 acetylation and

increased LKB1 cytoplasmic localization and activity (Lan et al., 2008). Hou et al., demonstrated that activation of AMP by polyphenols requires the presence of both SIRT1 and LKB1 (Hou et al., 2008). Suchankova et al. show that SIRT1 inhibitors downregulated the activities of both AMPK and SIRT, while SIRT1 activators increased both proteins' activities (Suchankova et al., 2009). Simultaneously, AMPK has also been shown to activate SIRT1. Fulco et al. proposed that AMPK activates SIRT1 by upregulating the gene encoding the NAD+ synthetic enzyme nicotinamide phosphoribosyltransferase (NAMPT) (Fulco et al., 2008), while Canto et al. demonstrated that activated AMPK increased NAD+ levels and the NAD+/NADH ratio, resulting in SIRT1 activation (Canto et al., 2009). Our study supports SIRT1 activation of AMPK through deacetylation of LKB1, which can be further enforced by a feedback mechanism from AMPK activating SIRT1.

Further, while our study proposes direct regulation of SIRT1 by MAP4K3, indirect regulation of SIRT1 by MAP4K3 is certainly possible via the JNK pathway. MAP4K3 activates the JNK pathway upon stimulation with UV radiation and TNF-α and induces apoptosis by modulating pro-apoptotic Bcl-2 homology domain 3 (BH3)-only proteins post-transcriptionally via the JNK signaling pathway (Diener et al., 1997; Lam et al., 2009; Lam et al., 2010). SIRT1 has been shown to be downstream of JNK1 signaling in multiple studies. JNK1 phosphorylates SIRT1 at serine 27 and 47 and threonine 530 and increases its nuclear localization and enzymatic activity (Nasrin et al., 2009), while knockdown of JNK2 decreased SIRT1 phosphorylation at serine 27 and reduced the half-life of SIRT1 (Ford et al., 2008). Growth factors have also been shown to increase SIRT1 expression through JNK1-dependent signaling (Vinciguerra et al., 2012). Further work is necessary to elucidate how direct regulation

of SIRT1 by MAP4K3 is functionally different from indirect regulation via the JNK pathway.

In addition to the mTORC1 and JNK signaling pathway, the EGFR and Hippo signaling pathways have also been implicated to be downstream of MAP4K3. *Happyhour*, the *Drosophila* homologue of MAP4K3, was shown to inhibit the EGFR signaling pathway to regulate ethanol sensitivity (Corl et al., 2009). Separately, the MAP4K family of proteins were shown to be important physiological LATS-activating kinases in the Hippo signaling pathway (Meng et al., 2015). Furthermore, in addition to the metabolic functions of MAP4K3 proposed in this study, dysregulation of MAP4K3 has been associated with pancreatic cancer, though the mechanism by which MAP4K3 mutations induce tumorigenicity is not understood (Jones et al., 2008; Lam et al., 2009). It will thus be important to elucidate the interplay between these different signaling pathways and how MAP4K3 integrates regulation of these different pathways to cause physiological and pathological effects.

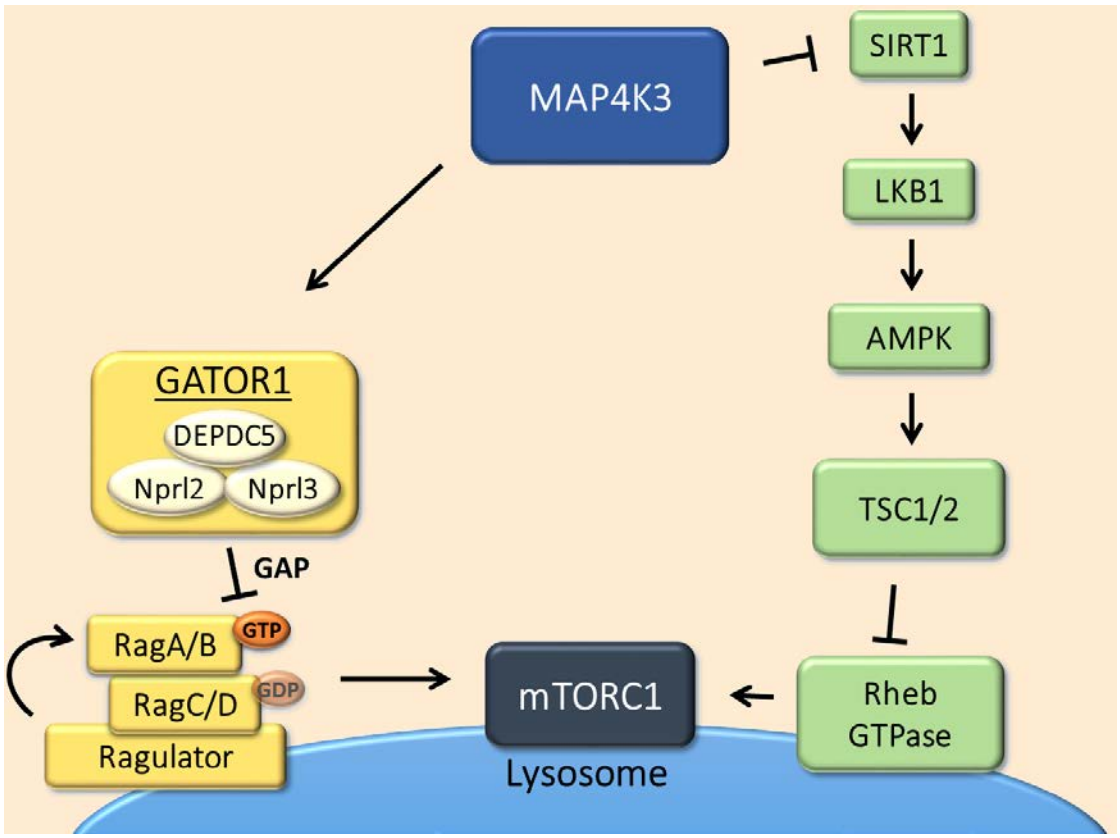

Figure 4.22. Schematic of mechanisms by which MAP4K3 mediates mTORC1 localization via the GATOR1 complex and mTORC1 activity via SIRT1 and the LKB1-AMPK axis.

Acknowledgements

Chapter 4 is an original document describing scientific work that is currently being prepared as a manuscript for submission in a much revised form. Hsu, C.L., Ohnishi, K., Lee, E.X., Meisenhelder, J., Paz, E.P., Hunter, T., and La Spada, A.R. “MAP4K3 regulates mTORC1 activity via AMPK signaling.” The dissertation author is the principal author of this work.

MATERIALS AND METHODS

Cell culture

HEK293A and HeLa cells were grown in DMEM media with 10% FBS. For amino acid deprivation (AAD), cells were treated with Earle's balanced salt solution (EBSS). For autophagic flux determination, Neuro2a cells were co-transfected with the mCherry-GFP-LC3 vector using Lipofectamine 2000, according to the manufacturer's instructions (Invitrogen). After 24 hrs, the media was replaced.

Primary Neuron Studies

Primary cortical neurons were cultured from postnatal day 0 (P0) C57BL/6J mice or GFP-LC3 transgenic mice (Mizushima et al., 2004). The primary neurons were prepared as described (Young et al., 2009). On day 4 after cell seeding, primary neurons were subjected to siRNA transfection, mimic transfection, anti-miR transfection, or lentiviral infection. On day 5, primary neurons were cultured in CM, NLM, or amino acid deprivation media (Earle's balanced salt solution, EBSS) for specific time courses, as described (Young et al., 2009). For mimic transfections, CM and NLM controls were run both with or without scrambled mimic control. For siRNA knockdown experiments, primary neurons were transfected with Silencer Select predesigned siRNA's using RNAi Max (Invitrogen). For mimic transfections, primary neurons were transfected with a stabilized miRNA mimic oligonucleotide let-7 or a scrambled miR-let-7 negative control, containing a 6 bp mismatch in the seed site (Dharmacon). The mimic negative control was used in all transfections, along with a siGLO red indicator to monitor transfection efficiency (Dharmacon). RT-PCR analysis

of mimic-transfected cells revealed a 4- to 10-fold increase in the expression level of the corresponding mature miRNA. For anti-miR transfections, primary neurons were transfected with 4 μg (6-well) or 1.6 μg (12-well) of a 2′-F/MOE modified anti-miR complementary to let-7 (Regulus Therapeutics) using Lipofectamine 2000 (Invitrogen).

Lentivirus infection

Transduction of primary neurons with Rheb Q64L lentivirus was confirmed by immunostaining of fixed neurons with anti-Flag antibody, and consistently revealed nearly complete transduction (>95%) of neurons, permitting counting of all neurons in experiments featuring Rheb Q64L lentivirus infection.

Luciferase Assays

Putative let-7 regulatory sites in amino acid sensing pathway genes were cloned from mouse cDNA libraries prepared from (1) wild-type mouse brain, (2) wild-type postnatal day 3 primary cortical neurons, or (3) mouse genomic DNA (gDNA; Promega). For cDNA synthesis, total RNA was extracted using TRIZOL and cDNA synthesized using SuperScript III first-strand synthesis system for RT-PCR with random hexamer primers (Invitrogen). Regions containing predicted let-7 binding sites are given in Supplemental Experimental Procedures. PCR amplicons were directionally cloned into the 3′ UTR of Renilla luciferase in the psiCHECK-2 dual luciferase plasmid (Promega), using XhoI and NotI restriction enzymes. PCR products were ligated using T4 DNA ligase (NEB) for 30 min at RT and transformed into DH5α competent E. coli cells (Invitrogen). Plasmid DNAs were obtained using

QIAprep Miniprep (QIAGEN) and sequenced. For dual luciferase experiments, HEK293T cells were cotransfected with 20 ng of psiCHECK-2 plasmid and 15 or 30 nM of miRVana miRNA mimic negative control #1 (#4464058), or mimic hsa-let-7f-5p (#4464066) using Lipofectamine 2000 (Invitrogen). Changes in relative luciferase were measured 24 hr later using the dual-luciferase reporter assay system (Promega) and quantified in triplicate using a Promega 96-well plate luminometer. Luciferase experiments were performed in triplicate, are shown as relative luciferase units (RLUs) after normalization of Renilla luciferase to endogenous firefly luciferase, and are shown relative to readouts obtained with mimic negative-control-treated samples.

Cell lysis and immunoprecipitation

Cells were rinsed twice with ice-cold PBS and lysed in ice-cold lysis buffer (25mM HEPES-KOH pH 7.4, 150mM NaCL, 5mM EDTA, 1% Triton X-10040 mM, one tablet of EDTA-free protease inhibitors (#11873580001 from Roche) per 10 mL of lysis buffer, and one tablet of PhosStop phosphatase inhibitor, as necessary. The soluble fractions from cell lysates were isolated by centrifugation at 8,000 rpm for 10 mins in a microfuge. Protein lysates were quantified using Pierce BCA Protein Assay Kit (Thermo Scientific) following the manufactures protocol. For immunoprecipitations, primary antibodies were incubated with Dynabeads® (Invitrogen) overnight, then washed with sterile PBS. Antibodies bound to Dynabeads were then incubated with lysates with rotation for 2 hours at 4°C. Immunoprecipitates were washed three times with lysis buffer. Immunoprecipitated proteins were denatured by the addition of 20 µl of sample buffer and boiling for 10 minutes at 70°C, resolved by SDS-PAGE, and analyzed via Western blot analysis.

Western Blot analysis

After SDS-PAGE, proteins were transferred to a 0.45 mm PVDF Immobilon-P membrane (EMD Millipore), and blocked for 1 hr at RT with 5% PBS-T milk. Membranes were incubated overnight with primary antibodies against: LC3 (Novus Biologicals, #NB100-2331) 1/3000; beta actin (abcam, #ab8226) 1/10000; Map4k3 (Cell Signaling #9613) 1/1000; RagA (Cell Signaling #4357) 1/1000; RagC (Cell Signaling #5466) 1/1000; and Lamtor1 (Cell Signaling #8975) 1/1000 in 5% PBST BSA. Antibodies and conditions for immunoblotting of mTOR, phospho-mTOR (S2448), S6K1, phospho-S6K1 (T421/S424), S6RP, and phospho-S6RP (S240/244) have already been described (Dubinsky 2014). Species-specific secondary antibodies were goat anti-rabbit IgG-HRP (Santa Cruz, #sc-2004) or goat anti-mouse IgG-HRP (Santa Cruz, #sc-2005), diluted 1/10,000 in 2% PBS-T milk and incubated for 1 hr at RT. Chemiluminescent signal detection was captured using Pierce ECL Plus Western Blotting Substrate (Thermo Scientific), and autoradiographic film, using standard techniques. Densitometry analysis was performed using ImageJ.

RNA analysis

RNA was extracted from cells using Trizol (Invitrogen). For quantification of mRNA expression, cDNA synthesis was performed using SuperScript III first-strand synthesis system and qRT-PCR was performed using SyberGreen master mix (Invitrogen) and probes (Sardiello 2009). qRT-PCR samples were prepared in triplicate, and fold change determined after normalization to GAPDH and negative

control treatment conditions. All QPCR was performed on an Applied Biosystem HT7500 RealTime PCR machine.

Immunocytochemistry

Cells were seeded in CC2-coated 8-chamber slides (Thermo Fisher) two days prior to experimentation and transfected as indicated. PBS-MC (1mM $MgCl_2$, 0.1mM $CaCl_2$, in PBS) was used for all washes and as a diluent for all solutions. Cells were fixed with 4% paraformaldehyde in PBS-MC for 12 minutes, then washed 3 times. Then 0.05% Triton-X in PBS-MC was used to permeabilize the cells for 5 minutes, followed by 2 washes in PBS-MC. Primary and secondary antibodies were diluted in 5% normal goat serum in PBS-MC. Cells were incubated in primary antibodies for 2 hours at room temperature, followed by 4 washes in PBS-MC. Cells were incubated in secondary antibodies for 1 hour at room temperature. Cells were washed 4 times in PBS-MC, then mounted with Prolong gold antifade reagent with DAPI (#P-36931 from Invitrogen). Images were captured with a Zeiss LSM 780 confocal microscopy and analyzed with Zen 2011 LSM 780 software and Image J.

Autophagy Assays

For autophagic induction in GFP-LC3 primary neurons, cells were scored as positive when >5 green puncta were observed. Cell counting for primary neurons was performed, using a Zeiss LSM 780 Observer.Z1 with Zen 2011 LSM 780 software, and only puncta superimposed on soma or within neurite processes were counted for at least 100 cells, from at least three fields per transfection, per experiment. For autophagic flux determination based on LC3 immunoblotting, we measured LC3-II

and actin levels by densitometry using NIH ImageJ and divided LC3-II:actin in the presence of NH4Cl by LC3-II:actin at baseline. For autophagic flux determination in HEK293A cells and primary cortical neurons transfected with the mCherry-GFP-LC3 vector, we performed confocal imaging as above, categorized puncta as yellow (autophagosomes) or red (autolysosomes), imaged ≥100 cells per experimental condition from at least three fields per transfection, and performed at least three separate experiments per condition.

Generation of MAP4K3 and TFEB knockout cells using CRISPR/Cas9 genome editing

The 20 nucleotide guide sequences targeting human TFEB and MAP4K3 were designed using the CRISPR design tool at http://crispr.mit.edu/ (Hsu et al., 2013) and cloned into a bicistronic expression vector (pX330) containing human codon–optimized Cas9 and the RNA components (Addgene).

The guide sequence targeting Exon 1 of human MAP4K3 and Exon 3 of TFEB are shown below.

MAP4K3: 5’ – TACCTTGTAGACGTCGCCGT – 3’

TFEB: 5’ – GAGTACCTGTCCGAGACCTA – 3’

The single guide RNAs (sgRNAs) in the pX330 vector (1 µg) were mixed with EGFP (0.1 µg; Clonetech) and co-transfected into HEK293A cells using Lipofectamine 2000 (Life Technologies) according to manufacturer’s instructions. 24 hrs post transfection, the cells were trypsinized, washed with PBS, and re-suspended in fluorescence-activated cell sorting (FACs) buffer (PBS, 5 mM EDTA, 2% FBS and Pen/Strep). GFP positive cells were single cell sorted by FACs (UCSD; Human

Embryonic Stem Cell Core, BDInflux) into 96- well plate format into DMEM containing 20% FBS and 50 µg ml-1 penicillin/streptomycin. Single clones were expanded, and screened for MAP4K3 and TFEB by protein immunoblotting. Genomic DNA (gDNA) was purified from clones using the DNeasy Blood & Tissue Kit (QIAGEN), and the region surrounding the protospacer adjacent motif (PAM) was amplified with Phusion® High-Fidelity DNA Polymerase (New England Biolabs) using the following primers:

MAP4K3:

Forward: 5' – GGAGCCGGGTGATTGTGA – 3'

Reverse: 5' – AGAAGGGAGGTGGCAAAAAT – 3'

TFEB:

Forward: 5' – CGTCACGCATAGGGTTGC – 3'

Reverse: 5' – CGTCCAGACGCATAATGTTG – 3'

PCR products were purified using the QIAquick PCR Purification Kit (QIAGEN) and cloned using the TOPO® TA Cloning (Life Technologies). To determine the exact mutations of individual alleles, at least 10 bacterial colonies were expanded and the plasmid DNA purified and sequenced.

In vitro kinase assay and phosphopeptide mapping

Respective proteins were transfected into HEK293T cells, immunoprecipitated individually, mixed with γ-32P-ATP in kinase buffer () at 30°C for 15 min, separated by SDS/PAGE and the gel dried. 32P incorporation into TFEB was determined by autoradiography and analyzed with a phosphorimager. For phosphopeptide mapping, 32P-labeled TFEB was extracted from the dried gel and precipitated with TCA. The

precipitated protein was oxidized, digested with trypsin, lyophilized, and the tryptic peptide mix spotted onto a TLC plate. The peptides were then resolved by electrophoresis and chromatography in two dimensions and visualized by autoradiography. Circles indicate location of the phospho-S3 peptide.

Statistical Analysis

All data were prepared for analysis with standard spread sheet software (Microsoft Excel). Statistical analysis was done using Microsoft Excel, Prism 5.0 (Graph Pad), or the VassarStats website (http://faculty.vassar.edu/lowry/VassarStats.html). For ANOVA, if statistical significance ($p < 0.05$) was achieved, we performed post hoc analysis to account for multiple comparisons. The level of significance (alpha) was always set at 0.05.

REFERENCES

Avruch, J. (2007). MAP kinase pathways: the first twenty years. Biochim Biophys Acta *1773*, 1150-1160.

Bar-Peled, L., Chantranupong, L., Cherniack, A.D., Chen, W.W., Ottina, K.A., Grabiner, B.C., Spear, E.D., Carter, S.L., Meyerson, M., and Sabatini, D.M. (2013). A Tumor suppressor complex with GAP activity for the Rag GTPases that signal amino acid sufficiency to mTORC1. Science *340*, 1100-1106.

Bar-Peled, L., Schweitzer, L.D., Zoncu, R., and Sabatini, D.M. (2012). Ragulator is a GEF for the rag GTPases that signal amino acid levels to mTORC1. Cell *150*, 1196-1208.

Bartel, D.P. (2009). MicroRNAs: target recognition and regulatory functions. Cell *136*, 215-233.

Boudeau, J., Baas, A.F., Deak, M., Morrice, N.A., Kieloch, A., Schutkowski, M., Prescott, A.R., Clevers, H.C., and Alessi, D.R. (2003). MO25alpha/beta interact with STRADalpha/beta enhancing their ability to bind, activate and localize LKB1 in the cytoplasm. The EMBO journal *22*, 5102-5114.

Boya, P., Reggiori, F., and Codogno, P. (2013). Emerging regulation and functions of autophagy. Nat Cell Biol *15*, 713-720.

Bryk, B., Hahn, K., Cohen, S.M., and Teleman, A.A. (2010). MAP4K3 regulates body size and metabolism in Drosophila. Dev Biol *344*, 150-157.

Canto, C., Gerhart-Hines, Z., Feige, J.N., Lagouge, M., Noriega, L., Milne, J.C., Elliott, P.J., Puigserver, P., and Auwerx, J. (2009). AMPK regulates energy expenditure by modulating NAD+ metabolism and SIRT1 activity. Nature *458*, 1056-1060.

Carroll, B., Maetzel, D., Maddocks, O.D., Otten, G., Ratcliff, M., Smith, G.R., Dunlop, E.A., Passos, J.F., Davies, O.R., Jaenisch, R., Tee, A.R., Sarkar, S., and Korolchuk, V.I. (2016). Control of TSC2-Rheb signaling axis by arginine regulates mTORC1 activity. Elife *5*.

Chantranupong, L., Scaria, S.M., Saxton, R.A., Gygi, M.P., Shen, K., Wyant, G.A., Wang, T., Harper, J.W., Gygi, S.P., and Sabatini, D.M. (2016). The CASTOR Proteins Are Arginine Sensors for the mTORC1 Pathway. Cell *165*, 153-164.

Chen, D.Y., Chuang, H.C., Lan, J.L., Chen, Y.M., Hung, W.T., Lai, K.L., and Tan, T.H. (2012). Germinal center kinase-like kinase (GLK/MAP4K3) expression is increased in adult-onset Still's disease and may act as an activity marker. BMC Med *10*, 84.

Chi, S.W., Zang, J.B., Mele, A., and Darnell, R.B. (2009). Argonaute HITS-CLIP decodes microRNA-mRNA interaction maps. Nature *460*, 479-486.

Corl, A.B., Berger, K.H., Ophir-Shohat, G., Gesch, J., Simms, J.A., Bartlett, S.E., and Heberlein, U. (2009). Happyhour, a Ste20 family kinase, implicates EGFR signaling in ethanol-induced behaviors. Cell *137*, 949-960.

Dazert, E., and Hall, M.N. (2011). mTOR signaling in disease. Current opinion in cell biology *23*, 744-755.

Dhanasekaran, D.N., and Johnson, G.L. (2007). MAPKs: function, regulation, role in cancer and therapeutic targeting. Oncogene *26*, 3097-3099.

Diener, K., Wang, X.S., Chen, C., Meyer, C.F., Keesler, G., Zukowski, M., Tan, T.H., and Yao, Z. (1997). Activation of the c-Jun N-terminal kinase pathway by a novel protein kinase related to human germinal center kinase. Proceedings of the National Academy of Sciences of the United States of America *94*, 9687-9692.

Dubinsky, A.N., Dastidar, S.G., Hsu, C.L., Zahra, R., Djakovic, S.N., Duarte, S., Esau, C.C., Spencer, B., Ashe, T.D., Fischer, K.M., MacKenna, D.A., Sopher, B.L., Masliah, E., Gaasterland, T., Chau, B.N., Pereira de Almeida, L., Morrison, B.E., and La Spada, A.R. (2014). Let-7 coordinately suppresses components of the amino acid sensing pathway to repress mTORC1 and induce autophagy. Cell metabolism *20*, 626-638.

Efeyan, A., Zoncu, R., Chang, S., Gumper, I., Snitkin, H., Wolfson, R.L., Kirak, O., Sabatini, D.D., and Sabatini, D.M. (2013). Regulation of mTORC1 by the Rag GTPases is necessary for neonatal autophagy and survival. Nature *493*, 679-683.

Escande, C., Chini, C.C., Nin, V., Dykhouse, K.M., Novak, C.M., Levine, J., van Deursen, J., Gores, G.J., Chen, J., Lou, Z., and Chini, E.N. (2010). Deleted in breast cancer-1 regulates SIRT1 activity and contributes to high-fat diet-induced liver steatosis in mice. The Journal of clinical investigation *120*, 545-558.

Findlay, G.M., Yan, L., Procter, J., Mieulet, V., and Lamb, R.F. (2007). A MAP4 kinase related to Ste20 is a nutrient-sensitive regulator of mTOR signalling. The Biochemical journal *403*, 13-20.

Fineberg, S.K., Kosik, K.S., and Davidson, B.L. (2009). MicroRNAs potentiate neural development. Neuron *64*, 303-309.

Ford, J., Ahmed, S., Allison, S., Jiang, M., and Milner, J. (2008). JNK2-dependent regulation of SIRT1 protein stability. Cell Cycle *7*, 3091-3097.

Fulco, M., Cen, Y., Zhao, P., Hoffman, E.P., McBurney, M.W., Sauve, A.A., and Sartorelli, V. (2008). Glucose restriction inhibits skeletal myoblast differentiation by activating SIRT1 through AMPK-mediated regulation of Nampt. Developmental cell *14*, 661-673.

Ganley, I.G., Lam du, H., Wang, J., Ding, X., Chen, S., and Jiang, X. (2009). ULK1.ATG13.FIP200 complex mediates mTOR signaling and is essential for autophagy. The Journal of biological chemistry *284*, 12297-12305.

Gao, M., and Kaiser, C.A. (2006). A conserved GTPase-containing complex is required for intracellular sorting of the general amino-acid permease in yeast. Nat Cell Biol *8*, 657-667.

Garami, A., Zwartkruis, F.J., Nobukuni, T., Joaquin, M., Roccio, M., Stocker, H., Kozma, S.C., Hafen, E., Bos, J.L., and Thomas, G. (2003). Insulin activation of Rheb, a mediator of mTOR/S6K/4E-BP signaling, is inhibited by TSC1 and 2. Molecular cell *11*, 1457-1466.

Gwinn, D.M., Shackelford, D.B., Egan, D.F., Mihaylova, M.M., Mery, A., Vasquez, D.S., Turk, B.E., and Shaw, R.J. (2008). AMPK phosphorylation of raptor mediates a metabolic checkpoint. Molecular cell *30*, 214-226.

Haghighat, A., Mader, S., Pause, A., and Sonenberg, N. (1995). Repression of cap-dependent translation by 4E-binding protein 1: competition with p220 for binding to eukaryotic initiation factor-4E. The EMBO journal *14*, 5701-5709.

Han, J.M., Jeong, S.J., Park, M.C., Kim, G., Kwon, N.H., Kim, H.K., Ha, S.H., Ryu, S.H., and Kim, S. (2012). Leucyl-tRNA synthetase is an intracellular leucine sensor for the mTORC1-signaling pathway. Cell *149*, 410-424.

Hara, K., Maruki, Y., Long, X., Yoshino, K., Oshiro, N., Hidayat, S., Tokunaga, C., Avruch, J., and Yonezawa, K. (2002). Raptor, a binding partner of target of rapamycin (TOR), mediates TOR action. Cell *110*, 177-189.

Hara, K., Yonezawa, K., Kozlowski, M.T., Sugimoto, T., Andrabi, K., Weng, Q.P., Kasuga, M., Nishimoto, I., and Avruch, J. (1997). Regulation of eIF-4E BP1 phosphorylation by mTOR. The Journal of biological chemistry *272*, 26457-26463.

Hara, K., Yonezawa, K., Weng, Q.P., Kozlowski, M.T., Belham, C., and Avruch, J. (1998). Amino acid sufficiency and mTOR regulate p70 S6 kinase and eIF-4E BP1 through a common effector mechanism. The Journal of biological chemistry *273*, 14484-14494.

Hawley, S.A., Boudeau, J., Reid, J.L., Mustard, K.J., Udd, L., Makela, T.P., Alessi, D.R., and Hardie, D.G. (2003). Complexes between the LKB1 tumor suppressor, STRAD alpha/beta and MO25 alpha/beta are upstream kinases in the AMP-activated protein kinase cascade. J Biol *2*, 28.

Holz, M.K., Ballif, B.A., Gygi, S.P., and Blenis, J. (2005). mTOR and S6K1 mediate assembly of the translation preinitiation complex through dynamic protein interchange and ordered phosphorylation events. Cell *123*, 569-580.

Hosokawa, N., Hara, T., Kaizuka, T., Kishi, C., Takamura, A., Miura, Y., Iemura, S., Natsume, T., Takehana, K., Yamada, N., Guan, J.L., Oshiro, N., and Mizushima, N.

(2009a). Nutrient-dependent mTORC1 association with the ULK1-Atg13-FIP200 complex required for autophagy. Molecular biology of the cell *20*, 1981-1991.

Hosokawa, N., Sasaki, T., Iemura, S., Natsume, T., Hara, T., and Mizushima, N. (2009b). Atg101, a novel mammalian autophagy protein interacting with Atg13. Autophagy *5*, 973-979.

Hou, X., Xu, S., Maitland-Toolan, K.A., Sato, K., Jiang, B., Ido, Y., Lan, F., Walsh, K., Wierzbicki, M., Verbeuren, T.J., Cohen, R.A., and Zang, M. (2008). SIRT1 regulates hepatocyte lipid metabolism through activating AMP-activated protein kinase. The Journal of biological chemistry *283*, 20015-20026.

Howell, J.J., and Manning, B.D. (2011). mTOR couples cellular nutrient sensing to organismal metabolic homeostasis. Trends Endocrinol Metab *22*, 94-102.

Hsu, P.D., Scott, D.A., Weinstein, J.A., Ran, F.A., Konermann, S., Agarwala, V., Li, Y., Fine, E.J., Wu, X., Shalem, O., Cradick, T.J., Marraffini, L.A., Bao, G., and Zhang, F. (2013). DNA targeting specificity of RNA-guided Cas9 nucleases. Nature biotechnology *31*, 827-832.

Huang, Y., Shen, X.J., Zou, Q., Wang, S.P., Tang, S.M., and Zhang, G.Z. (2011). Biological functions of microRNAs: a review. J Physiol Biochem *67*, 129-139.

Inoki, K., Li, Y., Xu, T., and Guan, K.L. (2003a). Rheb GTPase is a direct target of TSC2 GAP activity and regulates mTOR signaling. Genes & development *17*, 1829-1834.

Inoki, K., Li, Y., Zhu, T., Wu, J., and Guan, K.L. (2002). TSC2 is phosphorylated and inhibited by Akt and suppresses mTOR signalling. Nat Cell Biol *4*, 648-657.

Inoki, K., Ouyang, H., Zhu, T., Lindvall, C., Wang, Y., Zhang, X., Yang, Q., Bennett, C., Harada, Y., Stankunas, K., Wang, C.Y., He, X., MacDougald, O.A., You, M., Williams, B.O., and Guan, K.L. (2006). TSC2 integrates Wnt and energy signals via a coordinated phosphorylation by AMPK and GSK3 to regulate cell growth. Cell *126*, 955-968.

Inoki, K., Zhu, T., and Guan, K.L. (2003b). TSC2 mediates cellular energy response to control cell growth and survival. Cell *115*, 577-590.

Jacinto, E., Loewith, R., Schmidt, A., Lin, S., Ruegg, M.A., Hall, A., and Hall, M.N. (2004). Mammalian TOR complex 2 controls the actin cytoskeleton and is rapamycin insensitive. Nat Cell Biol *6*, 1122-1128.

Jaeschke, A., Hartkamp, J., Saitoh, M., Roworth, W., Nobukuni, T., Hodges, A., Sampson, J., Thomas, G., and Lamb, R. (2002). Tuberous sclerosis complex tumor suppressor-mediated S6 kinase inhibition by phosphatidylinositide-3-OH kinase is mTOR independent. The Journal of cell biology *159*, 217-224.

Jewell, J.L., Russell, R.C., and Guan, K.L. (2013). Amino acid signalling upstream of mTOR. Nature reviews. Molecular cell biology *14*, 133-139.

Johnson, S.M., Grosshans, H., Shingara, J., Byrom, M., Jarvis, R., Cheng, A., Labourier, E., Reinert, K.L., Brown, D., and Slack, F.J. (2005). RAS is regulated by the let-7 microRNA family. Cell *120*, 635-647.

Jones, S., Zhang, X., Parsons, D.W., Lin, J.C., Leary, R.J., Angenendt, P., Mankoo, P., Carter, H., Kamiyama, H., Jimeno, A., Hong, S.M., Fu, B., Lin, M.T., Calhoun, E.S., Kamiyama, M., Walter, K., Nikolskaya, T., Nikolsky, Y., Hartigan, J., Smith, D.R., Hidalgo, M., Leach, S.D., Klein, A.P., Jaffee, E.M., Goggins, M., Maitra, A., Iacobuzio-Donahue, C., Eshleman, J.R., Kern, S.E., Hruban, R.H., Karchin, R., Papadopoulos, N., Parmigiani, G., Vogelstein, B., Velculescu, V.E., and Kinzler, K.W. (2008). Core signaling pathways in human pancreatic cancers revealed by global genomic analyses. Science *321*, 1801-1806.

Jung, C.H., Jun, C.B., Ro, S.H., Kim, Y.M., Otto, N.M., Cao, J., Kundu, M., and Kim, D.H. (2009). ULK-Atg13-FIP200 complexes mediate mTOR signaling to the autophagy machinery. Molecular biology of the cell *20*, 1992-2003.

Kaeberlein, M., McVey, M., and Guarente, L. (1999). The SIR2/3/4 complex and SIR2 alone promote longevity in Saccharomyces cerevisiae by two different mechanisms. Genes & development *13*, 2570-2580.

Kaizuka, T., Hara, T., Oshiro, N., Kikkawa, U., Yonezawa, K., Takehana, K., Iemura, S., Natsume, T., and Mizushima, N. (2010). Tti1 and Tel2 are critical factors in mammalian target of rapamycin complex assembly. The Journal of biological chemistry *285*, 20109-20116.

Kanazawa, T., Taneike, I., Akaishi, R., Yoshizawa, F., Furuya, N., Fujimura, S., and Kadowaki, M. (2004). Amino acids and insulin control autophagic proteolysis through different signaling pathways in relation to mTOR in isolated rat hepatocytes. The Journal of biological chemistry *279*, 8452-8459.

Khan, M.H., Hart, M.J., and Rea, S.L. (2012). The role of MAP4K3 in lifespan regulation of Caenorhabditis elegans. Biochemical and biophysical research communications *425*, 413-418.

Kilpatrick, K., Zeng, Y., Hancock, T., and Segatori, L. (2015). Genetic and chemical activation of TFEB mediates clearance of aggregated alpha-synuclein. PloS one *10*, e0120819.

Kim, D.H. (2003). GbetaL, a positive regulator of the rapamycin-sensitive pathway required for the nutrient-sensitive interaction between raptor and mTOR. Mol. Cell *11*, 895-904.

Kim, E., Goraksha-Hicks, P., Li, L., Neufeld, T.P., and Guan, K.L. (2008a). Regulation of TORC1 by Rag GTPases in nutrient response. Nat Cell Biol *10*, 935-945.

Kim, J.E., Chen, J., and Lou, Z. (2008b). DBC1 is a negative regulator of SIRT1. Nature *451*, 583-586.

Kim, Y.C., Park, H.W., Sciarretta, S., Mo, J.S., Jewell, J.L., Russell, R.C., Wu, X., Sadoshima, J., and Guan, K.L. (2014). Rag GTPases are cardioprotective by regulating lysosomal function. Nat Commun *5*, 4241.

Klionsky, D.J., Abdalla, F.C., Abeliovich, H., Abraham, R.T., Acevedo-Arozena, A., Adeli, K., Agholme, L., Agnello, M., Agostinis, P., Aguirre-Ghiso, J.A., Ahn, H.J., Ait-Mohamed, O., Ait-Si-Ali, S., Akematsu, T., Akira, S., Al-Younes, H.M., Al-Zeer, M.A., Albert, M.L., Albin, R.L., Alegre-Abarrategui, J., Aleo, M.F., Alirezaei, M., Almasan, A., Almonte-Becerril, M., Amano, A., Amaravadi, R., Amarnath, S., Amer, A.O., Andrieu-Abadie, N., Anantharam, V., Ann, D.K., Anoopkumar-Dukie, S., Aoki, H., Apostolova, N., Arancia, G., Aris, J.P., Asanuma, K., Asare, N.Y., Ashida, H., Askanas, V., Askew, D.S., Auberger, P., Baba, M., Backues, S.K., Baehrecke, E.H., Bahr, B.A., Bai, X.Y., Bailly, Y., Baiocchi, R., Baldini, G., Balduini, W., Ballabio, A., Bamber, B.A., Bampton, E.T., Banhegyi, G., Bartholomew, C.R., Bassham, D.C., Bast, R.C., Jr., Batoko, H., Bay, B.H., Beau, I., Bechet, D.M., Begley, T.J., Behl, C., Behrends, C., Bekri, S., Bellaire, B., Bendall, L.J., Benetti, L., Berliocchi, L., Bernardi, H., Bernassola, F., Besteiro, S., Bhatia-Kissova, I., Bi, X., Biard-Piechaczyk, M., Blum, J.S., Boise, L.H., Bonaldo, P., Boone, D.L., Bornhauser, B.C., Bortoluci, K.R., Bossis, I., Bost, F., Bourquin, J.P., Boya, P., Boyer-Guittaut, M., Bozhkov, P.V., Brady, N.R., Brancolini, C., Brech, A., Brenman, J.E., Brennand, A., Bresnick, E.H., Brest, P., Bridges, D., Bristol, M.L., Brookes, P.S., Brown, E.J., Brumell, J.H., Brunetti-Pierri, N., Brunk, U.T., Bulman, D.E., Bultman, S.J., Bultynck, G., Burbulla, L.F., Bursch, W., Butchar, J.P., Buzgariu, W., Bydlowski, S.P., Cadwell, K., Cahova, M., Cai, D., Cai, J., Cai, Q., Calabretta, B., Calvo-Garrido, J., Camougrand, N., Campanella, M., Campos-Salinas, J., Candi, E., Cao, L., Caplan, A.B., Carding, S.R., Cardoso, S.M., Carew, J.S., Carlin, C.R., Carmignac, V., Carneiro, L.A., Carra, S., Caruso, R.A., Casari, G., Casas, C., Castino, R., Cebollero, E., Cecconi, F., Celli, J., Chaachouay, H., Chae, H.J., Chai, C.Y., Chan, D.C., Chan, E.Y., Chang, R.C., Che, C.M., Chen, C.C., Chen, G.C., Chen, G.Q., Chen, M., Chen, Q., Chen, S.S., Chen, W., Chen, X., Chen, X., Chen, X., Chen, Y.G., Chen, Y., Chen, Y., Chen, Y.J., Chen, Z., Cheng, A., Cheng, C.H., Cheng, Y., Cheong, H., Cheong, J.H., Cherry, S., Chess-Williams, R., Cheung, Z.H., Chevet, E., Chiang, H.L., Chiarelli, R., Chiba, T., Chin, L.S., Chiou, S.H., Chisari, F.V., Cho, C.H., Cho, D.H., Choi, A.M., Choi, D., Choi, K.S., Choi, M.E., Chouaib, S., Choubey, D., Choubey, V., Chu, C.T., Chuang, T.H., Chueh, S.H., Chun, T., Chwae, Y.J., Chye, M.L., Ciarcia, R., Ciriolo, M.R., Clague, M.J., Clark, R.S., Clarke, P.G., Clarke, R., Codogno, P., Coller, H.A., Colombo, M.I., Comincini, S., Condello, M., Condorelli, F., Cookson, M.R., Coombs, G.H., Coppens, I., Corbalan, R., Cossart, P., Costelli, P., Costes, S., Coto-Montes, A., Couve, E., Coxon, F.P., Cregg, J.M., Crespo, J.L., Cronje, M.J., Cuervo, A.M., Cullen, J.J., Czaja, M.J., D'Amelio, M., Darfeuille-Michaud, A., Davids, L.M., Davies, F.E., De Felici, M., de Groot, J.F., de Haan, C.A., De Martino, L., De Milito, A., De Tata, V., Debnath, J., Degterev, A., Dehay, B., Delbridge, L.M., Demarchi, F., Deng, Y.Z., Dengjel, J., Dent, P., Denton, D., Deretic, V., Desai, S.D., Devenish, R.J., Di Gioacchino, M., Di Paolo, G., Di Pietro, C., Diaz-Araya, G., Diaz-Laviada, I., Diaz-Meco, M.T., Diaz-Nido, J., Dikic, I., Dinesh-Kumar, S.P., Ding, W.X., Distelhorst, C.W., Diwan, A., Djavaheri-

Mergny, M., Dokudovskaya, S., Dong, Z., Dorsey, F.C., Dosenko, V., Dowling, J.J., Doxsey, S., Dreux, M., Drew, M.E., Duan, Q., Duchosal, M.A., Duff, K., Dugail, I., Durbeej, M., Duszenko, M., Edelstein, C.L., Edinger, A.L., Egea, G., Eichinger, L., Eissa, N.T., Ekmekcioglu, S., El-Deiry, W.S., Elazar, Z., Elgendy, M., Ellerby, L.M., Eng, K.E., Engelbrecht, A.M., Engelender, S., Erenpreisa, J., Escalante, R., Esclatine, A., Eskelinen, E.L., Espert, L., Espina, V., Fan, H., Fan, J., Fan, Q.W., Fan, Z., Fang, S., Fang, Y., Fanto, M., Fanzani, A., Farkas, T., Farre, J.C., Faure, M., Fechheimer, M., Feng, C.G., Feng, J., Feng, Q., Feng, Y., Fesus, L., Feuer, R., Figueiredo-Pereira, M.E., Fimia, G.M., Fingar, D.C., Finkbeiner, S., Finkel, T., Finley, K.D., Fiorito, F., Fisher, E.A., Fisher, P.B., Flajolet, M., Florez-McClure, M.L., Florio, S., Fon, E.A., Fornai, F., Fortunato, F., Fotedar, R., Fowler, D.H., Fox, H.S., Franco, R., Frankel, L.B., Fransen, M., Fuentes, J.M., Fueyo, J., Fujii, J., Fujisaki, K., Fujita, E., Fukuda, M., Furukawa, R.H., Gaestel, M., Gailly, P., Gajewska, M., Galliot, B., Galy, V., Ganesh, S., Ganetzky, B., Ganley, I.G., Gao, F.B., Gao, G.F., Gao, J., Garcia, L., Garcia-Manero, G., Garcia-Marcos, M., Garmyn, M., Gartel, A.L., Gatti, E., Gautel, M., Gawriluk, T.R., Gegg, M.E., Geng, J., Germain, M., Gestwicki, J.E., Gewirtz, D.A., Ghavami, S., Ghosh, P., Giammarioli, A.M., Giatromanolaki, A.N., Gibson, S.B., Gilkerson, R.W., Ginger, M.L., Ginsberg, H.N., Golab, J., Goligorsky, M.S., Golstein, P., Gomez-Manzano, C., Goncu, E., Gongora, C., Gonzalez, C.D., Gonzalez, R., Gonzalez-Estevez, C., Gonzalez-Polo, R.A., Gonzalez-Rey, E., Gorbunov, N.V., Gorski, S., Goruppi, S., Gottlieb, R.A., Gozuacik, D., Granato, G.E., Grant, G.D., Green, K.N., Gregorc, A., Gros, F., Grose, C., Grunt, T.W., Gual, P., Guan, J.L., Guan, K.L., Guichard, S.M., Gukovskaya, A.S., Gukovsky, I., Gunst, J., Gustafsson, A.B., Halayko, A.J., Hale, A.N., Halonen, S.K., Hamasaki, M., Han, F., Han, T., Hancock, M.K., Hansen, M., Harada, H., Harada, M., Hardt, S.E., Harper, J.W., Harris, A.L., Harris, J., Harris, S.D., Hashimoto, M., Haspel, J.A., Hayashi, S., Hazelhurst, L.A., He, C., He, Y.W., Hebert, M.J., Heidenreich, K.A., Helfrich, M.H., Helgason, G.V., Henske, E.P., Herman, B., Herman, P.K., Hetz, C., Hilfiker, S., Hill, J.A., Hocking, L.J., Hofman, P., Hofmann, T.G., Hohfeld, J., Holyoake, T.L., Hong, M.H., Hood, D.A., Hotamisligil, G.S., Houwerzijl, E.J., Hoyer-Hansen, M., Hu, B., Hu, C.A., Hu, H.M., Hua, Y., Huang, C., Huang, J., Huang, S., Huang, W.P., Huber, T.B., Huh, W.K., Hung, T.H., Hupp, T.R., Hur, G.M., Hurley, J.B., Hussain, S.N., Hussey, P.J., Hwang, J.J., Hwang, S., Ichihara, A., Ilkhanizadeh, S., Inoki, K., Into, T., Iovane, V., Iovanna, J.L., Ip, N.Y., Isaka, Y., Ishida, H., Isidoro, C., Isobe, K., Iwasaki, A., Izquierdo, M., Izumi, Y., Jaakkola, P.M., Jaattela, M., Jackson, G.R., Jackson, W.T., Janji, B., Jendrach, M., Jeon, J.H., Jeung, E.B., Jiang, H., Jiang, H., Jiang, J.X., Jiang, M., Jiang, Q., Jiang, X., Jiang, X., Jimenez, A., Jin, M., Jin, S., Joe, C.O., Johansen, T., Johnson, D.E., Johnson, G.V., Jones, N.L., Joseph, B., Joseph, S.K., Joubert, A.M., Juhasz, G., Juillerat-Jeanneret, L., Jung, C.H., Jung, Y.K., Kaarniranta, K., Kaasik, A., Kabuta, T., Kadowaki, M., Kagedal, K., Kamada, Y., Kaminskyy, V.O., Kampinga, H.H., Kanamori, H., Kang, C., Kang, K.B., Kang, K.I., Kang, R., Kang, Y.A., Kanki, T., Kanneganti, T.D., Kanno, H., Kanthasamy, A.G., Kanthasamy, A., Karantza, V., Kaushal, G.P., Kaushik, S., Kawazoe, Y., Ke, P.Y., Kehrl, J.H., Kelekar, A., Kerkhoff, C., Kessel, D.H., Khalil, H., Kiel, J.A., Kiger, A.A., Kihara, A., Kim, D.R., Kim, D.H., Kim, D.H., Kim, E.K., Kim, H.R., Kim, J.S., Kim, J.H., Kim, J.C., Kim, J.K., Kim, P.K., Kim, S.W., Kim, Y.S., Kim, Y., Kimchi, A., Kimmelman, A.C., King, J.S., Kinsella, T.J., Kirkin, V., Kirshenbaum, L.A., Kitamoto, K., Kitazato, K., Klein, L., Klimecki, W.T., Klucken, J., Knecht, E., Ko, B.C., Koch, J.C., Koga, H., Koh, J.Y.,

Koh, Y.H., Koike, M., Komatsu, M., Kominami, E., Kong, H.J., Kong, W.J., Korolchuk, V.I., Kotake, Y., Koukourakis, M.I., Kouri Flores, J.B., Kovacs, A.L., Kraft, C., Krainc, D., Kramer, H., Kretz-Remy, C., Krichevsky, A.M., Kroemer, G., Kruger, R., Krut, O., Ktistakis, N.T., Kuan, C.Y., Kucharczyk, R., Kumar, A., Kumar, R., Kumar, S., Kundu, M., Kung, H.J., Kurz, T., Kwon, H.J., La Spada, A.R., Lafont, F., Lamark, T., Landry, J., Lane, J.D., Lapaquette, P., Laporte, J.F., Laszlo, L., Lavandero, S., Lavoie, J.N., Layfield, R., Lazo, P.A., Le, W., Le Cam, L., Ledbetter, D.J., Lee, A.J., Lee, B.W., Lee, G.M., Lee, J., Lee, J.H., Lee, M., Lee, M.S., Lee, S.H., Leeuwenburgh, C., Legembre, P., Legouis, R., Lehmann, M., Lei, H.Y., Lei, Q.Y., Leib, D.A., Leiro, J., Lemasters, J.J., Lemoine, A., Lesniak, M.S., Lev, D., Levenson, V.V., Levine, B., Levy, E., Li, F., Li, J.L., Li, L., Li, S., Li, W., Li, X.J., Li, Y.B., Li, Y.P., Liang, C., Liang, Q., Liao, Y.F., Liberski, P.P., Lieberman, A., Lim, H.J., Lim, K.L., Lim, K., Lin, C.F., Lin, F.C., Lin, J., Lin, J.D., Lin, K., Lin, W.W., Lin, W.C., Lin, Y.L., Linden, R., Lingor, P., Lippincott-Schwartz, J., Lisanti, M.P., Liton, P.B., Liu, B., Liu, C.F., Liu, K., Liu, L., Liu, Q.A., Liu, W., Liu, Y.C., Liu, Y., Lockshin, R.A., Lok, C.N., Lonial, S., Loos, B., Lopez-Berestein, G., Lopez-Otin, C., Lossi, L., Lotze, M.T., Low, P., Lu, B., Lu, B., Lu, B., Lu, Z., Luciano, F., Lukacs, N.W., Lund, A.H., Lynch-Day, M.A., Ma, Y., Macian, F., MacKeigan, J.P., Macleod, K.F., Madeo, F., Maiuri, L., Maiuri, M.C., Malagoli, D., Malicdan, M.C., Malorni, W., Man, N., Mandelkow, E.M., Manon, S., Manov, I., Mao, K., Mao, X., Mao, Z., Marambaud, P., Marazziti, D., Marcel, Y.L., Marchbank, K., Marchetti, P., Marciniak, S.J., Marcondes, M., Mardi, M., Marfe, G., Marino, G., Markaki, M., Marten, M.R., Martin, S.J., Martinand-Mari, C., Martinet, W., Martinez-Vicente, M., Masini, M., Matarrese, P., Matsuo, S., Matteoni, R., Mayer, A., Mazure, N.M., McConkey, D.J., McConnell, M.J., McDermott, C., McDonald, C., McInerney, G.M., McKenna, S.L., McLaughlin, B., McLean, P.J., McMaster, C.R., McQuibban, G.A., Meijer, A.J., Meisler, M.H., Melendez, A., Melia, T.J., Melino, G., Mena, M.A., Menendez, J.A., Menna-Barreto, R.F., Menon, M.B., Menzies, F.M., Mercer, C.A., Merighi, A., Merry, D.E., Meschini, S., Meyer, C.G., Meyer, T.F., Miao, C.Y., Miao, J.Y., Michels, P.A., Michiels, C., Mijaljica, D., Milojkovic, A., Minucci, S., Miracco, C., Miranti, C.K., Mitroulis, I., Miyazawa, K., Mizushima, N., Mograbi, B., Mohseni, S., Molero, X., Mollereau, B., Mollinedo, F., Momoi, T., Monastyrska, I., Monick, M.M., Monteiro, M.J., Moore, M.N., Mora, R., Moreau, K., Moreira, P.I., Moriyasu, Y., Moscat, J., Mostowy, S., Mottram, J.C., Motyl, T., Moussa, C.E., Muller, S., Muller, S., Munger, K., Munz, C., Murphy, L.O., Murphy, M.E., Musaro, A., Mysorekar, I., Nagata, E., Nagata, K., Nahimana, A., Nair, U., Nakagawa, T., Nakahira, K., Nakano, H., Nakatogawa, H., Nanjundan, M., Naqvi, N.I., Narendra, D.P., Narita, M., Navarro, M., Nawrocki, S.T., Nazarko, T.Y., Nemchenko, A., Netea, M.G., Neufeld, T.P., Ney, P.A., Nezis, I.P., Nguyen, H.P., Nie, D., Nishino, I., Nislow, C., Nixon, R.A., Noda, T., Noegel, A.A., Nogalska, A., Noguchi, S., Notterpek, L., Novak, I., Nozaki, T., Nukina, N., Nurnberger, T., Nyfeler, B., Obara, K., Oberley, T.D., Oddo, S., Ogawa, M., Ohashi, T., Okamoto, K., Oleinick, N.L., Oliver, F.J., Olsen, L.J., Olsson, S., Opota, O., Osborne, T.F., Ostrander, G.K., Otsu, K., Ou, J.H., Ouimet, M., Overholtzer, M., Ozpolat, B., Paganetti, P., Pagnini, U., Pallet, N., Palmer, G.E., Palumbo, C., Pan, T., Panaretakis, T., Pandey, U.B., Papackova, Z., Papassideri, I., Paris, I., Park, J., Park, O.K., Parys, J.B., Parzych, K.R., Patschan, S., Patterson, C., Pattingre, S., Pawelek, J.M., Peng, J., Perlmutter, D.H., Perrotta, I., Perry, G., Pervaiz, S., Peter, M., Peters, G.J., Petersen, M., Petrovski, G., Phang, J.M., Piacentini, M., Pierre, P., Pierrefite-Carle, V., Pierron, G., Pinkas-Kramarski, R., Piras, A., Piri, N., Platanias, L.C.,

Poggeler, S., Poirot, M., Poletti, A., Pous, C., Pozuelo-Rubio, M., Praetorius-Ibba, M., Prasad, A., Prescott, M., Priault, M., Produit-Zengaffinen, N., Progulske-Fox, A., Proikas-Cezanne, T., Przedborski, S., Przyklenk, K., Puertollano, R., Puyal, J., Qian, S.B., Qin, L., Qin, Z.H., Quaggin, S.E., Raben, N., Rabinowich, H., Rabkin, S.W., Rahman, I., Rami, A., Ramm, G., Randall, G., Randow, F., Rao, V.A., Rathmell, J.C., Ravikumar, B., Ray, S.K., Reed, B.H., Reed, J.C., Reggiori, F., Regnier-Vigouroux, A., Reichert, A.S., Reiners, J.J., Jr., Reiter, R.J., Ren, J., Revuelta, J.L., Rhodes, C.J., Ritis, K., Rizzo, E., Robbins, J., Roberge, M., Roca, H., Roccheri, M.C., Rocchi, S., Rodemann, H.P., Rodriguez de Cordoba, S., Rohrer, B., Roninson, I.B., Rosen, K., Rost-Roszkowska, M.M., Rouis, M., Rouschop, K.M., Rovetta, F., Rubin, B.P., Rubinsztein, D.C., Ruckdeschel, K., Rucker, E.B., 3rd, Rudich, A., Rudolf, E., Ruiz-Opazo, N., Russo, R., Rusten, T.E., Ryan, K.M., Ryter, S.W., Sabatini, D.M., Sadoshima, J., Saha, T., Saitoh, T., Sakagami, H., Sakai, Y., Salekdeh, G.H., Salomoni, P., Salvaterra, P.M., Salvesen, G., Salvioli, R., Sanchez, A.M., Sanchez-Alcazar, J.A., Sanchez-Prieto, R., Sandri, M., Sankar, U., Sansanwal, P., Santambrogio, L., Saran, S., Sarkar, S., Sarwal, M., Sasakawa, C., Sasnauskiene, A., Sass, M., Sato, K., Sato, M., Schapira, A.H., Scharl, M., Schatzl, H.M., Scheper, W., Schiaffino, S., Schneider, C., Schneider, M.E., Schneider-Stock, R., Schoenlein, P.V., Schorderet, D.F., Schuller, C., Schwartz, G.K., Scorrano, L., Sealy, L., Seglen, P.O., Segura-Aguilar, J., Seiliez, I., Seleverstov, O., Sell, C., Seo, J.B., Separovic, D., Setaluri, V., Setoguchi, T., Settembre, C., Shacka, J.J., Shanmugam, M., Shapiro, I.M., Shaulian, E., Shaw, R.J., Shelhamer, J.H., Shen, H.M., Shen, W.C., Sheng, Z.H., Shi, Y., Shibuya, K., Shidoji, Y., Shieh, J.J., Shih, C.M., Shimada, Y., Shimizu, S., Shintani, T., Shirihai, O.S., Shore, G.C., Sibirny, A.A., Sidhu, S.B., Sikorska, B., Silva-Zacarin, E.C., Simmons, A., Simon, A.K., Simon, H.U., Simone, C., Simonsen, A., Sinclair, D.A., Singh, R., Sinha, D., Sinicrope, F.A., Sirko, A., Siu, P.M., Sivridis, E., Skop, V., Skulachev, V.P., Slack, R.S., Smaili, S.S., Smith, D.R., Soengas, M.S., Soldati, T., Song, X., Sood, A.K., Soong, T.W., Sotgia, F., Spector, S.A., Spies, C.D., Springer, W., Srinivasula, S.M., Stefanis, L., Steffan, J.S., Stendel, R., Stenmark, H., Stephanou, A., Stern, S.T., Sternberg, C., Stork, B., Stralfors, P., Subauste, C.S., Sui, X., Sulzer, D., Sun, J., Sun, S.Y., Sun, Z.J., Sung, J.J., Suzuki, K., Suzuki, T., Swanson, M.S., Swanton, C., Sweeney, S.T., Sy, L.K., Szabadkai, G., Tabas, I., Taegtmeyer, H., Tafani, M., Takacs-Vellai, K., Takano, Y., Takegawa, K., Takemura, G., Takeshita, F., Talbot, N.J., Tan, K.S., Tanaka, K., Tanaka, K., Tang, D., Tang, D., Tanida, I., Tannous, B.A., Tavernarakis, N., Taylor, G.S., Taylor, G.A., Taylor, J.P., Terada, L.S., Terman, A., Tettamanti, G., Thevissen, K., Thompson, C.B., Thorburn, A., Thumm, M., Tian, F., Tian, Y., Tocchini-Valentini, G., Tolkovsky, A.M., Tomino, Y., Tonges, L., Tooze, S.A., Tournier, C., Tower, J., Towns, R., Trajkovic, V., Travassos, L.H., Tsai, T.F., Tschan, M.P., Tsubata, T., Tsung, A., Turk, B., Turner, L.S., Tyagi, S.C., Uchiyama, Y., Ueno, T., Umekawa, M., Umemiya-Shirafuji, R., Unni, V.K., Vaccaro, M.I., Valente, E.M., Van den Berghe, G., van der Klei, I.J., van Doorn, W., van Dyk, L.F., van Egmond, M., van Grunsven, L.A., Vandenabeele, P., Vandenberghe, W.P., Vanhorebeek, I., Vaquero, E.C., Velasco, G., Vellai, T., Vicencio, J.M., Vierstra, R.D., Vila, M., Vindis, C., Viola, G., Viscomi, M.T., Voitsekhovskaja, O.V., von Haefen, C., Votruba, M., Wada, K., Wade-Martins, R., Walker, C.L., Walsh, C.M., Walter, J., Wan, X.B., Wang, A., Wang, C., Wang, D., Wang, F., Wang, F., Wang, G., Wang, H., Wang, H.G., Wang, H.D., Wang, J., Wang, K., Wang, M., Wang, R.C., Wang, X., Wang, X., Wang, Y.J., Wang, Y., Wang, Z.,

Wang, Z.C., Wang, Z., Wansink, D.G., Ward, D.M., Watada, H., Waters, S.L., Webster, P., Wei, L., Weihl, C.C., Weiss, W.A., Welford, S.M., Wen, L.P., Whitehouse, C.A., Whitton, J.L., Whitworth, A.J., Wileman, T., Wiley, J.W., Wilkinson, S., Willbold, D., Williams, R.L., Williamson, P.R., Wouters, B.G., Wu, C., Wu, D.C., Wu, W.K., Wyttenbach, A., Xavier, R.J., Xi, Z., Xia, P., Xiao, G., Xie, Z., Xie, Z., Xu, D.Z., Xu, J., Xu, L., Xu, X., Yamamoto, A., Yamamoto, A., Yamashina, S., Yamashita, M., Yan, X., Yanagida, M., Yang, D.S., Yang, E., Yang, J.M., Yang, S.Y., Yang, W., Yang, W.Y., Yang, Z., Yao, M.C., Yao, T.P., Yeganeh, B., Yen, W.L., Yin, J.J., Yin, X.M., Yoo, O.J., Yoon, G., Yoon, S.Y., Yorimitsu, T., Yoshikawa, Y., Yoshimori, T., Yoshimoto, K., You, H.J., Youle, R.J., Younes, A., Yu, L., Yu, L., Yu, S.W., Yu, W.H., Yuan, Z.M., Yue, Z., Yun, C.H., Yuzaki, M., Zabirnyk, O., Silva-Zacarin, E., Zacks, D., Zacksenhaus, E., Zaffaroni, N., Zakeri, Z., Zeh, H.J., 3rd, Zeitlin, S.O., Zhang, H., Zhang, H.L., Zhang, J., Zhang, J.P., Zhang, L., Zhang, L., Zhang, M.Y., Zhang, X.D., Zhao, M., Zhao, Y.F., Zhao, Y., Zhao, Z.J., Zheng, X., Zhivotovsky, B., Zhong, Q., Zhou, C.Z., Zhu, C., Zhu, W.G., Zhu, X.F., Zhu, X., Zhu, Y., Zoladek, T., Zong, W.X., Zorzano, A., Zschocke, J., and Zuckerbraun, B. (2012). Guidelines for the use and interpretation of assays for monitoring autophagy. Autophagy *8*, 445-544.

Krishna, M., and Narang, H. (2008). The complexity of mitogen-activated protein kinases (MAPKs) made simple. Cellular and molecular life sciences : CMLS *65*, 3525-3544.

Krol, J., Loedige, I., and Filipowicz, W. (2010). The widespread regulation of microRNA biogenesis, function and decay. Nat Rev Genet *11*, 597-610.

Kwiatkowski, D.J., Zhang, H., Bandura, J.L., Heiberger, K.M., Glogauer, M., el-Hashemite, N., and Onda, H. (2002). A mouse model of TSC1 reveals sex-dependent lethality from liver hemangiomas, and up-regulation of p70S6 kinase activity in Tsc1 null cells. Human molecular genetics *11*, 525-534.

Lam, D., Dickens, D., Reid, E.B., Loh, S.H., Moisoi, N., and Martins, L.M. (2009). MAP4K3 modulates cell death via the post-transcriptional regulation of BH3-only proteins. Proceedings of the National Academy of Sciences of the United States of America *106*, 11978-11983.

Lam, D., Shah, S., de Castro, I.P., Loh, S.H., and Martins, L.M. (2010). Drosophila happyhour modulates JNK-dependent apoptosis. Cell Death Dis *1*, e66.

Lamming, D.W., Ye, L., Sabatini, D.M., and Baur, J.A. (2013). Rapalogs and mTOR inhibitors as anti-aging therapeutics. The Journal of clinical investigation *123*, 980-989.

Lan, F., Cacicedo, J.M., Ruderman, N., and Ido, Y. (2008). SIRT1 modulation of the acetylation status, cytosolic localization, and activity of LKB1. Possible role in AMP-activated protein kinase activation. The Journal of biological chemistry *283*, 27628-27635.

Laplante, M., and Sabatini, D.M. (2009). mTOR signaling at a glance. Journal of cell science *122*, 3589-3594.

Laplante, M., and Sabatini, D.M. (2012). mTOR signaling in growth control and disease. Cell *149*, 274-293.

Lin, S.J., Defossez, P.A., and Guarente, L. (2000). Requirement of NAD and SIR2 for life-span extension by calorie restriction in Saccharomyces cerevisiae. Science *289*, 2126-2128.

Lizcano, J.M., Goransson, O., Toth, R., Deak, M., Morrice, N.A., Boudeau, J., Hawley, S.A., Udd, L., Makela, T.P., Hardie, D.G., and Alessi, D.R. (2004). LKB1 is a master kinase that activates 13 kinases of the AMPK subfamily, including MARK/PAR-1. The EMBO journal *23*, 833-843.

Lock, C., Hermans, G., Pedotti, R., Brendolan, A., Schadt, E., Garren, H., Langer-Gould, A., Strober, S., Cannella, B., Allard, J., Klonowski, P., Austin, A., Lad, N., Kaminski, N., Galli, S.J., Oksenberg, J.R., Raine, C.S., Heller, R., and Steinman, L. (2002). Gene-microarray analysis of multiple sclerosis lesions yields new targets validated in autoimmune encephalomyelitis. Nature medicine *8*, 500-508.

Long, X., Ortiz-Vega, S., Lin, Y., and Avruch, J. (2005). Rheb binding to mammalian target of rapamycin (mTOR) is regulated by amino acid sufficiency. The Journal of biological chemistry *280*, 23433-23436.

Lopez-Otin, C., Blasco, M.A., Partridge, L., Serrano, M., and Kroemer, G. (2013). The hallmarks of aging. Cell *153*, 1194-1217.

Ma, X.M., and Blenis, J. (2009). Molecular mechanisms of mTOR-mediated translational control. Nature reviews. Molecular cell biology *10*, 307-318.

Ma, X.M., Yoon, S.O., Richardson, C.J., Julich, K., and Blenis, J. (2008). SKAR links pre-mRNA splicing to mTOR/S6K1-mediated enhanced translation efficiency of spliced mRNAs. Cell *133*, 303-313.

Manning, B.D., Tee, A.R., Logsdon, M.N., Blenis, J., and Cantley, L.C. (2002). Identification of the tuberous sclerosis complex-2 tumor suppressor gene product tuberin as a target of the phosphoinositide 3-kinase/akt pathway. Molecular cell *10*, 151-162.

Martina, J.A., Chen, Y., Gucek, M., and Puertollano, R. (2012). MTORC1 functions as a transcriptional regulator of autophagy by preventing nuclear transport of TFEB. Autophagy *8*, 903-914.

Martina, J.A., and Puertollano, R. (2013). Rag GTPases mediate amino acid-dependent recruitment of TFEB and MITF to lysosomes. The Journal of cell biology *200*, 475-491.

Mayer, C., Zhao, J., Yuan, X., and Grummt, I. (2004). mTOR-dependent activation of the transcription factor TIF-IA links rRNA synthesis to nutrient availability. Genes & development *18*, 423-434.

Mayr, C., Hemann, M.T., and Bartel, D.P. (2007). Disrupting the pairing between let-7 and Hmga2 enhances oncogenic transformation. Science *315*, 1576-1579.

McGale, E.H., Pye, I.F., Stonier, C., Hutchinson, E.C., and Aber, G.M. (1977). Studies of the inter-relationship between cerebrospinal fluid and plasma amino acid concentrations in normal individuals. J Neurochem *29*, 291-297.

Meng, Z., Moroishi, T., Mottier-Pavie, V., Plouffe, S.W., Hansen, C.G., Hong, A.W., Park, H.W., Mo, J.S., Lu, W., Lu, S., Flores, F., Yu, F.X., Halder, G., and Guan, K.L. (2015). MAP4K family kinases act in parallel to MST1/2 to activate LATS1/2 in the Hippo pathway. Nat Commun *6*, 8357.

Mizushima, N., and Komatsu, M. (2011). Autophagy: renovation of cells and tissues. Cell *147*, 728-741.

Mizushima, N., Sugita, H., Yoshimori, T., and Ohsumi, Y. (1998). A new protein conjugation system in human. The counterpart of the yeast Apg12p conjugation system essential for autophagy. The Journal of biological chemistry *273*, 33889-33892.

Nasrin, N., Kaushik, V.K., Fortier, E., Wall, D., Pearson, K.J., de Cabo, R., and Bordone, L. (2009). JNK1 phosphorylates SIRT1 and promotes its enzymatic activity. PloS one *4*, e8414.

Nicklin, P., Bergman, P., Zhang, B., Triantafellow, E., Wang, H., Nyfeler, B., Yang, H., Hild, M., Kung, C., Wilson, C., Myer, V.E., MacKeigan, J.P., Porter, J.A., Wang, Y.K., Cantley, L.C., Finan, P.M., and Murphy, L.O. (2009). Bidirectional transport of amino acids regulates mTOR and autophagy. Cell *136*, 521-534.

Noda, T., and Ohsumi, Y. (1998). Tor, a phosphatidylinositol kinase homologue, controls autophagy in yeast. The Journal of biological chemistry *273*, 3963-3966.

Palmieri, M., Impey, S., Kang, H., di Ronza, A., Pelz, C., Sardiello, M., and Ballabio, A. (2011). Characterization of the CLEAR network reveals an integrated control of cellular clearance pathways. Human molecular genetics *20*, 3852-3866.

Peterson, T.R., Laplante, M., Thoreen, C.C., Sancak, Y., Kang, S.A., Kuehl, W.M., Gray, N.S., and Sabatini, D.M. (2009). DEPTOR is an mTOR inhibitor frequently overexpressed in multiple myeloma cells and required for their survival. Cell *137*, 873-886.

Pimienta, G., and Pascual, J. (2007). Canonical and alternative MAPK signaling. Cell Cycle *6*, 2628-2632.

Polito, V.A., Li, H., Martini-Stoica, H., Wang, B., Yang, L., Xu, Y., Swartzlander, D.B., Palmieri, M., di Ronza, A., Lee, V.M., Sardiello, M., Ballabio, A., and Zheng, H. (2014). Selective clearance of aberrant tau proteins and rescue of neurotoxicity by transcription factor EB. EMBO Mol Med *6*, 1142-1160.

Potter, C.J., Pedraza, L.G., and Xu, T. (2002). Akt regulates growth by directly phosphorylating Tsc2. Nat Cell Biol *4*, 658-665.

Ramjaun, A.R., Angers, A., Legendre-Guillemin, V., Tong, X.K., and McPherson, P.S. (2001). Endophilin regulates JNK activation through its interaction with the germinal center kinase-like kinase. The Journal of biological chemistry *276*, 28913-28919.

Rebsamen, M., Pochini, L., Stasyk, T., de Araujo, M.E., Galluccio, M., Kandasamy, R.K., Snijder, B., Fauster, A., Rudashevskaya, E.L., Bruckner, M., Scorzoni, S., Filipek, P.A., Huber, K.V., Bigenzahn, J.W., Heinz, L.X., Kraft, C., Bennett, K.L., Indiveri, C., Huber, L.A., and Superti-Furga, G. (2015). SLC38A9 is a component of the lysosomal amino acid sensing machinery that controls mTORC1. Nature *519*, 477-481.

Resnik-Docampo, M., and de Celis, J.F. (2011). MAP4K3 is a component of the TORC1 signalling complex that modulates cell growth and viability in Drosophila melanogaster. PloS one *6*, e14528.

Roczniak-Ferguson, A., Petit, C.S., Froehlich, F., Qian, S., Ky, J., Angarola, B., Walther, T.C., and Ferguson, S.M. (2012). The Transcription Factor TFEB Links mTORC1 Signaling to Transcriptional Control of Lysosome Homeostasis. Sci. Signal. *5*, ra42-.

Roush, S., and Slack, F.J. (2008). The let-7 family of microRNAs. Trends Cell Biol *18*, 505-516.

Sancak, Y., Bar-Peled, L., Zoncu, R., Markhard, A.L., Nada, S., and Sabatini, D.M. (2010). Ragulator-Rag complex targets mTORC1 to the lysosomal surface and is necessary for its activation by amino acids. Cell *141*, 290-303.

Sancak, Y., Peterson, T.R., Shaul, Y.D., Lindquist, R.A., Thoreen, C.C., Bar-Peled, L., and Sabatini, D.M. (2008). The Rag GTPases bind raptor and mediate amino acid signaling to mTORC1. Science *320*, 1496-1501.

Sancak, Y., Thoreen, C.C., Peterson, T.R., Lindquist, R.A., Kang, S.A., Spooner, E., Carr, S.A., and Sabatini, D.M. (2007). PRAS40 is an insulin-regulated inhibitor of the mTORC1 protein kinase. Molecular cell *25*, 903-915.

Sardiello, M., Palmieri, M., di Ronza, A., Medina, D.L., Valenza, M., Gennarino, V.A., Di Malta, C., Donaudy, F., Embrione, V., Polishchuk, R.S., Banfi, S., Parenti, G., Cattaneo, E., and Ballabio, A. (2009). A gene network regulating lysosomal biogenesis and function. Science *325*, 473-477.

Saucedo, L.J., Gao, X., Chiarelli, D.A., Li, L., Pan, D., and Edgar, B.A. (2003). Rheb promotes cell growth as a component of the insulin/TOR signalling network. Nat Cell Biol *5*, 566-571.

Saxton, R.A., Knockenhauer, K.E., Wolfson, R.L., Chantranupong, L., Pacold, M.E., Wang, T., Schwartz, T.U., and Sabatini, D.M. (2016). Structural basis for leucine sensing by the Sestrin2-mTORC1 pathway. Science *351*, 53-58.

Scott, S.V., Hefner-Gravink, A., Morano, K.A., Noda, T., Ohsumi, Y., and Klionsky, D.J. (1996). Cytoplasm-to-vacuole targeting and autophagy employ the same machinery to deliver proteins to the yeast vacuole. Proceedings of the National Academy of Sciences of the United States of America *93*, 12304-12308.

Sekiguchi, T., Hirose, E., Nakashima, N., Ii, M., and Nishimoto, T. (2001). Novel G proteins, Rag C and Rag D, interact with GTP-binding proteins, Rag A and Rag B. The Journal of biological chemistry *276*, 7246-7257.

Settembre, C., Di Malta, C., Polito, V.A., Garcia Arencibia, M., Vetrini, F., Erdin, S., Erdin, S.U., Huynh, T., Medina, D., Colella, P., Sardiello, M., Rubinsztein, D.C., and Ballabio, A. (2011). TFEB links autophagy to lysosomal biogenesis. Science *332*, 1429-1433.

Settembre, C., Zoncu, R., Medina, D.L., Vetrini, F., Erdin, S., Huynh, T., Ferron, M., Karsenty, G., Vellard, M.C., Facchinetti, V., Sabatini, D.M., and Ballabio, A. (2012). A lysosome-to-nucleus signalling mechanism senses and regulates the lysosome via mTOR and TFEB. The EMBO journal *31*, 1095-1108.

Shaw, R.J., Kosmatka, M., Bardeesy, N., Hurley, R.L., Witters, L.A., DePinho, R.A., and Cantley, L.C. (2004). The tumor suppressor LKB1 kinase directly activates AMP-activated kinase and regulates apoptosis in response to energy stress. Proceedings of the National Academy of Sciences of the United States of America *101*, 3329-3335.

Shintani, T., and Klionsky, D.J. (2004). Autophagy in health and disease: a double-edged sword. Science *306*, 990-995.

Small, E.M., and Olson, E.N. (2011). Pervasive roles of microRNAs in cardiovascular biology. Nature *469*, 336-342.

Smith, E.M., Finn, S.G., Tee, A.R., Browne, G.J., and Proud, C.G. (2005). The tuberous sclerosis protein TSC2 is not required for the regulation of the mammalian target of rapamycin by amino acids and certain cellular stresses. The Journal of biological chemistry *280*, 18717-18727.

Spampanato, C., Feeney, E., Li, L., Cardone, M., Lim, J.A., Annunziata, F., Zare, H., Polishchuk, R., Puertollano, R., Parenti, G., Ballabio, A., and Raben, N. (2013). Transcription factor EB (TFEB) is a new therapeutic target for Pompe disease. EMBO Mol Med *5*, 691-706.

Stocker, H., Radimerski, T., Schindelholz, B., Wittwer, F., Belawat, P., Daram, P., Breuer, S., Thomas, G., and Hafen, E. (2003). Rheb is an essential regulator of S6K in controlling cell growth in Drosophila. Nat Cell Biol *5*, 559-565.

Suchankova, G., Nelson, L.E., Gerhart-Hines, Z., Kelly, M., Gauthier, M.S., Saha, A.K., Ido, Y., Puigserver, P., and Ruderman, N.B. (2009). Concurrent regulation of AMP-activated protein kinase and SIRT1 in mammalian cells. Biochemical and biophysical research communications *378*, 836-841.

Suter, M., Riek, U., Tuerk, R., Schlattner, U., Wallimann, T., and Neumann, D. (2006). Dissecting the role of 5'-AMP for allosteric stimulation, activation, and deactivation of AMP-activated protein kinase. The Journal of biological chemistry *281*, 32207-32216.

Tee, A.R., Manning, B.D., Roux, P.P., Cantley, L.C., and Blenis, J. (2003). Tuberous sclerosis complex gene products, Tuberin and Hamartin, control mTOR signaling by acting as a GTPase-activating protein complex toward Rheb. Curr Biol *13*, 1259-1268.

Tissenbaum, H.A., Hawdon, J., Perregaux, M., Hotez, P., Guarente, L., and Ruvkun, G. (2000). A common muscarinic pathway for diapause recovery in the distantly related nematode species Caenorhabditis elegans and Ancylostoma caninum. Proceedings of the National Academy of Sciences of the United States of America *97*, 460-465.

van der Geer, P., and Hunter, T. (1994). Phosphopeptide mapping and phosphoamino acid analysis by electrophoresis and chromatography on thin-layer cellulose plates. Electrophoresis *15*, 544-554.

van der Vos, K.E., Eliasson, P., Proikas-Cezanne, T., Vervoort, S.J., van Boxtel, R., Putker, M., van Zutphen, I.J., Mauthe, M., Zellmer, S., Pals, C., Verhagen, L.P., Groot Koerkamp, M.J., Braat, A.K., Dansen, T.B., Holstege, F.C., Gebhardt, R., Burgering, B.M., and Coffer, P.J. (2012). Modulation of glutamine metabolism by the PI(3)K-PKB-FOXO network regulates autophagy. Nat Cell Biol *14*, 829-837.

Vander Haar, E., Lee, S.I., Bandhakavi, S., Griffin, T.J., and Kim, D.H. (2007). Insulin signalling to mTOR mediated by the Akt/PKB substrate PRAS40. Nat Cell Biol *9*, 316-323.

Vinciguerra, M., Santini, M.P., Martinez, C., Pazienza, V., Claycomb, W.C., Giuliani, A., and Rosenthal, N. (2012). mIGF-1/JNK1/SirT1 signaling confers protection against oxidative stress in the heart. Aging Cell *11*, 139-149.

Wang, S., Tsun, Z.Y., Wolfson, R.L., Shen, K., Wyant, G.A., Plovanich, M.E., Yuan, E.D., Jones, T.D., Chantranupong, L., Comb, W., Wang, T., Bar-Peled, L., Zoncu, R., Straub, C., Kim, C., Park, J., Sabatini, B.L., and Sabatini, D.M. (2015). Metabolism. Lysosomal amino acid transporter SLC38A9 signals arginine sufficiency to mTORC1. Science *347*, 188-194.

Wang, X., Li, W., Williams, M., Terada, N., Alessi, D.R., and Proud, C.G. (2001). Regulation of elongation factor 2 kinase by p90(RSK1) and p70 S6 kinase. The EMBO journal *20*, 4370-4379.

Wilson, K.F., Wu, W.J., and Cerione, R.A. (2000). Cdc42 stimulates RNA splicing via the S6 kinase and a novel S6 kinase target, the nuclear cap-binding complex. The Journal of biological chemistry *275*, 37307-37310.

Wolfson, R.L., Chantranupong, L., Saxton, R.A., Shen, K., Scaria, S.M., Cantor, J.R., and Sabatini, D.M. (2016). Sestrin2 is a leucine sensor for the mTORC1 pathway. Science *351*, 43-48.

Xiao, Q., Yan, P., Ma, X., Liu, H., Perez, R., Zhu, A., Gonzales, E., Tripoli, D.L., Czerniewski, L., Ballabio, A., Cirrito, J.R., Diwan, A., and Lee, J.M. (2015). Neuronal-Targeted TFEB Accelerates Lysosomal Degradation of APP, Reducing Abeta Generation and Amyloid Plaque Pathogenesis. The Journal of neuroscience : the official journal of the Society for Neuroscience *35*, 12137-12151.

Yan, J., Kuroyanagi, H., Kuroiwa, A., Matsuda, Y., Tokumitsu, H., Tomoda, T., Shirasawa, T., and Muramatsu, M. (1998). Identification of mouse ULK1, a novel protein kinase structurally related to C. elegans UNC-51. Biochemical and biophysical research communications *246*, 222-227.

Yan, L., and Lamb, R.F. (2012). Amino acid sensing and regulation of mTORC1. Seminars in cell & developmental biology *23*, 621-625.

Yan, L., Mieulet, V., Burgess, D., Findlay, G.M., Sully, K., Procter, J., Goris, J., Janssens, V., Morrice, N.A., and Lamb, R.F. (2010). PP2A T61 epsilon is an inhibitor of MAP4K3 in nutrient signaling to mTOR. Molecular cell *37*, 633-642.

Young, J.E., Martinez, R.A., and La Spada, A.R. (2009). Nutrient deprivation induces neuronal autophagy and implicates reduced insulin signaling in neuroprotective autophagy activation. The Journal of biological chemistry *284*, 2363-2373.

Zaia, K.A., and Reimer, R.J. (2009). Synaptic Vesicle Protein NTT4/XT1 (SLC6A17) Catalyzes Na+-coupled Neutral Amino Acid Transport. The Journal of biological chemistry *284*, 8439-8448.

Zhang, Y., Gao, X., Saucedo, L.J., Ru, B., Edgar, B.A., and Pan, D. (2003). Rheb is a direct target of the tuberous sclerosis tumour suppressor proteins. Nat Cell Biol *5*, 578-581.

Zhu, H., Shyh-Chang, N., Segre, A.V., Shinoda, G., Shah, S.P., Einhorn, W.S., Takeuchi, A., Engreitz, J.M., Hagan, J.P., Kharas, M.G., Urbach, A., Thornton, J.E., Triboulet, R., Gregory, R.I., Consortium, D., Investigators, M., Altshuler, D., and Daley, G.Q. (2011). The Lin28/let-7 axis regulates glucose metabolism. Cell *147*, 81-94.